Wear of PEEK All-Polymer Articulations for Cervical Spinal Disc Arthroplasty

by

Heather Austin

A thesis
presented to the University of Waterloo
in fulfillment of the
thesis requirement for the degree of
Master of Applied Science
in
Mechanical Engineering

Waterloo, Ontario, Canada, 2008
© Heather Austin 2008

I hereby declare that I am the sole author of this thesis. This is a true copy of the thesis, including any required final revisions, as accepted by my examiners.

I understand that my thesis may be made electronically available to the public.

Abstract

The conventional treatment for degenerative disc disease (DDD) and disc herniation is spinal fusion, a process consisting of fusing two segments of the spine together. Arthroplasty treatments that preserve the natural motion of the spine are still in the early stages of development. Cervical disc arthroplasty (CDA) involves removal of the existing damaged disc and replacement with an articulating implant.

The materials used for implants must possess excellent biocompatibility, strength, and wear resistance properties. Spinal implants in particular should also allow precise post-operative imaging because surgeons rely on imaging tools to check for migration of the implant and nerve impingement post-operatively.

The purpose of the current thesis is to investigate the wear behaviour of three different versions of poly-ether-ether-ketone (PEEK), a radiolucent polymer that does not distort MRI images, articulating against themselves. The materials tested include: PEEK OPTIMA (OPT), carbon-fiber reinforced (CFR) PEEK and carbon-nanofiber (CNF) PEEK.

A series of wear tests were performed on a pin-on-plate apparatus that imposed reciprocating crossing-path motion to the articulating specimens. The first series of wear tests, "normal conditions tests", consisted of application of 80 N for 2.0 million cycles (Mc). Continuation of testing was aimed at evaluating the tribological behaviour of the materials under "adverse conditions". The adverse conditions involved increasing the load every 0.15 Mc until the material showed significant surface damage. The materials were tested in a 12g/L protein concentration alpha calf fraction serum, at 37˚C. The wear of the specimens were evaluated using volumetric wear calculations and microscopy.

The lowest wear, at the end of the normal conditions test, occurred with the articulation of CFR PEEK-on-CFR PEEK, and the highest wear, after 2.0 Mc, occurred with CNF PEEK-on-CNF PEEK. The adverse conditions revealed the highest wear value for PEEK OPT. Surface damage was apparent on both the PEEK OPT and CFR PEEK specimens; however, volumetric wear measurements performed on the specimens did not indicate a rise in wear for CFR PEEK, though surface damage was visibly noted. CNF

PEEK was not tested to failure, although surface damage was evident as the material neared the end of the adverse conditions test.

The PEEK OPT wear values after the normal conditions test are similar to those reported for spine simulator studies on a PEEK OPT-on-PEEK OPT all-polymer lumbar nucleus implant. This tentatively suggests that the normal test conditions represent a clinically realistic range.

CFR PEEK shows the most promise for application in cervical disc arthroplasty. The other versions of PEEK possess excellent imaging qualities but had inferior wear resistance compared with CFR PEEK. However, wear volumes found in the present thesis for all three versions of PEEK after the "normal conditions" test were considerably lower than those found for stainless steel (SS) in similar testing. Prestige® STLP, composed of SS, is an FDA approved product that is currently implanted in patients in the United States.

Acknowledgments

I would like to extend thanks to my supervisor, Dr. J.B. Medley, for providing me with many opportunities, including the chance to observe orthopaedic surgery and the experience of travelling to both local and international conferences. Dr. J.B. Medley's challenge of my results and reasoning has led to a much improved thesis and a deeper understanding of the material presented. Dr. C.M. Hanson is credited for me maintaining my sanity towards the end of this project. Thank you for taking on the task of co-supervision and for your constant support and insight into my research.

I would like to thank my research group consisting of Kyle Anders, Brad Bergsma, Neal Damgaard, Rana Islam, Shahzma Jaffer, Katherine Olsen and Ken Su for all the feedback. Thank you to Dan Langohr for his assistance with experimental procedures.

I am grateful for the financial support from Medtronic Spinal and Biologics, Memphis, TN. Many thanks to Megan Harper for her expertise in wear research. Thank you to Jan Brandt for his insight into lubricant composition. The precise results presented in this thesis would not have been possible without the help of the team at London Health Sciences Centre who graciously lent me their analytical balance for the duration of my research.

Thank you to Tom Gawel for the design and fabrication of the load soak used throughout this project and for the technical support provided when issues arose with the OrthoPOD^{TM}. I would like Charlie Boyle, from the University of Waterloo machine shop, for fabricating the specimen holders used in the wear tests.

Thank you to my family and friends for your support and patience throughout this endeavor. Finally, thank you Tom and Ruby for making me laugh at least once day, everyday.

Dedication

The current thesis is dedicated to the following individuals:

Sandy Austin

Don Austin

Stephanie Wood

Neil Gibson

Kirk D'Souza

Dr. M. J. Berber

Thank you.

TABLE OF CONTENTS

List of Tables ix
List of Figures x
List of Equations xii
Nomenclature xiii
1.0 INTRODUCTION 1
2.0 LITERATURE REVIEW 3
2.1. Anatomy and Biomechanics of the Cervical Spine 3
2.1.1. General Anatomy 3
2.1.1. Loads and Motions of the Cervical Spine 5
2.1.2. Intervertebral Disc 11
2.2. Basic Tribology 13
2.2.1. Surface Topography 14
2.2.2. Friction 16
2.2.3. Lubrication 16
2.2.4. Wear 18
2.3. Surgery for Damaged Cervical Discs 22
2.3.1. Fusion 22
2.3.2. Cervical Disc Arthroplasty 23
2.3.2.1. Implant Design Principles 23
2.3.2.2. Implants 24
2.3.2.3. Biomechanical and Wear Tests 28
2.3.2.4. Wear Particles and Osteolysis 30
2.3.2.5. Evidence of Osteolysis in Spinal Disc Arthroplasty 32
2.3.2.6. Post Operative Medical Imaging 33
2.4 Polyetheretherkeytone (PEEK) 34
2.4.1 Types of PEEK 35
2.4.2 Properties 37
2.4.3 Wear Testing of PEEK Surfaces 38
2.4.3.1 Configurations 38
2.4.3.2 Reciprocating Pin-on-plate Wear Results 40
2.4.3.3 PEEK Simulator Studies 41
2.4.3.4 Lubricants 43
2.4.3.5 Wear Particles 43
2.4.3.6 Fluid Adsorption 44
2.5 Objectives and Scope of Research 45
3.0 WEAR TESTING OF PEEK 46
3.1. Test Apparatus 46
3.1.1 Pin-on-Disc Apparatus 46
3.1.2 Temperature 47
3.1.3 Chamber Sealing 47
3.1.4 Hardware and Software 50
5.1.1. Motion 52
3.1.6 Load 53
3.2 Load-Soak Apparatus 54
3.2.1 Design & Fabrication 54

4.0 MATERIALS AND METHODS 56
4.1. Specimens 56
4.2. Protocols 58
4.2.1. Lubricant 61
4.2.2. Dis-assembly and Cleaning 63
4.2.3. Weighing and Re-assembly 64
4.2.4. Wear Measurements 65
4.2.5. Contact Stress 66
4.2.6. Microscopy 68
4.3. Concluding Remarks 68
5.0 RESULTS AND DISCUSSION 69
5.1. Preliminary Tests 69
5.1.1. Effect of Fluid Composition, Temperature and Load on Fluid Uptake 69
5.1.2. Fluid Uptake – Load Soak vs. OrthoPOD™ 71
5.2. Normal Conditions 73
5.2.1. PEEK OPTIMA 73
5.2.2. CFR PEEK 75
5.2.3. CNF PEEK Wear Curves 76
5.2.4. Comparison of PEEK OPTIMA, CFR PEEK and CNF PEEK 77
5.2.4.1. Comparison of Wear Rates for Different Contacts 79
5.2.4.2. Comparison of Wear Rates for Various PEEK pin-on-plate Studies 81
5.3. Observations on the Effect of Protein Degradation on Wear 82
5.4. Adverse Conditions 84
5.4.1. Wear Curves for PEEK OPTIMA, CFR PEEK and CNF PEEK 84
5.4.2. Modes of Failure 87
5.5. Microscopy of Surface Failure 88
5.5.1. PEEK OPTIMA 89
5.5.1.1. SEM 91
5.5.2. CFR PEEK 94
5.5.2.1. Scanning Electron Microscopy 94
5.5.3. CNF PEEK 98
5.6. Concluding Remarks 98
5.7. Clinical Implications 99
6.0 CONCLUSIONS AND RECOMMENDATIONS 101
6.1. Conclusions 101
6.2. Recommendations 103
References 105

Appendices
APPENDIX A 114
APPENDIX B 125
APPENDIX C 127
APPENDIX D 134
APPENDIX E 136

List of Tables

Table 1: Motions for C3-C7 segments in the Cervical Spine 6
Table 2: ISO & ASTM Standards for Loads and Motion 9
Table 3: FDA Summary of Safety and Effectiveness Data Report Results- Prestige® [21] 29
Table 4: FDA Summary of Safety and Effectiveness Data Report - ProDisc-C® [20] 29
Table 5: Wear Results for the Bryan® [7] 30
Table 6: PEEK Properties 37
Table 7: Comparison of Pin-on-plate tests with Different Articulating Materials and Test Conditions 40
Table 8: Specimen Pairings 57
Table 9: Preliminary Test Protocol 59
Table 10: PEEK OPTIMA Test Protocol 60
Table 11: CFR PEEK Protocol 61
Table 12: CNF PEEK Protocol 61
Table 13: Bovine Lubricant 62
Table 14: Alpha Lubricant 62
Table 15: Volumetric Wear & Wear Factors for PEEK OPTIMA - Normal Conditions 74
Table 16: Volumetric Wear and Wear Factors for CFR PEEK - Normal Conditions 76
Table 17: Volumetric Wear and Wear Factor for CNF PEEK - Normal Conditions 77
Table 18: Average Volumetric Wear Values after 2.0 Mc for PEEK OPT, CFR PEEK & CNF PEEK 78
Table 19: Adverse Conditions Wear Results 85
Table 21: Percentage of Wear Experienced by the Pin and the Plate 98

List of Figures

Fig. 1: Bryan Cervical Disc Implant (Medtronic) [7] 1
Fig. 2: Regions of the Spine (Top Left [17], Bottom Right [16]) 4
Fig. 3: Motions of the Spine [18] 5
Fig. 4: Cervical Disc Segment: Forces, Translations, Rotations [19] 6
Fig. 5: Cervical Intradiscal Pressures and Axial Loads [12, 18] 10
Fig. 6: Intervertebral Disc [25] 12
Fig. 7: Facet Joints[15] 13
Fig. 8: A worn surface of 20wt% commercial grade PAN CFR PEEK pin after articulating against a 100Cr6 steel plate [45] 14
Fig. 9A&B: Micrographs of PEEK OPT - Normal vs. Severe Test Conditions [45, 46] 15
Fig. 10: Micrograph of 30wt% PAN CFR PEEK - Severe test conditions [46] 16
Fig. 11: Types of Lubrication [48] 17
Fig. 12: Typical Wear Behaviour [44] 20
Fig. 13: The Transition Phenomena in Wear [50] 21
Fig. 14: Prestige®LP (Medtronic Spinal a Biologics) [6] 25
Fig. 15: ProDisc-C® (Synthes, Paoli, PA) [62] 26
Fig. 16: Bryan® Cervical Disc Implant (Medtronic Sofamor Danek) [64][66] 27
Fig. 17: PCM® (Cervitech®, Rockway, NJ) [68, 68] 28
Fig. 18: MRI of A) ProDisc-C® B) PCM® [11] 34
Fig. 19: Radiopacity of Different Spinal Implants [13] 36
Fig. 20: PEEK vs. UHMWPE [85] 42
Fig. 21: Schematic of OrthoPOD™ [108] 46
Fig. 22: OrthoPOD lubricant levels after 0.2 Mc cycles 48
Fig. 23: Fluid Level Difference between Chamber 1 and Chamber 4 48
Fig. 24: Volume of lubricant in the OrthoPOD™ and Load Soak 49
Fig. 25: Incorrect “Home” Position 51
Fig. 26: Load Soak Apparatus 55
Fig. 27: Specimens A) Pin B) Plate 56
Fig. 28: Confirm of Radius on Pins (PEEK OPT) 57
Fig. 29: Numbering Scheme for A) OrthoPOD™ B) Load Soak 58
Fig. 30: Wear Paths on PEEK OPTIMA Specimen 59
Fig. 31: Effect of Temperature (Above Left) & Load (Above Right) on Fluid Uptake – Study 1 70
Fig. 32: Effect of Temperature and Load - Study 2 70
Fig. 33: Change in Mass (mg) for PEEK OPTIMA pairs (plate+pin) 71
Fig. 34: Fluid Uptake Test A) Original Location B) Reversed Location 72
Fig. 35: Average Fluid Uptake Study A) Original Locations B) Locations Reversed 72
Fig. 36: PEEK OPTIMA Wear Curves 74
Fig. 37: CFR PEEK Wear Curves 75
Fig. 38: CNF Wear Curves 76
Fig. 39: Normal Conditions Wear Curves 78
Fig. 40: Comparison of Results and Studies from the Literature (wear rates < 20 mm^3/Nm x 10^{-7}) 80
Fig. 41: Comparison of PEEK Wear Rates 81

Fig. 42: Comparison of Results to PEEK studies from the literature (2 studies not shown in graph) 82
Fig. 43: Protein Degradation and Wear Curves for PEEK OPTIMA Normal Condtions 83
Fig. 44: Wear Curves for Adverse Condition Tests 85
Fig. 45: Volumetric Wear of All Versions of PEEK after Normal and Adverse Conditions 86
Fig. 46: PEEK OPTIMA – Plate 2 at the 300 N load level of the Adverse Conditions Test 87
Fig. 47: CFR PEEK – Plate 2 at the 400N load level of the Adverse Conditions Test 88
Fig. 48: Worn End of CFR Pin 1 and OPT Pin 2 88
Fig. 49: Macrographs of PEEK OPT Plates 2 & 4 after Adverse Conditions Test (300N, 2.75 Mc) 90
Fig. 50: Overview of Damaged Region on PEEK OPT Plate 2 91
Fig. 51: Different Locations in the Damaged Zone – PEEK OPT (plate 4) 92
Fig. 52: Microscopy of Plate 5 - Unworn (A) and Plate 4 - Severely Damaged (B) PEEK OPT 93
Fig. 53: Pin 4 after Adverse Conditions (300N, 2.75 Mc) 93
Fig. 54: Damage seen at 2.90 Mc and 350 N - CFR PEEK Plate 2 A) Centre of hole B) Polished wear track 95
Fig. 55: Images of Unworn (A) and Severely Damaged (B) CFR PEEK Plate 3 96
Fig. 56: Max Damage in A) PEEK OPT – Plate 2 @ 2.75 Mc, 300N and in B) CFR PEEK – Plate 2 @ 3.05 Mc, 400 N 96
Fig. 57: Pin hole damage on a CFR PEEK pin specimen after 2.9 Mc and 350 N 97
Fig. 58: Carbon Fiber Orientation in Pin and Plate Specimens 97
Fig. 59: CNF PEEK plate @ 0.25 Mc, 80 N 98

List of Equations

Eqn. 1: Definition of the Coefficient of Friction [47] 16
Eqn. 2: Archard's Law [44] 21
Eqn. 3: Wear in mg 65
Eqn. 4: Volumetric Wear 65
Eqn. 5: Wear Factor 66
Eqn. 6: Contact Stress Formula [110] 67
Eqn. 7: Hertzian Theory 67

Nomenclature

ACRONYMS

CDA	Cervical Disc Arthroplasty
CDA	Cervical Disc Arthroplasty
CFR	Carbon Fibre Reinforced
CNF	Carbon Nanofiber
CoCrMo	Cobalt chromium molybedeum
CT	Computer Tomography
DDD	Degenerative Disc Disease
FE	Flexion/Extension
HC	High carbon
Hz	Hertz
ISO	International Standard Organization
kPa	kiloPascals
LB	Lateral Bending
LC	Low carbon
Mc	Million cycles
N	Newton
OPT	OPTIMA
PAN	Polyacrylomitrile
PEEK	Poly-ether-ether-ketone
ROM	Range of Motion
SD	Standard Deviation
SS	Stainless Steel
TiC	Titanium Carbide
™	Trade Mark
UHMWPE	Ultra High Molecular Weight Polyethylene

MATHEMATICAL SYMBOLS

ΔV	Change in Volume
μ	Coefficient of friction
ρ	Density of the specimen
m	mass
N	Number of samples
π	pi
x	sliding distance
V	Volumetric wear
K	Wear Factor

1.0 INTRODUCTION

Cervical degenerative disc disease (DDD), which can include facet joint degeneration and cervical disc herniation result in tingling and clumsiness of the hands and possible gait disturbance. DDD and disc herniation also affect the roots of the nerves that run along the spine and can result in shoulder and arm pain [1]. If untreated, severe DDD or disc herniation can lead to loss of normal disc mechanical function, tissue injury, pain and ultimately paralysis. Less severe cases can be treated with physiotherapy, braces and other non-surgical devices therapies but spinal fusion, the fusion of two or more vertebrae to form a single rigid unit, is the conventional treatment for severe cervical DDD and disc herniation. Adjacent disc degeneration, above or below a fused segment, is not uncommon and can create a need for additional fusions in the future [2]. This increasingly impairs motion and overall functionality of the cervical spine.

Cervical disc arthroplasty (CDA), in which the intervertebral disc between two adjacent vertebrae is replaced by an articulating implant, is a relatively new and increasingly popular surgical procedure used to treat DDD or cervical disc herniation [3]. It preserves the natural motion of the spine and, thus, reduces the risk of adjacent disc degeneration [3]. CDA implants include the articulation of the following classes of materials; metal-polymer [4], ceramic-ceramic [5] and metal-metal [6]. Fig. 1 shows a metal-polymer CDA implant known as the Bryan®.

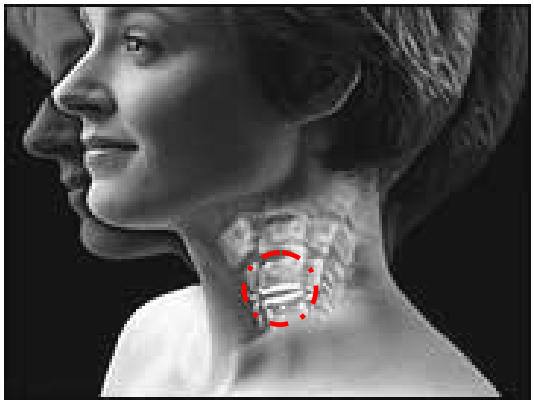

Fig. 1: Bryan Cervical Disc Implant (Medtronic) [7]

Wear particle-induced osteolysis, a time dependent process that arises from an inflammatory reaction to wear particles, can result in loosening of an implant. In addition, it is the main cause of hip replacement failure [8, 9] but is not life threatening. Loosening of a cervical implant, and possible migration, however, is a major concern due to the implant being situated adjacent to neural structures. Explant analysis [10] of metal-polymer and metal-metal implants has not shown wear particle-induced osteolysis but there has been some inflammatory response. Further clinical follow-up is required because the results of the explant analysis have been obtained only after short term implantation.

Almost all of the implant designs use tough, relatively rigid metallic materials to promote a stable fixation at the implant-bone interface. However, to varying extents, metals impair the clarity of medical imaging [11]. Obtaining quality images post-operatively is important because examination and confirmation of the decompression of neural structures is often required after CDA. Ability to see the implant and adjacent structures is imperative [11]. A radiolucent polymer implant would not distort MRI and could be an alternative to the conventional materials used in cervical implants. Structural strength, implant-bone interface stability and, in particular, wear resistance must be confirmed to deem a new material acceptable.

Medical grade polyetheretherketone (PEEK) is a polymer that has structural strength and stiffness to provide a stable implant-bone interface [12]. In addition, PEEK is a radiolucent polymer that does not distort MRI images [13]. Initial pin-on-plate wear of PEEK-PEEK pairings has been surprisingly low [14]. Thus, PEEK is a good candidate for an all-polymer cervical disc replacement. The purpose of the present study is to further explore the wear behavior of various PEEK-PEEK pairings, looking for governing principles and tribological limits in order to assess the risk of gross surface damage and/or wear particle-induced osteolysis. Investigation of PEEK is done with the intent to improve the CDA procedure and outcomes.

2.0 LITERATURE REVIEW

2.1. Anatomy and Biomechanics of the Cervical Spine

The present thesis investigates materials for application in the cervical spine. Knowledge of spinal anatomy and loads and motions of the cervical was required for this investigation.

2.1.1. General Anatomy

The spine is composed of both soft and hard tissue. The vertebral bodies compose the hard tissue, and the intervertebral discs, ligaments, cartilage on the facet joint surfaces and spinal cord compose the soft tissue. The role of the vertebrae is to protect the spinal cord, brainstem and neurovascular structures and to provide structural support for the soft tissues. The intervertebral discs, facet joints and ligaments connect the vertebrae to allow for flexibility and mobility of the spine. The discs, ligaments and muscles also provide support to the spine in an upright position and control movement. The ligaments primarily connect the vertebrae and prevent excessive flexion, extension, or rotation. The intervertebral discs transmit bending moments, axial torque and axial loads in addition to absorbing peak loads. They are composed of soft tissue that hold and contain fluid. Muscle activation results in the movement of the cervical spine and originates from nerve impulses that travel through the spinal cord [15]. Facet joints are hinge-like synovial joints with cartilage surfaces that slide over each other and are located on the medial and lateral sides of the posterior aspects of the spine that link the vertebrae together and carry a portion the axial load transmitted through a spinal segment.

The spine is divided into five regions, cervical, thoracic, lumber, sacral and coccyx. Regions of the spine are illustrated in Fig. 2. The vertebrae and connecting soft tissues are very similar within each regions of the spine, with the exceptional of the atlas and axis which are geometrically and functionally unique but are considered part of the cervical spine.

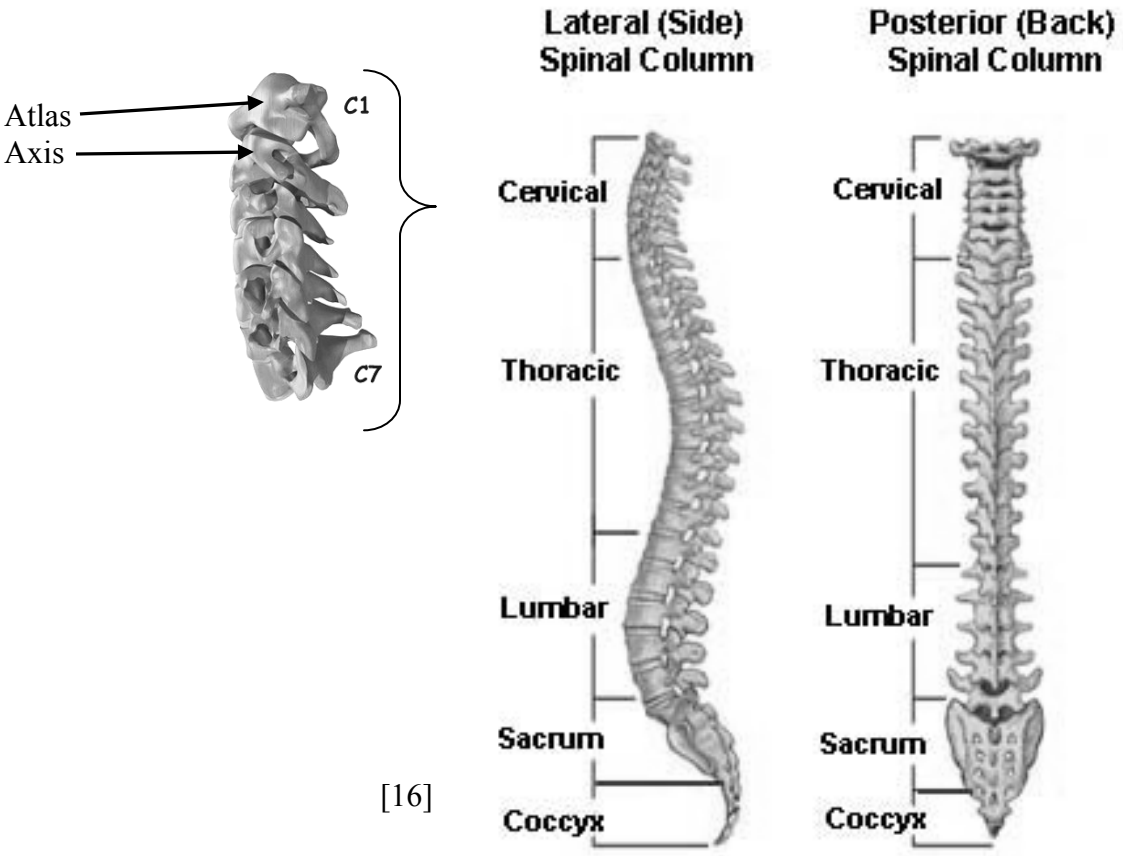

[16]

Fig. 2: Regions of the Spine (Top Left [17]**, Bottom Right** [16]**)**

The cervical spine provides: shock absorption for the brain, support for the skull and the greatest range in motion [15]. The vertebrae adjacent to the skull C1(atlas), and C2(axis) are very different than the rest of the cervical spine. The occiput is a saucer like membrane bone located at the base of the cranium. The atlas forms synovial joints with the occiput. The atlas also forms synovial joints with the axis. The synovial joints formed on both superior and inferior aspects of the atlas are responsible for approximately 40% of cervical flexion-extension and 60% of cervical rotation [15]. The occiput-C1 articulation is mostly responsible for the rotation in the cervical spine. Rotation is aided by the lack of an intervertebral disc between C1 and C2 [15]. The first intervertebral disc occurs between the C2 and C3 vertebral bodies. Generally, vertebrae

C2-C7 are similar in structure and are connected by intervertebral discs and facet joints that facilitate flexion-extension motion and rotation.

2.1.1. Loads and Motions of the Cervical Spine

The cervical spine experiences more motion and lower loads than the thoracic or lumbar spines. Fig. 3 illustrates the motions of the spine.

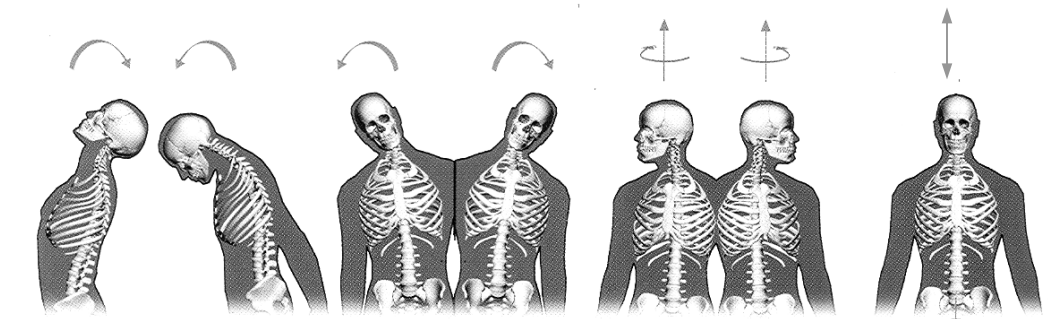

Fig. 3: Motions of the Spine [18]

A cervical spine segment has six degrees of freedom. A 3-D coordinate system with six different forces applied is shown in Fig. 4. The forces consist of anterior/posterior shear (+ F_z), left/right lateral shear (+/- F_x) and compression/distraction (+/- F_y). Translations are generally very small but the cervical spine motion includes a translation in the anterior-posterior or z-direction of a few millimeters. Rotation occurs about each of the axes.

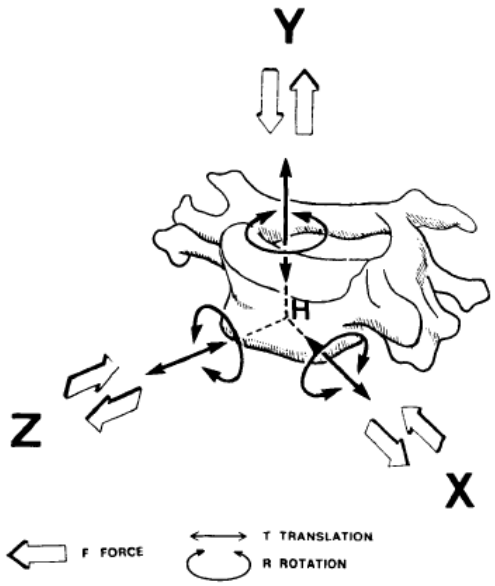

Fig. 4: Cervical Disc Segment: Forces, Translations, Rotations [19]

The loads and motions acting on individual discs in the cervical spine are of particular interest in the present thesis because wear tests of material pairs under consideration for cervical spine disc arthroplasty were performed. Wear is affected by both loads and motions and therefore estimation was required to establish these parameters. Cervical disc implants, including the recent FDA approved Prestige and ProDisc-C, are currently intended for use in the C3-C7 region [20, 21]. The loads and motions estimated to act on these discs are the focus of the present thesis.

There is considerable literature on loads and motions of the C3-C7 section of the spine. Axial rotation, lateral bending and flexion-extension values reported in the literature are presented in Table 1.

Table 1: Motions for C3-C7 segments in the Cervical Spine

Study	Details	Spinal Segment	ROM
AXIAL ROTATION			
IN VIVO			
Dvorak et al. 1987 [22]	*passive*: manually move head through ROM	C5-C6	**14**°
Penning et al. 1987 [23]	N=26 *active*: patient moves head through ROM	C5-C6	**13.8**°

IN VITRO			
Panjabi et al. 2001 [24]	Measured from neutral position to end position at a maximum load of 1.00 Nm (summates both right and left sides)	C4-C5	**6.8**˚
White & Panjabi 1990 [25]		C3-C4 & C4-C5 & C5-C6	**14**˚
White & Panjabi 1978 [26]	One side axial rotation = 12˚	C4-C5	**24.0**˚
FLEXION/EXTENSION			
IN VIVO			
Dvorak et al. 1988 [27]	passive	C5-C6	**23**˚
Dvorak et al. 1993 [28]	passive	C5-C6	**22.6**˚
Dvorak et al. 1988 [27]	active	C5-C6	**20**˚
Penning 1978 [29]	N=20 Young healthy adults	C4-C5 & C5-C6	**20**˚
Ordway et al. 1999 [30]	N=20 , active	C4-C5	**19**˚
Holmes et al. 1994 [31]	N=50, active	C4-C5	**17.9**˚
IN VITRO			
Panjabi et al. 1986 [19]	50 N applied at vertebrae centre Young healthy adult cadaveric spines	C5-C6	**9.9**˚
White & Panjabi 1990 [25]		C4-C5 & C5-C6	**20**˚
White & Panjabi 1978 [26]		C5-C6	**17**˚
Panjabi et al. 2001 [24]	Measured from neutral position to the end position at a maximum load of 1.00 Nm (sum of both right and left sides)	C5-C6	**9.9**˚
White & Panjabi 1990 [25]		C3-C4 & C4-C5 & C5-C6	**14**˚

LATERAL BENDING			
IN VIVO			
Penning 1978 [29]	active	C5-C6	**12**°
IN VITRO			
Panjabi et al. 2001 [24]	Measured from neutral position to the end position at a maximum load of 1.00 Nm (sum of both right and left sides)	C4-C5	**9.3**°
White & Panjabi 1990 [25]		C3-C4 &C4-C5	**22**°
White & Panjabi 1978 [26]		C3-C4 &C4-C5	**22**°

The variation of results reported for each study is substantial in some instances. The present author is not clear why certain studies, in some cases performed by the same individuals, i.e. Panjabi, report different results for the same motion.

Fortunately, there are two governing bodies involved in wear testing, the International Standard Organization (ISO) and the American Society for Testing and Materials (ASTM). An ISO standard (ISO 18192-1) [32] provides parameters for intervertebral spinal disc prostheses wear testing that include values for flexion/extension, lateral bending, axial rotation and axial load [32, 33]. Also, an ASTM standard (ASTM F 2423-05) [34] provides values for axial preload, flexion/extension, lateral bending and rotation. The parameters chosen for the standard are selected from studies available in literature at the time the standards were created. However, the standards seem to determine typical conditions and then moderately increase both loads and motions to create a "worst-case" scenario. Thus, the citations listed for the ISO and ASTM standards do not include studies reporting extreme conditions. An excessive load or motion may only occur occasionally but still cause enough damage to accelerate the wear of an implant. The standard states clearly that it is not designed with the intention of locating the point at which the material experiences significant surface damage, thus forth referred to in the present thesis as a failure point [32, 34]. The length of the wear test must be 10,000,000 cycles (10Mc) according to ASTM and ISO. The load and motion patterns that act on the C3-C7 section of the spine are generally considered to be

cyclic and the number of cycles applied in one year has been estimated to vary from 0.125-0.317 Mc [35]. The accuracy and precision of these estimates is not known [35].

The ISO and ASTM standards for range of motion (ROM) of a single cervical segment are summarized in Table 2.

Table 2: ISO & ASTM Standards for Loads and Motion

ISO 18192-1 [21]	
Load	100 N, sinusoidal – amplitude = 50 N
Flexion/Extension (FE)	15˚
Lateral Bending (LB)	12˚
Axial Rotation (AR)	8˚
Frequency	1 Hz
Duration	10^7 cycles
ASTM 2423-05 [23]	
Load	100 N – constant
Flexion/Extension (FE)	15˚
Lateral Bending (LB)	12˚
Axial Rotation (AR)	12˚
Frequency	< 2 Hz
Duration	10^7 cycles

Unlike the lumbar region of the spine, there are very few studies that estimate in vivo loads on the disc of the C3-C7 section of the spine. A study performed by Hattorie et al. [36] in 1981 gathered in vivo intradiscal pressures for various positions of the head during daily living activity. The nucleus, the central region of the intervertebral disc, contains tissue that retains fluid. This fluid resists compression. Hydrostatic pressure of the nucleus is reported to be linearly related to the forces acting on the spine at that level. Various studies measure pressure both in vitro and in vivo to obtain forces acting on the intervertebral disc. Those pressures were converted to loads using the relationships given by Nachemson [37] between intradiscal pressure and applied compressive force. These data values from Hattorie et al [36] and Nachemson [37] were presented by Kurtz [18] in Fig. 5 and give the intradiscal pressure with the corresponding applied axial load in parentheses. Hattorie's pressure measurements do not differentiate between disc levels.

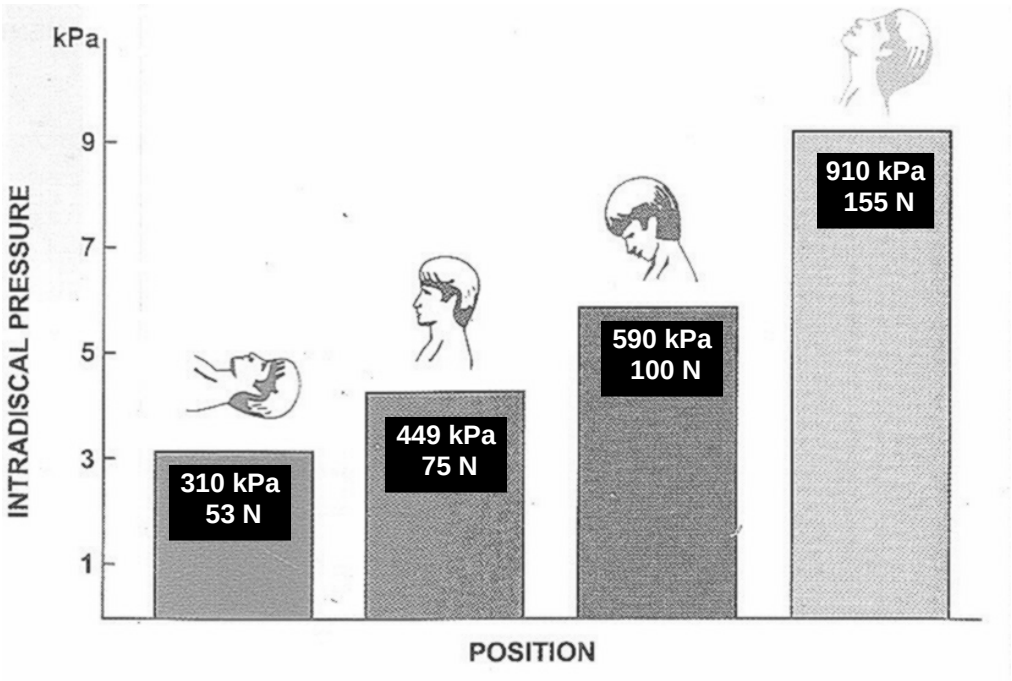

Fig. 5: Cervical Intradiscal Pressures and Axial Loads [12, 18]

The standard upright position of the head imposes 75 N on the each level of the cervical spine according to Hattori et al. [36]. Moroney et al. [38] supported this statement by suggesting a very similar value of 73.6 N and said it represented the weight of the head.

Moroney et al. [39] reported a C4 compressive force of 1,164 N with a standard deviation of 494 for the extension motion. Moroney et al. recorded compressive force values of 578 N for flexion motion. His study involved 14 patients sitting upright in a chair, with their upper bodies immobilized, asked to push their heads against a load cell at maximum voluntary strength.

Cripton et al. [40] measured intradiscal pressures for cervical discs under applied axial loads up to 800N. The relationship between disc pressure and applied force were found to be linear. Extrapolation of Cripton et al's data gives about 3.75 MPa for an axial load of 1000 N. The relevance of these findings is the confirmation of a relationship between intradiscal pressure and axial compressive loads.

The anterior-posterior translation distance between the C5-C6 vertebrae under a 50 N compressive load has been measured as 3.5 mm by Panjabi et al. in 1986 [19].

Moroney et al. measures [38] a total translation of 0.52 mm under a 19 N compressive load. Both studies are in vitro and are measured around the same anatomic point, the centre of the vertebral body.

2.1.2. Intervertebral Disc

The present thesis investigates material pairs for cervical spinal disc arthroplasty. Since spinal discs are to be replaced, it is considered useful to investigate this tissue in some detail. The intervertebral cervical discs, located between the vertebral bodies in the spine, are roughly elliptical in shape and constitute one third of the total height of the spinal column. Each disc is composed of three main components labeled in Fig. 6. These components are the nucleus pulposus, annular fibers and the cartilaginous endplates above and below the disc, adjacent to the vertebrae [41].

The centre of the intervertebral disc, the nucleus pulposus, is a translucent, gelatinous, semi-solid structure composed of a hydrated gel containing proteoglycans and collagen. The water content in the nucleus is a significant indicator of disc degeneration in the cervical spine because its concentration is highest at birth, 70%-90%, and decreases with age [41]. The amount of water in the tissue determines its ability to pressurize and subsequently absorb and transfer compressive loads [18].
The negatively charged prototgylcans in the nucleus repel each other and push apart to create a suction effect that pulls in water carrying positive ions. The water forms part of the nucleus and the positive ions give an electroneutrality condition in the nucleus. If axial forces are applied to the nucleus, water is squeezed outwards along with positive ions and the remaining fixed negatively charged ions repel each other and resist compression. The collagen is composed of helically organized proteins bundled into fibers that entrap and hold the proteoglycan gel thus preventing it from being extruded under axial loading. Thus, tensile forces in the collagen fibers help the composite nucleus resist axial compressive forces. Proteogylcans and collagen are both classified as type II collagen, which makes up 80% of the collagen found in the nucleus pulposus [42]. This type of collagen is stronger in tension than type I collagen fibrils [15]. Cartilage, another compressive load-bearing tissue found in the body, is also composed of type II collagen, preteoglycan gels and water [43].

The annulus fibrosus has a strong structure designed to provide most of the resistance to the lateral extrusion of the nucleus while maintaining some flexibility [15]. It consists of fibrocatilage in a series of concentric laminated bands that surround the nucleus. The helical fibers seen in Fig. 6 are oriented 30˚ to the disc "plane" and 120˚ to each other and run the same direction on each band and the reverse direction every two bands. The annulus is attached directly to the osseous tissue of the outer surface of the vertebra in the more peripheral area and to the cartilaginous endplates in the inner zone that form a transition to the osseous tissue of the more central region of the vertebra [25].

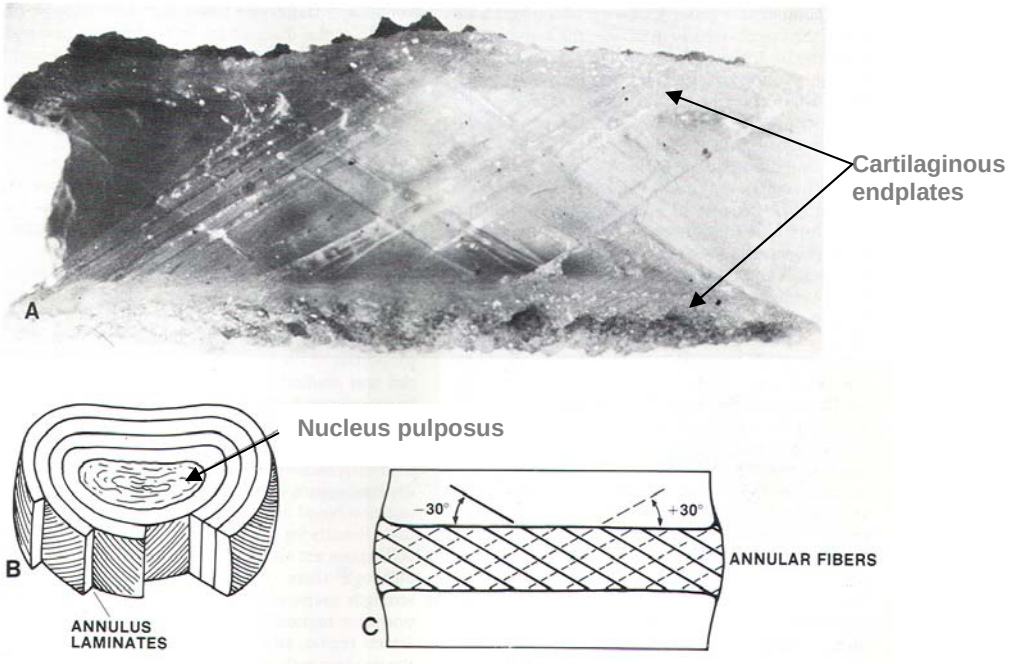

Fig. 6: Intervertebral Disc [25]

The decreased water content occurring with age within the nucleus plays a major role in the deterioration of the annulus. The inability of the nucleus to pressurize results in compressive rather than tensile forces acting on the annulus and thus the annulus begins to collapse inward rather than bulging outward in tension. The layers of the annulus delaminate and may tear or crack [18]. The change in the loading and deflection of the annulus causes the disc to lose height. This situation is made worse by the nucleus being extruded through a damaged zone in the annulus. The result can be pinched nerves or bending of the spinal cord giving a loss of neuro-muscular function and pain. The cartilaginous endplates connect the nucleus pulposus and annulus fibrosus to the

vertebrae [25]. Calcification of the cartilage in the endplate gives a barrier to fluid extrusion from the nucleus but also prevents the delivery of glucose and oxygen from the vertebral body to the intervertebral disc and inhibits the removal of lactic acid [18].

Four facet joint surfaces are on each vertebra, two on the upper side and two on the lower side. They articulate with corresponding surfaces on the vertebrae above and the vertebra below. Facet joints are responsible for controlling the flexion-extension, lateral bending and axial rotation motions that occurs in the cervical spine. They contribute to overall stability and are reported to resist 16% of the axial forces and the majority of the lateral or shear forces acting on the spine [15]. The cervical spine facet joints, illustrated in Fig. 7, are oriented at 45˚ to the "plane" of the disc [15].

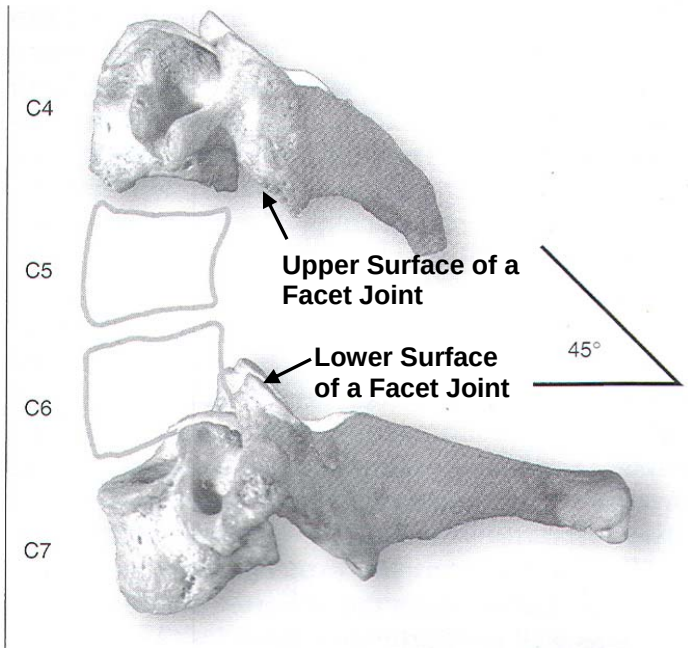

Fig. 7: Facet Joints[15]

2.2. Basic Tribology

The term tribology first emerged in the mid 1960's and is derived from the Greek words "tribo" meaning rub and "logia" meaning principal or logic. Tribology is defined as "the science and technology of interacting surfaces in relative motion". It is most often associated with the study and applications of the principals of friction, lubrication

and wear [44]. The current thesis examines tribology involving load, motion, lubrication, surface topography, microstructure, friction, wear and mechanisms of wear. An understanding of the tribology allows some interpretation of the wear of materials proposed for application in cervical disc arthroplasty.

2.2.1. Surface Topography

No surface is perfectly smooth; roughness exists at some level of magnification, usually as a result of material production techniques and underlying characteristics of a material [44]. Worn surface conditions can sometimes be compared with original surfaces to qualitatively measure the amount of wear. When polymeric material pairs are articulated against each other, the initial spike in wear often results in "smoothing". However, this is not always the case and surfaces may get rougher upon wear.

There are very few studies available in the literature that have used microscopy to examine the wear of PEEK. Pin-on-plate testing of commercial 20 wt% carbon fiber based polyetheretherketone (CFR PEEK) [45] against a 100Cr6 steel disc was performed. The test was completed without lubricant at 150˚C using a plane-ended pin of 4 mm diameter, a contact stress of 3 MPa (load 3.77 N) and a constant speed of 1 m/s. The composite surface was polished prior to testing. Fig. 8 reveals the damage.

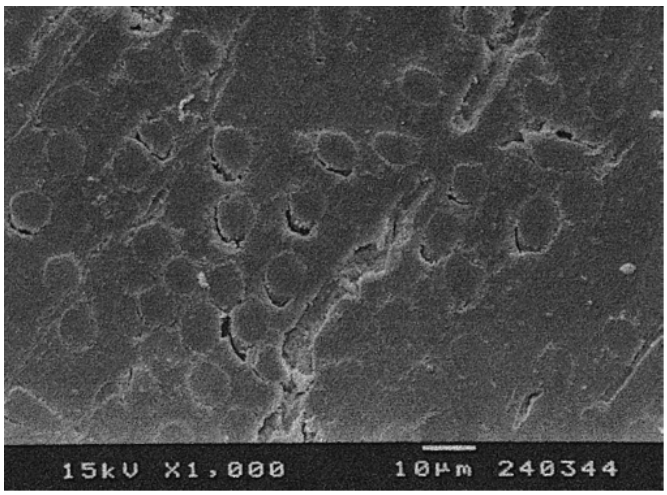

Fig. 8: A worn surface of 20wt% commercial grade PAN CFR PEEK pin after articulating against a 100Cr6 steel plate [45]

Another study [46] examined wear damage to medical grade PEEK OPT and 30wt% PAN-CFR PEEK using a pin-on-plate apparatus with reciprocating motion at a frequency of 1 Hz. These two versions of PEEK pins were worn against steel plate using distilled water held at 37˚C as lubricant. Two types of conditions were exerted on the materials, normal and severe. Normal conditions included 3 MPa contact stress and 20 mm/s sliding speed. Severe test conditions include 5 MPa contact stress and 10 m/s sliding speed. Fig. 9 A, normal conditions, reveals abrasive scratches and fold formations. Fig. 9 B, severe conditions, reveals abrasive scratches, fold formations, polishing and cavities created from material plucking [46]. The severe conditions appear to polish the surface and eventually create a cavity as the material experiences sub-surface fatigue.

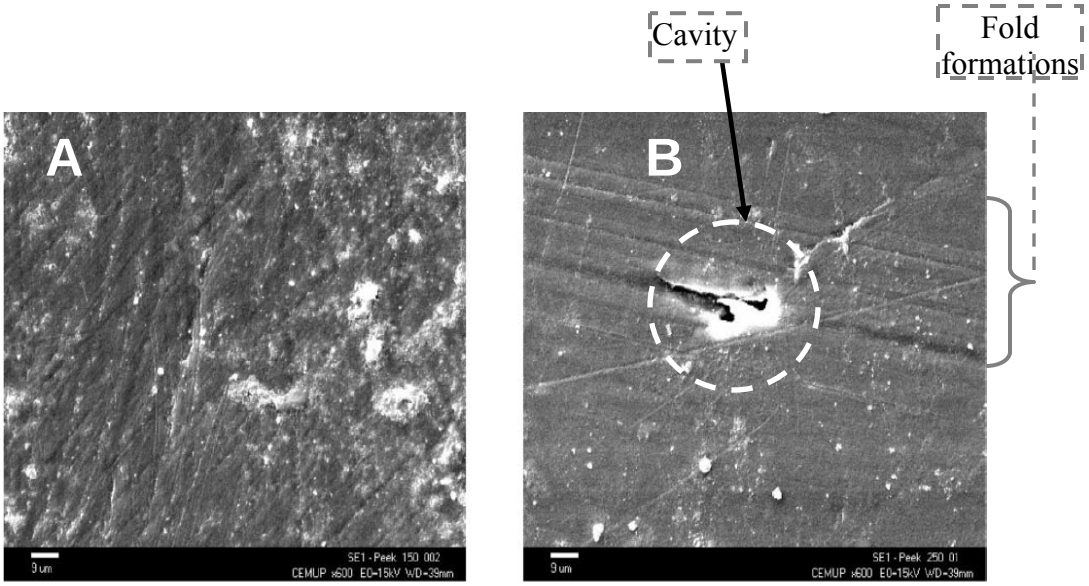

Fig. 9A&B: Micrographs of PEEK OPT - Normal vs. Severe Test Conditions [45, 46]

Low loads produced several cracks and cavities around the carbon fibers of the CFR PEEK. Fig. 11 is a micrograph of the CFR PEEK after being tested under severe conditions. The damage appears to be less severe than the PEEK OPT shown in Fig. 9 B [46]. The CFR displays roughness on the surface in Fig. 10. This can be compared to PEEK OPT shown in Fig 9 B, that appears polished and shows a large cavity.

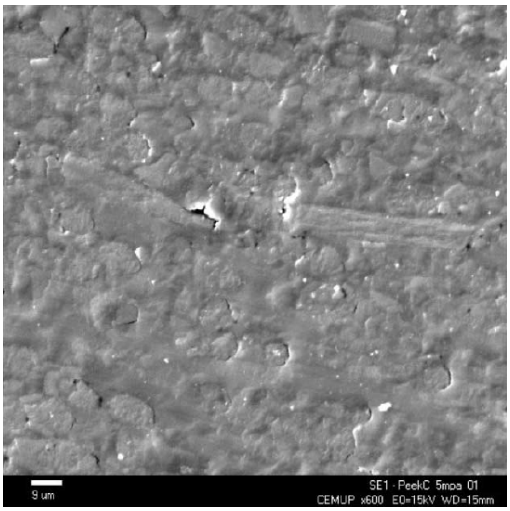

Fig. 10: Micrograph of 30wt% PAN CFR PEEK - Severe test conditions [46]

2.2.2. Friction

The friction force is the tangential resisting force encountered when bodies in contact move tangentially over one another [44]. Often the ratio of friction force (F_f) to normal force (F) is constant over a range of conditions [44] and this ratio is known as the coefficient of friction (μ) as shown in Eqn. 1.

$$\mu = \frac{F_f}{F}$$

Eqn. 1: Definition of the Coefficient of Friction [47]

2.2.3. Lubrication

Conventionally, fluid lubricants are used to minimize friction and reduce wear at the interface of materials [48]. Shoulder, hip and knee joints all contain synovial fluid and lubricant is available in vivo for implants in these areas [18]. Understanding of the lubricant available within the cervical spine is important. Currently the type and amount of lubricant available at the fibrocartilaginous cervical disc joint is unknown [49]. There are various regimes of self-acting (without the use of an external pump) fluid film lubrication shown in Fig. 11. The parameter (h/σ) is the mean film thickness over the composite root-mean-square of surface heights of the two surfaces [48] and it is often

used to determine the effectiveness of a fluid film in separating bearing surfaces**.**

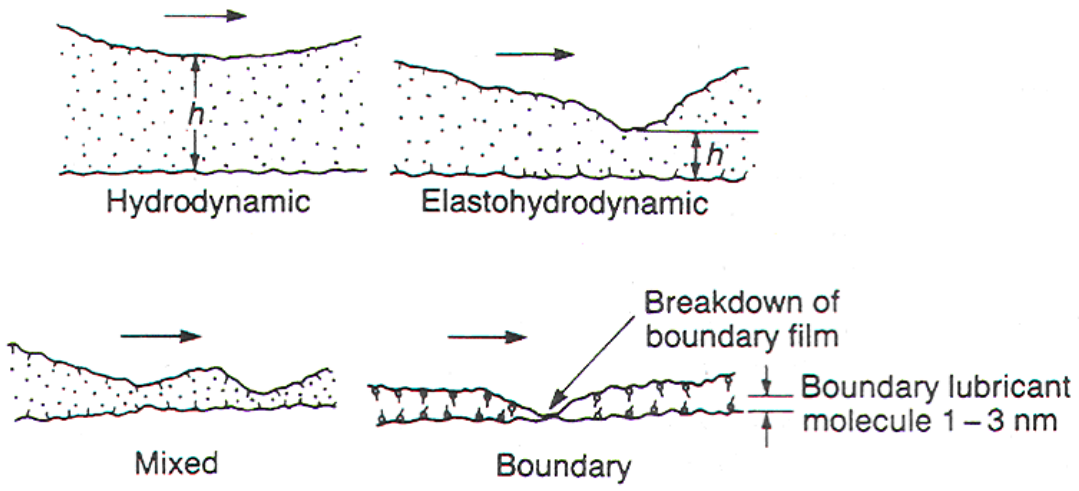

Fig. 11: Types of Lubrication [48]

The top left illustration of Fig. 11, titled hydrodynamic, is often referred to as fluid-film or thick-film lubrication with a fluid film thickness ranging from typically 5 - 500 μm thicker than the height of the irregularities on the bearing surface. A layer of fluid is pulled through a gap of decreasing thickness between two interacting surfaces and generates a hydrodynamic pressure that supports the load. The lubricant film prevents contact between asperities and can result in friction coefficients as low as 0.001. This value can be even lower in air lubricated bearings.

The top right lubrication region of Fig. 11, elastohydrodynamic, is similar to hydrodynamic with a fluid film thickness ranging from 0.5 - 5 μm. The film pressure is high enough to cause the contacting materials to experience elastic deformation and increases the viscosity of the lubricant. These two influences act to increase fluid film thickness but they may not be significant enough to avoid asperity contact. In the event of asperity contact, the lubricant is described as mixed. .

The bottom left illustration of Fig. 11 is called mixed lubrication. It is referred to as mixed because it represents the transition between elastohydrodynamic and boundary lubricant regimes. There is frequent contact between the tips of the asperities on each surface; however, a portion of the contacting surface is supported by a partial fluid film.

Boundary lubrication, shown in the bottom right illustration of Fig. 11, is a condition in which the surfaces are so close together that surface interaction between chemically adherent molecular films of lubricant and solid asperities tips dominate the contact. The transition to boundary lubrication can be caused by increased load, decreased speed or reduced lubricant viscosity. The coefficient of friction can increase quickly and can reach levels of as high as 0.1 or much higher. Boundary lubrication occurs at locations starved of lubricant. Friction coefficient levels can be higher than 1 in the absence of boundary lubricants. Boundary lubrication is experienced at the onset of motion of preloaded contacting surfaces. The failure mechanism is adhesive in boundary lubrication conditions [48].

2.2.4. Wear

Wear is progressive damage on a surface resulting in material loss from one or both surfaces [44, 50]. The material loss is most often quantified by the volume of the worn materials in mm^3 or the mass of the worn material in grams [51] . Assuming the properties of the materials in contact remain the same, wear is affected by changes in load, speed, lubrication and environmental conditions, surface geometry and topography, contact stress and "third" body wear to name a few [50]. Wear is sometimes described as a material property. However, it is the response to the entire tribological system.

Energy losses in the forms of heat, noise, fracture and/or deformation are results of friction forces. Wear occurs depending on how the material deals with the frictional force and the energy expended at its surface. High local temperatures play a large role in polishing. Melting of the polymer at the points of sliding contact occurs as a result of frictional heat rising to the melting point of the material. The melted polymer is smeared onto cooler areas, fills crevices adjacent to it and quickly solidifies creating a polished appearance. The sliding speed is relevant in the sense that it is directly related to the energy dissipation rate and thus the surface temperature [52]. The speed is relevant in the sense that if the cycle time were too low, the material would never reach high enough temperature to deform. The speed affects the ability of the lubricant to cool the interface [52].

Polymers generally have low thermal conductivities and sliding solids with poor thermal conducting properties retain frictional heat at the interface which often contributes to the surface damage [52]. Elevated temperatures caused from frictional heat can decrease the mechanical properties of a material and contribute to failure. This mechanism of failure, fatigue, is dependent on friction. Deformation occurs due to external friction at separate points on the surface which can lead to abrasive wear in the forms of fracture and tearing. Deformation is dependent on sliding velocity, pressure, temperature, surface geometry and material properties [51].

There are four basic mechanisms of wear: adhesive, abrasive, surface fatigue and corrosion [50]. Polymers are unaffected by many corrosive environments, however they often have the potential to react in certain fluids and swell with degradation in mechanical properties. This can make the polymer susceptible to wear [48]. Polymer wear is conventionally divided into adhesive, abrasive(micro-cutting) and fatigue [48, 51].

Adhesive wear is a result of the chemical bonding of asperity tips between two articulating surfaces. These bonded tips are broken as the materials sliding against one another and form wear debris. The debris remains in the interface, most likely causing further wear by third body abrasion, or attaches to one of the two articulating surfaces. [44, 48]. A scuffed like appearance may occur on either wear surface in the event of polymer-on-polymer material combinations, lubrication starvation or high temperature/sliding speed. The scuffing is a result of a breakdown of lubricant film and subsequent onset of adhesive wear [44].

Abrasive wear consists of a hard surface, or harder particle ripping up a softer surface. Abrasion can, thus, be classified as either two or three body abrasion: two-body abrasion occurs when wear on one surface is a direct result of the opposing surface. Three-body abrasion occurs when wear is caused by particles, most likely wear debris, however they can be foreign particles, caught between the two articulating surfaces [44]. Plowing, micro-cutting and wedge formation are methods of material removal from the surface caused by plastic deformation during abrasion.

Surface fatigue wear, either surface or sub-surface is caused by repetitive moving contact, i.e. sliding. Cracks can form on the surface or below it as a result of constant

loading and unloading of the surface. The material can reach a threshold where the cracks cause fragmentation of the surface, and eventual pits or cavities [48]. Pits can also be caused by adhesion, abrasion and corrosion. It is possible for surface fatigue to occur with continuous fluid film formed between surfaces as a result of reciprocating motion, without direct surface contact. Hard polymers such as thermoset polymers sliding against smooth surfaces can be significantly affected by the fatigue mechanism [48]

The process of wear, shown in Fig. 13, often involves a run-in period with a much higher wear rate than the subsequent region of steady-state wear. The steady state wear rate is low and ends with the onset of fatigue mechanisms [44]. Fig. 12 represents the behaviour of materials under relatively normal conditions with a constant load. Fig. 13, on the other hand, highlights wear of metallic materials that are generally linear until the load reaches a certain threshold for the material after which fractures occurs at the surface with detachment of large wear particles and the wear rate increases suddenly to a severe level. The dip in wear shown in Fig. 13 is attributed to work hardening that makes the metallic materials more wear resistant..

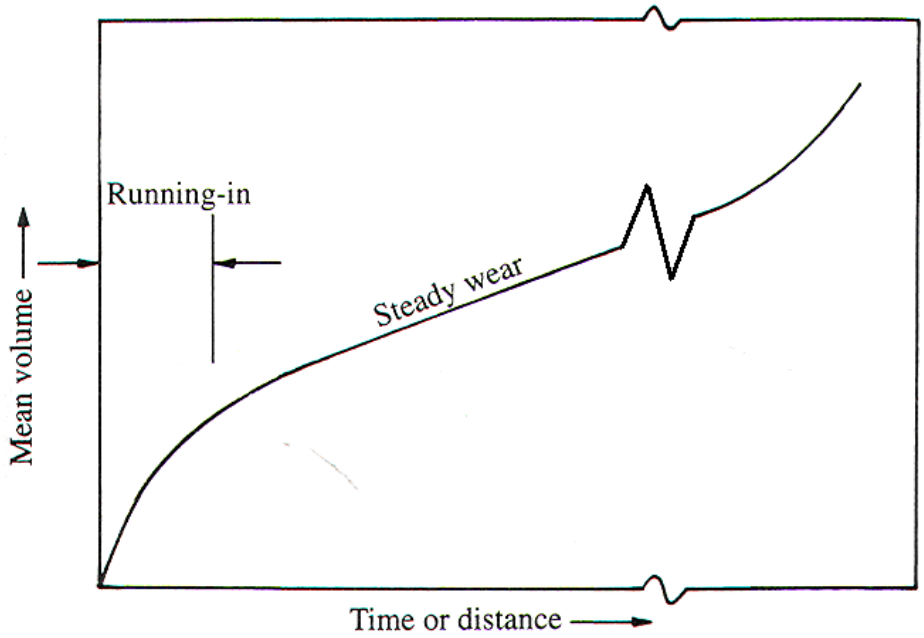

Fig. 12: Typical Wear Behaviour [44]

The effect of load on wear behaviour that is shown in Fig. 13 in the first transition can also occur in polymeric materials. Increasing load can result in a rapid transition from mild wear to severe wear [50]. This pattern of wear behaviour is evident in the findings of the current thesis and will be shown in the following chapters.

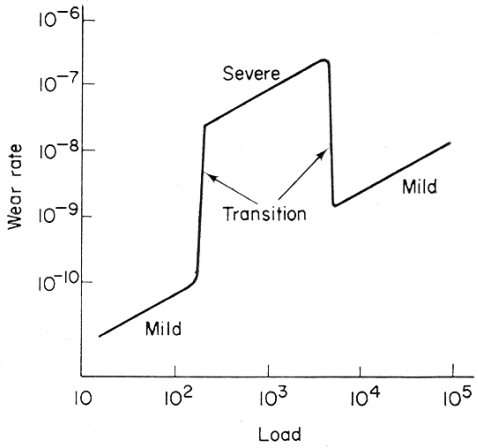

Gradual increase in load does not produce a gradual increase in wear rate. The transition for mild to severe wear is sudden once the load reaches a threshold for the material.

Fig. 13: The Transition Phenomena in Wear [50]

As mentioned previously, sliding interface temperature is a function of compressive force and sliding velocity. Once the two parameters surpass the limit for the material, the wear rate increases rapidly, due to the polymer melting at the interface which can occur at ambient temperatures [48].

Archard's Law proposed in 1953, shown in Eqn. 2, suggests that wear is mostly proportional to the applied load F(N) and sliding distance x(mm) [44]. The wear factor, k, is the proportionality constant in ($mm^3\ N^{-1}\ m^{-1}$), and V is volumetric wear in mm^3 [48].

$$k = \frac{V}{F \bullet x}$$

Eqn. 2: Archard's Law [44]

Wear factors are a useful tool used to compare studies with varying loads and sliding distances. However, there are many parameters that are not represented in Eqn. 2 that influence the wear including material properties, sliding speeds, surface topography and lubricant properties. These physical processes and contact parameters can result in a wear factor that may not be constant for a particular material. In spite of the above

mentioned facts, wear factors are often assumed to be constant and used to compare the same material with different geometries, loads and motions. Archard's law can be used for an approximation of wear, but it is not used exclusively for quantitative measurements in the present thesis.

Polymeric materials introduce an additional level of complexity in the area of wear measurement. Fluid absorption is continual with most polymers, with the exception of rubber, and without appropriate control mechanisms, has the potential to skew wear results. Fluid is absorbed into the polymer as the wear test progresses and the absorption rate is dependent on lubricant, temperature, and load. Wear is generally measured by weight loss and fluid uptake will mask wear by increasing the overall value of the weight measurement. Soaking the polymer while under load but not exposed to relative motion, known as "load soak", is conventionally used to determine the affect of fluid absorption. The intent is to maintain identical conditions with the exception of motion in both the wear test apparatus and load soak apparatus. ASTM Standard F 2025 [34] specifies a particular method for wear calculation. This method can be found in Appendix A. The average weight gain of all soak control specimens is subtracted from the weight measurement of each wear test sample for each interval of testing. The original weight is subtracted from the initial weight of the specimens. The final change in weight is divided by the density to give a volumetric wear value. The volumetric wear value is used in Eqn. 2 to calculate wear factors.

2.3. Surgery for Damaged Cervical Discs

2.3.1. Fusion

Spinal fusion, the fusion of two or more vertebrae to form a single rigid unit, is the standard treatment for severe degenerative disc disease (DDD) and disc herniation today. Degenerative disc disease and cervical disc herniation result in tingling and clumsiness of the hands together with gait disturbance. Disc herniation also causes problems at, or near, the root of the nerve which runs along the spine and may result in shoulder and arm pain [1]. The goal of fusion surgery is to relieve the cervical root and spinal cord compression. However, fusion alters the kinematics of the spine and places

additional stresses on adjacent vertebrae. Increased biomechanical stresses accelerate degenerative changes at adjacent levels [53]. According to Ishihara et al. [54], the chance of having no adjacent disc degeneration after spinal fusion surgery is 89% at 5 years, 84% at 10 years and 67% at 17 years. Therefore, a significant number of spinal fusion patients are in need of additional surgeries due to adjacent level degeneration. Fusion surgery requires iliac crest harvest, i.e. bone material taken from the pelvis to be used for bone grafts in the surgery. Auerbach et al. [53] stated that post-operative complications developed in 20% of patients and included chronic pain, infection, and pelvic fractures at the donor site. Nevertheless, fusion is still the primary choice of many surgeries as the long term clinical performance of alternatives is unknown.

2.3.2. Cervical Disc Arthroplasty

Cervical disc arthroplasty (CDA) is an attractive alternative to cervical disc fusion and appeals to younger, active patients who require a 30-50 year life span for a spinal implant. This would equal 37.5 – 62.5 Mc experienced by the spine in a lifetime based on a study [55] that found the spine underwent approximately 125,000 significant bends per year. Whereas knee and hip joints maintain stability from ligamentous structures, the discs in the spine are themselves responsible for maintaining some of the stability [56]. The goal of CDA is to relieve disc compression and, hence, the pain, by restoring disc height and segmental motion. This preserves the kinematics [56] of the spine at both operative and adjacent levels and reduces the chance of degenerative disease at adjacent levels. There are two cervical disc implants approved by the Food and Drug Administration (FDA) in the United States today. The Prestige® (Medtronic Inc, Memphis, TN, USA) was approved in July, 2007 and the The ProDisc-C® (Snythes, Paoli, PA, USA) was approved in December, 2007. The Bryan® (Medtronic Inc, Memphis, TN, USA) and the PCM® (Cervitech, Rockaway, NJ, USA) are currently at the advanced stage of the FDA approval process.

2.3.2.1. Implant Design Principles

Articulation of the implant is a crucial component of the design. The way in which the implant articulates can determine the stroke length and the amount of crossing-

path motion of the two surfaces rubbing against each other. The stroke length and the crossing-path motion have a direct effect on wear [44].

The interface between the bone and the implant is a design challenge that has been attacked from various angles. The intervertebral disc is firmly attached to the vertebrae in vivo and it is the goal of the implant endplate to do the same. Temporary fixation modes such as the rails shown in Fig. 14 and 15, are often used. However, the intent of the porous endplate and other end plate coatings is to initiate permanent, long term bone ingrowth, meaning the bone actually grows into the end plate and reduces movement between the end plate and the vertebrae. Micromotion, movement between an implant and the bone can introduce debris particles into the environment and potentially accelerate wear and cause pain and gross loosening of the implant.

A general issue with implant design is "end of motion stopping". Certain implants, for example the Prestige® LP shown in Fig. 15 and the Bryan® discussed in the following section, give such a large range of motion that, with good surgical positioning, the spine itself will stop the motion of the implant. Other implants invite metal-metal or metal-polymer contact. Both can be disastrous as impact on the surface on the implant could cause fracture or release of material into the system. Wear could potentially increase rapidly if loose debris was to get caught between the articulating surfaces

There are many more implants in the early design stages and some of them are available in Europe. The implants reviewed below are examples of different articulating biomaterials, fixation modes and bearing designs. We are concerned with implant designs in the current thesis because a new material, like the one we are investigating, may require a new implant design.

2.3.2.2. Implants

The idea behind the Prestige® was first conceived in 1989 by Brian Cummins [57]. The first clinical trial began in 1991 and consisted of a 316 Stainless Steel (SS) joint that allowed minimal translation [57]. The second generation of the implant, designed by Medtronic Inc., the Prestige®I, converted the ball and socket design to a ball and trough [58]. Coupling translation with the flexion-extension motion resulted in a closer replication of the motion experienced by the cervical disc in vivo [59]

The third generation of the Prestige®, the Prestige®II was designed in 1999 and included grit blasted end-plates to promote bone ingrowth and attempt to eliminate the possibility of implant loosening [59]. In 2002, the implant was further redesigned and renamed the Prestige® STLP. Primary fixation was achieved using parallel rails on each side, and the back surface was roughed to provide secondary fixation. The final modification of the implant, renamed the Prestige®LP, shown in Fig. 14, changed the material of the bearing surface. Stainless steel is not MRI compatible, so the new implant was made from a composite consisting of titanium carbide (TiC) and Ti6A14V metal matrix [18].

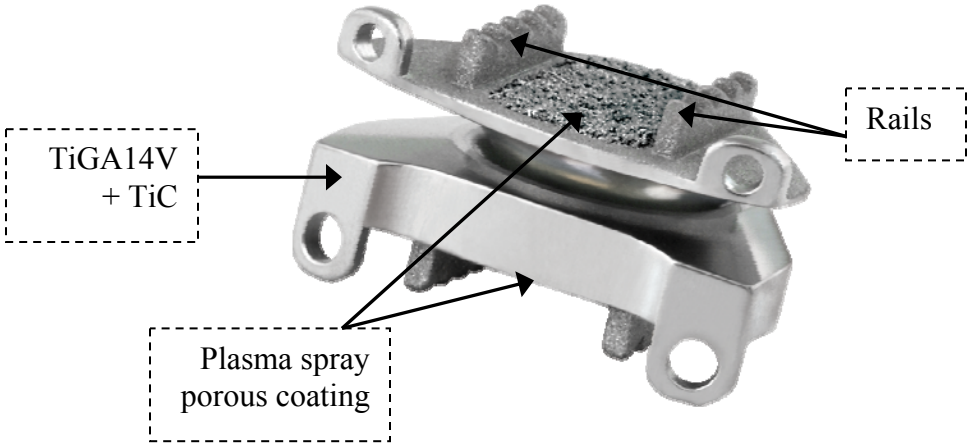

Fig. 14: Prestige®LP (Medtronic Spinal a Biologics) [6]

The ProDisc-C®, shown in Fig. 15, is a cervical disc implant produced by Synthes that utilizes a metal-polymer ball-and-socket bearing design. The metal endplates are made from a cobalt chromium alloy (Co-Cr) and the polymer insert is made from ultra-high molecular weight polyethylene (UHMWPE). There are two central rails on the endplates for immediate fixation to the vertebrae. Then bone ingrowth is promoted by a plasma sprayed titanium coating on all surfaces in contact with the bone [60]. Recent studies [61] on the ProDisc-C prothesis (Synthes, Paoli, PA) confirmed the increased motion in comparison to fusion patients 12 months after surgery.

Fig. 15: ProDisc-C® (Synthes, Paoli, PA) [62]

The Bryan®, unlike the Prestige®, ProDisc-C® and PCM® is a single component device rather than the standard two piece implant. Vincent Bryan Jr. invented this device in the early 1990's [4]. The Bryan® is composed of two titanium endplates and a polyurethane core [63]. A polyurethane sheath surrounds the nucleus and is attached to the shells with titanium wire. The polyurethane nucleus is seated between two titanium shells and moves with respect to them so that some sliding occurs. The titanium shells have inward facing posts that fit into flared holes in the nucleus. This design controls range of motion and ensures no hard stops occur at extreme ranges of motion and maximum translation. A soft stop occurring by squeezing the polyurethane could lead to fatigue problems unless the contact stresses are low. It is possible that the stresses are low enough in the cervical spine and extreme motions are infrequent enough, that this might not be a problem. The shell posts are not in contact with the nucleus during normal motion [64]. A cross-sectional view of the implant is shown in Fig. 16. The device is somewhat unconstrained and has a variable instantaneous axis of rotation [65]. The polymer sheath that surrounds the hyperelastic core, shown in Fig. 16, is filled with saline solution during implantation to lubricate the bearing surfaces. The sheath is designed to contain any wear debris and reduce soft tissue growth in and around the bearing interface. The core and sheath are made of two different resins of polyurethane. The softer resin is used for the sheath and the stiffer resin is used for the core [18]. Fixation of the Bryan® to the vertebral bodies is achieved though convex porous ingrowth surfaces on shaped titanium plates [4].

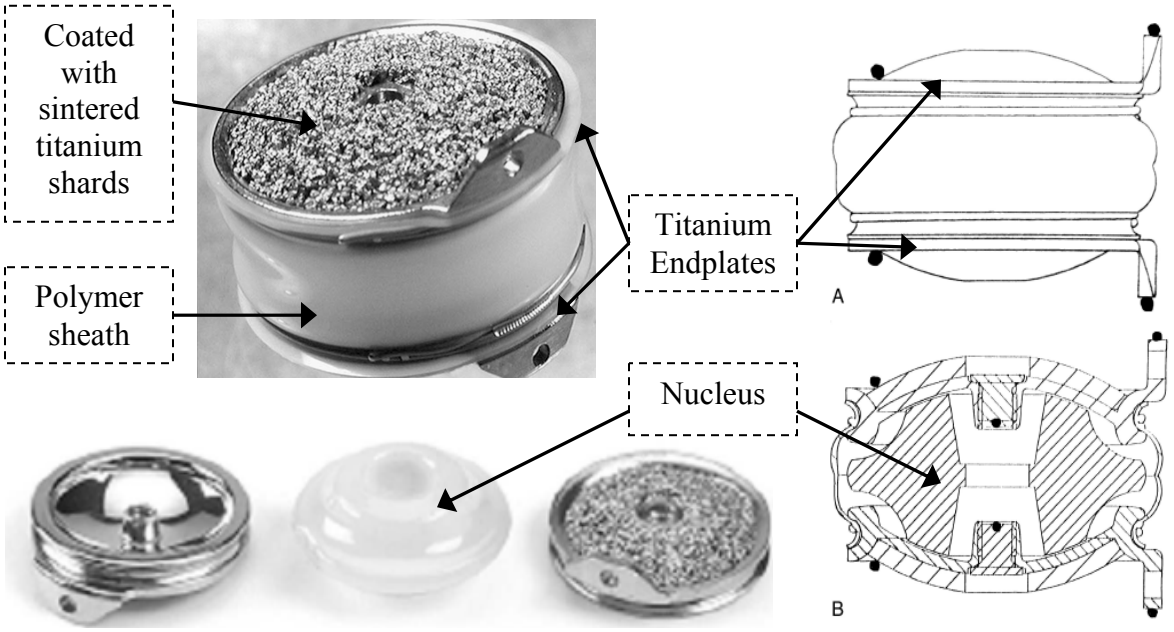

Fig. 16: Bryan® Cervical Disc Implant (Medtronic Sofamor Danek) [64][66]

The Bryan® began clinical trials in the United States in 2002, while European trials began in 2000 [2]. After two years of implantation, favorable outcomes are seen with the Bryan cervical disc replacement versus anterior cervical fusion. The Bryan® is in the advanced stages of the FDA approval process.

The porous coated motion (PCM®) cervical disc replacement was first invented by Paul C. McAfee and has been improved over the years by Helmut Link and Arnold Keller [67]. The PCM®, shown below in Fig. 17, is produced by Cervitech and is manufactured from Co-Cr alloy and UHMWPE. The minimally constrained bearing design consists of a smooth, concave, Co-Cr top endplate interfaced with a large radius convex UHMWPE core. The core is fixed to the bottom endplate restricting all motion at that interface [18]. The top plate glides around and across the core to accommodate the motion of the natural cervical spine. The PCM® is a surface replacement that depends on surrounding muscles and ligaments for proper kinematics [67]. Early fixation of the cervical implant is established from the serrated profile on the endplates. Bone ingrowth is encouraged by two ultra-thin layers of titanium with electrochemically coated Calcium Phospate known in industry as TiCaP® [67].

Fig. 17: PCM® (Cervitech®, Rockway, NJ) [68, 68]

2.3.2.3. Biomechanical and Wear Tests

Prior to implantation in humans, implants must undergo biomechanical and wear testing to assess the risk of failure. Wear tests are all different and thus comparison is approximate.

The FDA produced a "Summary of Safety and Effectiveness Data" report in 2006 [21], at the time of the approval of the Prestige®. Results, shown in Table 3, were reported for wear tests. Two groups of three specimens were tested using simulators in 25% bovine serum held at 37˚C. The two groups differ in the order of application of 10 Mc of flexion-extension (FE) and 5 Mc lateral bending combined with axial rotation (LB/AR) [21]: one test involved 10 Mc FE followed by 5 Mc LB/AR and the other test involved 5 Mc LB/AR and then 10 Mc FE. The flexion-extension is performed in the range of ± 9.7˚, at a frequency of 2 Hz, under a compressive load of 148 N. The lateral bending and axial rotation are performed in the range of ± 4.7˚ and ± 3.8˚ respectively. Both motions are performed at a frequency of 2 Hz under a compressive load of 49 N [21].

Table 3: FDA Summary of Safety and Effectiveness Data Report Results- Prestige® [21]

Test	Details	Range of Volumetric Wear	Mean Volumetric Wear
Wear Simulator Tests	A) 10 Mc FE, 5 Mc LB/AR, n=3 B) 5 Mc LB/AR, 10 Mc FE, n=3 25% bovine, 37˚C	A) **2.61 – 5.15 mm^3** B) **2.20 – 4.48 mm^3**	A) **3.86 mm^3** B) **3.70 mm^3**

Wigfield [58] reported results for cycle testing and claimed the Prestige® implant did not experience permanent deformation in static fatigue testing. Wigfield's cyclic testing performed 10 Mc using 120 and 225 N and did not produce any significant findings. However, increasing the load to 500 and 700 N for the 8x12 mm and 8x14 mm implants respectively, produced cracks next to the screw heads at 5 Mc [58]. These failures were not noted in the 2006 FDA report. Extreme loads exceeding 1500 N produced cracks at 0.12 Mc in major joint components and screw holes. Wigfield's findings are significant in noting no catastrophic failures occurred even at loads as high as 3000 N [58].

A "Summary of Safety and Effectiveness of Data report" published by the FDA in 2007 [20], at the time of the approval of the ProDisc-C®, reported results for impingement tests and wear tests. The results are presented in Table 4. Two specimens were tested to evaluate the impact of high loads at extreme flexion/extension ranges of motion. The point of contact between the UHMWPE and metallic superior plate exhibited a small surface indentation; however, no fractures of the UHMWPE insert or metal plates were evident [20]. Six ProDisc-C® implants were subjected to 10 Mc at a frequency of 1 Hz under a constant load of 150 N in 37˚ C bovine calf serum. The implants were subjected to combined ±7.5˚ flexion/extension, ±6˚ lateral bending and ± 4˚ axial rotation.

Table 4: FDA Summary of Safety and Effectiveness Data Report - ProDisc-C® [20]

Test	Details	Mean Total Weight Loss	Mean Wear Rate
Wear Simulator Tests	10 Mc FE, LB, AR n=6, 150 N, 1 Hz 37˚C +/- 2˚C	**27.4 ± 4.1 mm^3**	**2.77 ± 0.39 mm^3** (determined over a 10Mc test, no evident run-in wear) assuming density of 0.935mg/mm^3

An in vitro simulator test [7] performed on the Bryan® in 2003 is summarized in Table 5. During the 10 Mc test, the implant was subjected to sinusoidal motion for both FE and AR. The tests were performed in bovine calf serum held at 37˚ ± 3˚ C under a constant load of 130 N. The motions included ± 4.9˚ FE and ± 3.8˚ AR at 4 Hz.

Table 5: Wear Results for the Bryan® [7]

Test	Details	Mean Total Volume Loss	Mean Wear Rate
Wear Simulator Tests	10 Mc FE, AR n=6 130 N 4 Hz 37˚C +/- 3˚C	**9.6 mm^3**	**0.96 mm^3/year**

An in vivo caprine(goat) study using the PCM® cervical implant reported no evidence of particulate debris or cytokines [69]. The present author must interpret these results to mean no particles were detected as it is impossible to have a tribological interaction with no wear particles. The present author was unable to locate any in vitro wear studies or mechanical tests performed on this implant.

2.3.2.4. Wear Particles and Osteolysis

Wear particles, causing osteolysis, is the leading cause of long-term failure in total hip arthroplasty (THA) [8]. Any particles within the size range of 0.2 - 0.8 μm has potential to cause osteolysis [70]. Each implant creates wear debris primarily from the articulating surfaces and potentially additional debris from micromotion between the implant and bone. Examination of hip stems reveals a polished surface on the femoral stem caused by micromotion between the femoral stem and the acrylic cement sheath. Metal and cement wear debris are produced from this phenomenon [9]. There is a wide range of clinical consequences of wear-induced osteolysis. Bone loss caused by wear activated macrophagic activity presents itself in the form of radiolucent lines on x-rays in less severe cases, to extreme cases of osteolysis resulting in implant loosening and movement and pain. Bone loss not only presents a need for revision surgery, it also creates a situation where there is much less material to attach a second implant. Severe bone loss can leave patients with much reduced options for future treatment [9].

The local effect of wear particles has been heavily researched and it is concluded that submicrometer and micrometer sized particles activate macrophages and cause phagocytosis. This process is the engulfment of the wear particle by the macrophage. The enlarged macrophage is unable to break down the particle and subsequently releases inflammatory and osteolytic factors. These signals, in addition to those released in the event of the death of the original macrophage cell (which usually occurs); recruit more macrophages in an attempt to rid the body of the wear particles [9, 71]. The inflammatory factors diminish bone stock and may cause the implant to lose its fixation. Bone chips lost from the implant fixation site, cement particles used to attach the implant and wear particles themselves have the potential to get in between the articulating surfaces and induced third body wear, escalating osteolysis [71].

Bioreactivity of particles is dependent on particle size, geometry, composition and concentration. Metallic wear particles, the dominant type of particulate found near spinal implants of various types, ranges from 0.5 - 5 μm, with 90% of metallic particles smaller than 1 μm [72]. UHMWPE particles can be larger but in the size range of 0.1-0.5 μm the strongest systemic response is produced [73]. In general, particles in the size range of 0.2 - 0.8 μm elicit the strongest macrophagic response [70]. The greater the concentration of wear particles within the critical size range, the greater the inflammatory response [70, 71]. Metallic particles are of concern if localized metal ion levels rise as this can cause cell death and tissue necrosis [73]. The effect of elevated metal ion concentration levels in the cervical spine region, adjacent to neural tissues requires further investigation.

Wear particle analysis was performed during in vitro wear testing of the Prestige® STLP [21], the Bryan® [65] and the ProDisc-C® [20]. The wear debris of three Prestige® STLP samples were examined at 20,000x nominal magnification in the scanning electron microscope (SEM). The 316 stainless steel particle sizes ranged from 0.13 μm to 1.58 μm [21].

The polymeric wear particles attained from tissue surrounding the implant during in vitro simulator testing of the Bryan® are larger than those produced in knee simulator tests. Over 2400 independent wear particles were assessed giving an average “equivalent circle diameter” of 3.89 μm [7]. There were no metallic particles found in the wear

debris. The Bryan disc implant particles are polyurethane and elliptical in shape rather than the more spherical particles usually seen [65].

Particle analysis was performed on two ProDisc-C® implants after a 10 Mc wear test conducted in bovine serum [20]. A minimum of 100 particles were analyzed per implant using 4000x nominal magnification in an SEM. The mean particle size for each implant, evaluated in two machines was 0.21 ± 0.13 μm and 0.22 ± 0.14 μm for implant 1. The mean particle size for implant 2 was 0.28 ± 0.17 μm and 0.19 ± 0.08 μm in machines 1 and 2 respectively [20].

The present author was unable to locate any particle analysis on the PCM® cervical implant. There is very little information available in comparison with studies by Catelas et al. [74], Cambell et al. [75] and Ingham et al. [70] on hip and knee wear particles.

2.3.2.5. Evidence of Osteolysis in Spinal Disc Arthroplasty

Spinal disc arthroplasty introduces unique concerns in comparison to other forms of total joint replacement. The effect of chronic inflammation on adjacent neural tissues and systemic effects is unknown and is cause for extreme caution [71]. The lower quantity of bone stock available at the vertebral location in comparison with the pelvis and the complexity of a reconstructive procedure in the event of osteolysis make wear particle-induced osteolysis a major clinical concern for spinal disc arthroplasty [76].

There are very few in vivo studies examining wear particle size and tissue reactions at the implant site. Kurtz et al. [77] using tissue collected during revision surgery of the Charité lumbar spinal implant found polyethylene particles above ~ 0.49 μm in 11 of 17 patients. The number of particles increased as the particle size decreased. This study dismisses the notion that "osteolysis is impossible in lumbar total disc arthroplasty as a result of minimal or no synovial fluid and small amount of movement at the joint". The above mentioned study confirms the presence of periprosthetic inflammatory reactions in the region of artificial disc that were requiring revision. The data from this study supports the hypothesis that inflammatory reactions are related to the presence of wear particles.

A second study [78], performed in 2007, examined serum levels pre-operatively and at 3 and 6 months post-operatively of patients implanted with the Prestige® STLP. The particles were isolated from the serum using a high-resolution inductively-coupled plasma-mass spectrometry. Metal levels were compared to those of stainless steel spinal instrumentation used for fusion surgery and cobalt-alloy metal-on-metal hip implants at similar points post operatively. The short-term metal levels for the Prestige® STLP study were an order of magnitude lower that those observed in both the spinal instrumentation and hip implant cases at similar points in time [78]. Short term conclusions could possibly indicate osteolysis is not as likely with CDA as it might be with spinal fusion and hip implants but realistically, we know the amount of wear particles is significantly higher in hip implants and therefore osteolysis would take longer to develop in CDA that has considerable lower wear. The two above mentioned studies [77, 78] present some of the most current findings in this area of research. The conclusions from these studies were obtained from abstracts presented at the North American Spine Society 22nd Annual Meeting.

2.3.2.6. Post Operative Medical Imaging

Cervical spinal disc arthroplasty requires clear postoperative images due to the danger of implant migration in regions adjacent to neural tissue. X-rays are a useful postoperative tool to determine implant positioning and potential migration [11]. Magnetic resonance imaging (MRI) is required for any neural tissue assessment [11]. It is a crucial tool used by surgeons to assess adequacy of neural decompression and monitor adjacent levels of the spine. Magnetic susceptibility of a metallic implant produces local inhomogeneous artifacts around the implant in the MRI field which distort the resonance frequency due to interference with imager gradients [79]. Eddy currents caused from gradient switching in highly electro conductive material disturb the magnetic field [79]. The disturbance around the implant causes signal alterations, regional hypointensities, increased peripheral signals and geometric image distortions at the implant site [79].

Early studies of spinal fusion materials concluded that stainless steel implants had significant imaging artifacts in comparison with titanium implants [80]. Artifacts created

by metal implant components reduce the chance of successful identification of tumors, fractures, infections at the implant site, and loosening of the implant [81].

Studies conducted in 1994 [82] concluded that titanium alloys allowed better bone detail in comparison to cobalt-chrome alloys on CT scans. Artifact reducing methods have been explored in the past but these approaches are timely and costly, therefore not suitable for clinical imaging of metals[81, 82].

The biomaterials used in cervical disc prosthesis play a role in the quality of the images the surgeon is able to obtain post-operatively. Studies in 2007 [11], performed by Sekhon indicate the Bryan® and Prestige® LP allow satisfactory visualization versus the PCM® and ProDisc-C® that significantly impaired visualization. This is correlated to the titanium component in the implant. Non-titanium metals prevent the use of MRI for accurate post operative assessment of the surgical and adjacent levels [11]. A MRI image, presented by Sekhon et al., of the two of the above mentioned implants is shown in Fig. 18.

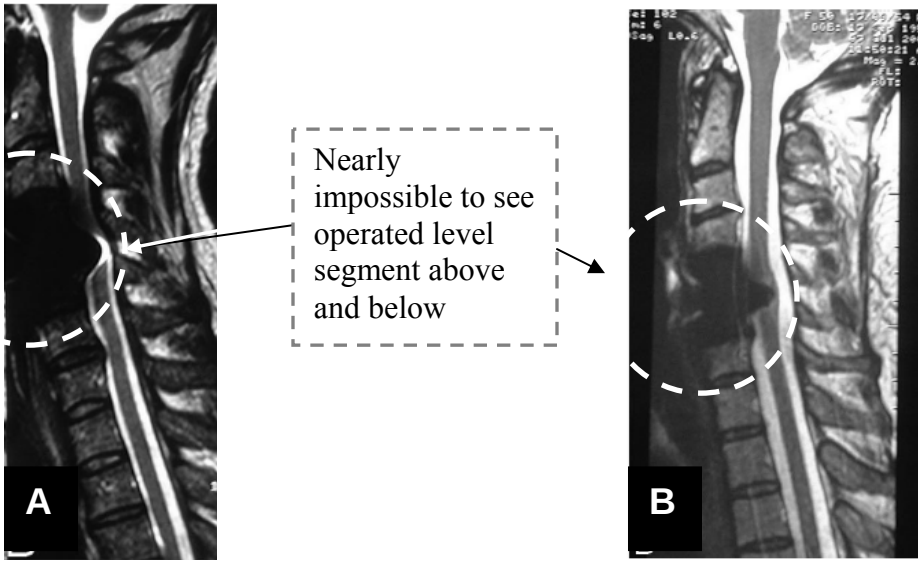

Fig. 18: MRI of A) ProDisc-C® B) PCM® [11]

2.4 Polyetheretherkeytone (PEEK)

Implantable versions of polyetheretherketone (PEEK) have been in use since 1999. The material is conventionally used for interbody spinal fusion cages, craniofacial

devices, dental and cardiovascular implants as a result of its biocompatibility, radiolucency and mechanical strength [83]. A background on PEEK is provided as it being investigated in the present thesis for application in cervical disc arthroplasty.

2.4.1 Types of PEEK

Polyetheretherkeytone is available in both commercial and medical grades. Medical grade PEEK, otherwise referred to as implantable PEEK, is manufactured to the highest purity level possible and is biostable, meaning the material invokes minimal immunological reactions. The body does not recognize the material in bulk as foreign and, therefore, does not attempt to eliminate it through an immune induced inflammatory response. However, there is a possibility the body will recognize PEEK wear debris as foreign, and attempt to eliminate it causing an osteolytic reaction.

PEEK maintains its physical and chemical properties during long periods of implantation. It also combines excellent strength, a stiffness similar to bone and excellent toughness. The ability to be repeatedly sterilized with gamma and electron beam radiation [12] without suffering any degradation in mechanical properties is a unique characteristic of implantable PEEK [84]. The radiation stability of PEEK has been heavily researched as a result of its potential application in spacecrafts and nuclear fusion reactors [12].

PEEK is available in both unfilled and carbon fiber reinforced (CFR PEEK) versions. The wt% of carbon fibers varies depending on the type of PEEK as does the nature of the fibers. Carbon fibers come in two forms; high strength, high modulus polyacrylonitrile (PAN) based carbon fibers or softer and graphitic pitch based fibers [85]. A PAN-based carbon fiber has a density of 1.76 mg/mm^3 versus pitch-based carbon fiber that has a density of 2.00 mg/mm^3. PAN-based fibers are much stronger but pitch-based fibers are much easier to produce and less costly [85]. The fibers can be short, chopped to an average length of 20 μm with an average diameter of 8 μm, or long and continuous throughout the PEEK matrix [85].

Carbon fibers have been used to reinforce artificial knee components in the past. Fibers were added to an ultra high molecular weight polyethylene (UHMWPE) matrix for use in both the acetabular and tibial components. Clinical catastrophic failure was noted

in the tibial component in articulation with a metal femoral component [85]. The following factors differentiate between the success of carbon fibers in PEEK and failure of carbon fibers in UHMWPE; carbon fibers debond with UHMWPE matrix under load due to poor creep resistance of the UHMWPE and weakness of bond between the fibers and matrix. Metallic surfaces articulating against UHMWPE can be scratched by carbon fibers. Finally the use of reinforced UHMWPE as a non-conforming tibial component can contribute to failure of carbon fibers in UHMWPE [85].

Carbon Nanofibre PEEK (CNF) has shown promise as a strengthening agent in commercial grade forms. A unidirectional sliding test, articulating CNF PEEK against 100Cr6 steet and X5CrNi18-10 steel was conducted [86]. The addition of nanofiber is reported to place the volumetric wear below PEEK OPT and CFR PEEK. This study suggested the nanofibers add a lubricating effect to the interface and this is what reduces the wear [86]. The biological response to CNF is not known to the best of the author's knowledge.

One advantage of PEEK is the fact that it is naturally radiolucent. The radiopacity can be varied with the addition of fillers which assists surgeon in identifying the location of the implant. Additions of barium sulfate to PEEK can tailor it to either mild or strong radiopacity depending on the concentration of the barium sulfate [84]. Fig. 19 shows the implants with high and low radiopacity resulting from additives to PEEK and compares them with implants made from unfilled PEEK and metal.

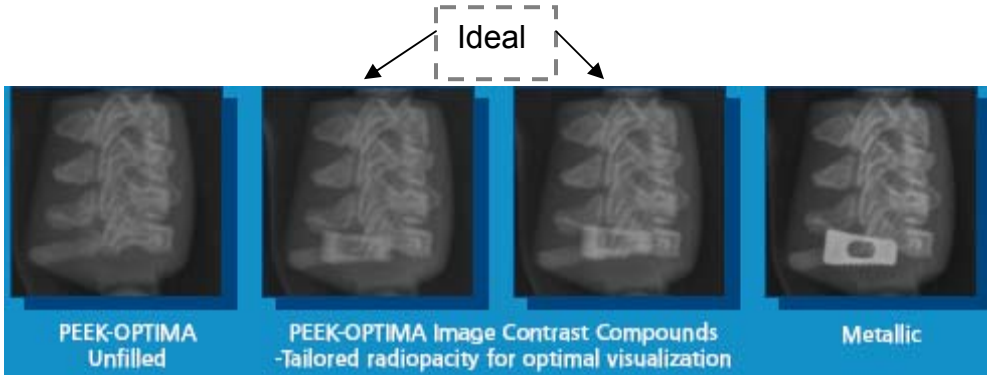

Fig. 19: Radiopacity of Different Spinal Implants [13]

Also, MRI imaging is an area where PEEK is superior to metallic materials as it does not cause artifacts on images. Titanium materials have proven [49] to reduce the

effect of artifacts, however, titanium alloys have been shown to exhibit high wear creating a need for a material that has good wear and imaging properties.

2.4.2 Properties

PEEK is a semi-crystalline thermoplastic with high strength, toughness and modulus. PEEK's thermal stability and chemical inertness place it high in the performance rankings of thermoplastics [87]. The material properties for the three different versions of PEEK are displayed in Table 6.

Table 6: PEEK Properties

Property	PEEK OPTIMA	PAN-CFR PEEK(30%)	CNF PEEK
Density (mg/mm^3)	1.265 [12]	1.4 [12]	2.0 +/- 0.4 [88]
Tensile Strength (MPa)	93 [12]	230 [89]	120 [88]
Elastic Modulus (GPa)**	4 [12]	20 [12]	5.6 +/- 0.2 [88]
Tensile Elongation (%)	30-40 [12]	1-2 [12]	
Glass Transition Temp (˚C)	143 [12]	289 [90]	163 [91]
Melting Point (˚C)	334-335 [12, 92]	400 [84]	400 [88]
Poisson's Ratio	0.36 [12]	0.40 [12]	0.31 [93]

**The elastic modulus of cortical bone is 18 GPa [12]. It is important for the material to mimic the elastic modulus of adjacent bone to avoid stress shielding.

Fixation to the bone is a potential problem with using PEEK for spinal applications. Countermeasures to date include bioactive composite additions to PEEK to aid with bone in-growth [12].

Commercial grade PEEK may be expected to operate at high temperatures. The mechanical properties of PEEK drop off gradually up to the transition glass temperature where a marked decrease in mechanical properties occurs [12]. Medical grade PEEK is intended for use in the body where the temperature remains at a constant value of 37˚C. The elastic behaviour of PEEK is unaffected at the low temperatures experienced in vivo; however, the yielding, plastic flow and fracture behaviour of PEEK are more sensitive at the lower in vivo temperatures. Spinal disc implants involve frictional contact and this

may result in surface temperatures far above 37˚C. Therefore, the thermal effects on PEEK are a topic of interest [12].

A study performed in 2008 [94] compared smooth and rough titanium to PEEK OPTIMA and 30wt% CFR PEEK manufactured by Invibio, the exact same supplier and material used in the present thesis. The study found CFR-PEEK to initiate the highest osteoblast formation. PEEK OPTIMA performed similarly to rough titanium with respect to bone growth on the surface of the material [94]. Bone ingrowth is important because it is the long term mode of fixation for implants.

2.4.3 Wear Testing of PEEK Surfaces

2.4.3.1 Configurations

Spine wear simulators are designed to produce similar wear to that seen in explanted devices. Hip and knee wear simulators have drawn comparisons between clinically observed wear mechanisms on explanted devices and simulator wear results [18]. Comparisons are facilitated by the length of clinical studies performed on both hips and knees and the walking cycle, a frequent activity that induces wear in knee and hip implants. Spinal implant technology and clinical application are still very immature and comprehensive comparisons cannot be made as explants are not readily available. Standards are published; both ASTM and ISO, for total disc replacement simulator wear tests; however confusion arises from the differences between the two standards and neither one has been compared with in vivo. Wear tests have been performed by applying axial compression load and then rotational motions in displacement control about three axes [18].

Pin-on-plate tests can be used to evaluate material combinations prior to implant design. These test devices often try to approximate some aspects of in vivo conditions. They can offer an assessment of the wear of two materials in contact under similar sliding speeds and contact stresses experienced in the body [95]. The pin-on-plate tests simulate conditions that occur in vivo by including crossing-path motion and utilizing a protein based lubricant. Simulator testing requires an implant design and can be both costly and time consuming; whereas the pin-on-plate test offers quick tribological results for new material combinations. Loads can be selected to replicate the weight of the head in

cervical spine applications or increased to represent more extreme conditions. Preliminary testing also provides the opportunity to evaluate the adverse conditions the implant may be required to endure for certain in vivo activites. Lubricant starvation conditions can be simulated along with increased loads and sliding speeds.

Equating the number of in vitro cycles to years in vivo proves to be a difficult task. There are some conflicting opinions expressed in the literature. Degenerative disc disease and disc herniation, the ailment spine implants treat, can occur at very young ages and it is not clear what exactly causes it. This can result in a spinal disc prosthesis requiring a longer life span than a hip or knee prosthesis that are most often implanted in patients experiencing arthritis, a condition that increases in frequency with age [96]. A study performed in 1991 by Hedman et al. [55] is often referenced with regard to correlating the number of cycles to time in vivo. In 1991, Hedman et al. suggested that the lifespan of disc prosthesis should exceed 40 years due to the risk involved with revision surgery [55]. The number of cycles and amplitude of load cycles experienced by a lumbar disc prosthesis remains a matter of speculation, similar to the situation in 1991. Hedman et al. calculated the frequency of certain daily activities in a moderately active person. They estimate that an average person goes through 1 million gait cycles resulting in 2 million strides per year and 125,000 significant flexion/extension bends. Hedman et al. states one significant bend produces 10x the wear debris of a single walk cycle. A conservative estimate correlates 85 million cycles to the loading cycles experienced in 40 years in vivo [55]. This would suggest materials should be tested for at least 100 million cycles. Implants were only tested for 10 Mc in 1991 regardless of Hedman et al. suggestions. Current FDA and ASTM standards only require 10 Mc for fatigue testing of implants which according to Hedman et al., would equal approximately 4.7 years in vivo [32, 34, 55]. The study is reported for a lumbar spine disc and do not necessarily correlate directly to cervical spine cycles. Another Hedman communication, reported by Kurtz [18] argues that walking cycles are less significant than the stated "significant" lumbar bends when the cervical spine is considered due to reduced angular displacement and load on an individual spine segment. However, the stress occurs on a smaller area and those cycles may produce increased wear, particularly in materials that exhibit fretting wear, an insidious type of adhesive wear that can occur when motions are

only in the order of micrometers. The cervical spine may experience many motions that could cause fretting.

A more recent study, Pare et al. [35] states there is no accepted correlation between in vivo and simulated cycles. Matthew et al. [96] suggests the spine goes through 317 460 cycles per year. Additional work is required to characterize the number of cycles per year of implanted device [35].

Estimating the number of cycles for an extremely active patient versus a more sedentary patient would allow surgeons to begin to match particular implants with the activity levels and potential lifespan of the patient.

2.4.3.2 Reciprocating Pin-on-plate Wear Results

Pin-on-plate results from various studies are presented in Table 7. There is a limited amount of quantified PEEK simulator wear data available in the literature.

Table 7: Comparison of Pin-on-plate tests with Different Articulating Materials and Test Conditions

Author & Study Details	Materials & Wear Factors ($mm^3\ N^{-1}\ m^{-1}\ 10^{-7}$)
Scholes et al. 2007 [97] Motion: Crossing-path Load: 40 N Pin Dia: 5 mm Freq: 1 Hz Stroke Length: 25 mm	CFR-PEEK OPT PAN-on-Biolox Delta = 1.8 CFR-PEEK OPT PAN-on-Biolox Forte = 2.15 CFR-PEEK OPT pitch-on-Biolox Delta = 2.26 CFR-PEEK OPT pitch-on-Biolox Forte = 1.53 (Biolox is a ceramic based material)
Scholes et al. 2001 [95] Motion: Crossing-path Load: 40 N Pin Dia: 5 mm Speed: 50 mm/s Stroke Length: 25 mm	LC CoCrMo-on-LC CoCrMo = 11.6 HC CoCrMo-on-HC CoCrMo = 8.43 LC = low carbon (0.06%) HC = high carbon (0.25%) CoCrMo = Cobalt, chromium and molybdenum
Powell 2005 [49] Motion: Crossing-path Load: 9.81 N Pin Dia: 12 mm, pin rot: 28˚/cyc Freq: 1.18 Hz Contact Stress: 91 MPa SS & 65 MPa TAC Stroke Length: 11 mm	 SS-on-SS = 393.38 TCC-on-TCC = 108.14 SS = Stainless Steel TCC = Titanium Ceramic Composite
Tipper et al. 1999 [49][98] Motion: Crossing-path Load: 80 N Pin Dia: 12 mm (spherical tip)	LC CC alloy-on-LC CC alloy = 20.77 HC CC alloy-on-HC CC alloy = 11.91 LC = low carbon (0.07%)

Freq: 1 Hz Contact Stess: 11.3 MPa Stroke Length: 30 mm	HC = high carbon (0.2%) CC = Cobalt, chromium
Joyce et al. 2000 [99] Motion: Crossing-path Load: 40 N Pin Dia: 5 mm Freq: 1 Hz Contact Stress: 2.04 MPa Stroke Length: 26 mm	316 SS-on-UHMWPE = 11
Scholes et al. 2008 [100] Motion: Crossing-path Load: 40 N Freq: 1 Hz Contact Stress: 2 MPa	PEEK OPT-on-PEEK OPT = 45 CFR-PEEK PAN-on-CFR PEEK PAN = 2.59 & 3.40 (2 tests) CFR-PEEK pitch-on-CFR PEEK pitch = 9.21 PEK-on-PEK = 9.92 & 16.4
Scholes et al. 2008 [101] Motion: Crossing-path Load: 40 N Freq: 1 Hz	PEEK-on-LC CoCrMo = 73.8 CFR-PEEK PAN-on-LC CoCrMo = 1.55 CFR-PEEK PAN-on-HC CoCrMo = 1.77 CFR-PEEK Pitch-on-HC CoCrMo = 1.29
Joyce et al. 2004 [102] Motion: Crossing-path Load: 40 N Pin Dia: 5 mm Freq: 1 Hz Distance: 56 km	UHMWPE-on-UHMWPE = 410 XLPE-on-XLPE = 33.6 XLPE = Cross-linked polyethylene
Howling et al. 2003 [73] Motion: Crossing-path Load: 160 N Pin rotation: 120˚ per cycle Distance: 5 km	CFR-PEEK PAN-on-alumina ceramic = 0.93 +/-0.3

It should be noted that all of the above studies ignored lateral sliding caused by pin rotation in the wear factor calculation with the exception of Powell et al.

2.4.3.3 PEEK Simulator Studies

A hip wear simulator study performed 1998 [85] examines the tribological performance of PEEK and CFR-PEEK(20wt% and 30wt%) as an acetabular cup liner insert for total hip replacement implants. The simulator tests included an acetabular cup liner composed of different types of PEEK articulating against a femoral head composed of various materials including; alumina, CoCr and zirconia. Specific wear values are not

stated for every material combination however the PEEK OPTIMA wear rate, shown in Fig. 20, is reported to be 100 times higher than the 20wt% PAN-CFR PEEK wear rate. The 30wt% PAN-CFR PEEK wear rate is half that of 20wt% PAN-CFR PEEK. Both wt% versions of PAN-CFR PEEK are 10 times lower than the wear rate on non-crosslinked UHMWPE but the PEEK OPTIMA wear rate is 8 times larger than the UHMWPE wear rate [85]. The findings discussed above are shown in Fig. 20.

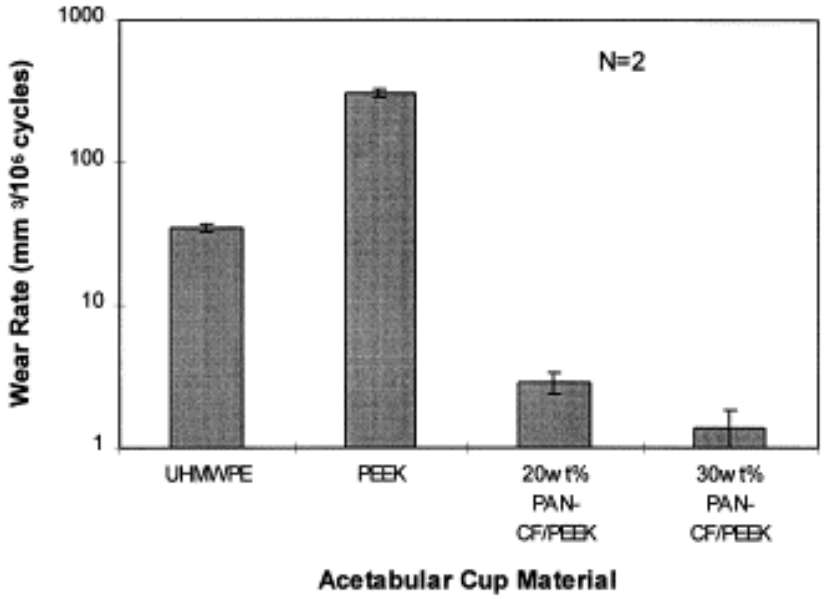

Fig. 20: PEEK vs. UHMWPE [85]

The 30wt% pitch-based CFR PEEK acetabular insert coupled with a zirconia ceramic head produces a wear rate almost two orders of magnitude lower than conventional UHMWPE-metal and UHMWPE-ceramic couples [85].

More recent spine simulator studies [103] have been performed on PEEK OPTIMA-PEEK OPTIMA lumbar nucleus implants. The linear-tracking study produced a wear rate of rate of 0.28 +/- 0.02 mg/Mc over a 40 Mc period. Specific wear rate values are not stated for the crossing-path test, however the graphical representation reveals a run-in wear period and wear rate of ~ 0.65 mg/Mc in the first 5 Mc and a decreased wear rate of ~0.45 mg/Mc in the 5-10 Mc range [103]. The multi-directional test results are most useful for comparison to the results present in the current thesis.

2.4.3.4 Lubricants

The wear testing standards for both hips and knees suggest a minimum protein concentration of 17g/L [35]. This value is intended to represent synovial fluid in the hip and knees. There is much debate surrounding the composition of the fluid in and around the intervertebral disc. The two standards used to define lubricant parameters for wear testing cervical disc implants reflect the composition of synovial fluid. The ASTM F 2423-05 standard suggests diluting bovine serum with de-ionized water to a protein concentration of 20g/L and holding it at 37˚C. The standard also suggests addition of 0.2% sodium azide or another antibiotic and 20-mM ethylene-diaminetetraacetic acid (EDTA) to minimize bacteria growth in the lubricant and calcium phosphate precipitation onto the bearing surface [34]. The ISO 18192-1 standard suggests using calf serum diluted with deionized water to a protein concentration of 30g/L +/- 2 g/L with an anti-microbial reagent such as sodium azide added. The addition of EDTA at 20 mM is suggested but justification of its addition is left to the user [32]. Recent work [104, 105] suggests that alpha calf serum is closer to synovial protein sub-constituents and also that phosphate buffer saline solution reflects the osmolality more accurately than de-ionized water. Sodium azide has shown inability to kill bacteria thus raising the need for other regimes of antibiotics to be used in serum [104, 105]. These findings relate to synovial fluid in the knee and a paper by Matthews et al. in 2004 [96] states there is no synovial fluid present in a spinal segment [96]. If the spinal segment doesn't in fact contain synovial fluid then it would more appropriate to test implants in a medium that mimics interstitial fluid. Pare et al. [35] uses a protein concentration of 10g/L for wear testing. This seems the most reasonable to the current author. However, it is clear that further work is required to determine the composition of the fluid in and around a cervical spinal segment.

2.4.3.5 Wear Particles

Wear resistance is important when selecting an implantable, articulating biomaterial. The wear debris for PEEK OPTIMA and CFR PEEK were reported to be biocompatible materials [12]. Studies on systemic, intracutaneous toxicity and intramuscular implantation show no adverse side effects. Biological reactions to

micrometer and sub-micrometer sized CFR PEEK particles have been investigated to evaluate potential bearing surface for artificial hips. CFR PEEK particles induce no cytotoxic effects in a petri dish. It is possible that CFR PEEK would not produce an adverse tissue reaction, as is the case with CoCr wear debris [73]. A study examining the immune response to rough titanium in comparison to both PEEK OPTIMA and CFR PEEK found the latter materials to demonstrate good cytocompatability and mineralization in vitro [94].

A simulator study [73] performed in 2003 examined PAN CFR PEEK particles and found the particles to induce no cytotoxic effects [73]. The CFR PEEK particles were similar in size to alumina ceramic. The author hypothesizes that particles less than 100-nm in size may not induce an inflammatory tissue response and therefore produce lower osteolytic reactions [73].

A literature search has not located any studies reporting on tissue response to CNF wear particles.

2.4.3.6 Fluid Adsorption

Fluid absorption is an issue in materials that absorb fluid and use weight measurements to attain wear values. The absorbed water can mask wear and must be accounted for to ensure accurate results. ASTM standard F 1634-95 [33] outlines the procedure to obtain a state of saturation for non-absorbable polymer matrix composites and implant devices [106]. Previous studies on PEEK fluid uptake use water as the fluid medium rather than the bovine lubricant described above. The water uptake does not vary significantly with temperature fluctuation. The mean value of absorption is 0.48% for PEEK OPTIMA [107]. Water absorption in CFR PEEK is noted in the literature as a possible concern due to the space between the matrix and the fibers. Medical grade CFR PEEK is reported to absorb up to 0.05% over a 24 hr period and after 96 hours immersion the material is considered saturated and has absorbed up to 0.11%, considerably less than unfilled PEEK OPTIMA [90]. No fluid absorption values were found for medical grade CNF PEEK.

2.5 Objectives and Scope of Research

There is uncertainty surrounding the correlation between in vivo conditions and wear test parameters. The actual load experienced by a cervical disc is known for the standing upright body position. The load parameters for specific activities, in particular, extreme motions and movements have not yet been determined. Imaging capability is necessary for cervical implant materials. Post operative movement of a cervical disc implant could have disastrous consequences. Surgeons require spinal implant materials to have adequate imaging capability in order to see in and around the implant post operatively.

The objective of the current study is to examine the wear performance of PEEK. Since simulator tests can be both costly and time consuming, the pin-on-plate test configuration is a useful tool to assess initial tribological behaviour of material candidates for cervical disc implants. An OrthoPOD^{TM} pin-on-disc apparatus is used in the current study to assess the wear behaviour of PEEK under normal and adverse conditions. Normal conditions are evaluated with a baseline test involving 2.0 Mc under an 80 N load. The load is subsequently increased until the material shows signs of failure to determine the performance of PEEK under adverse conditions. Microscopy is used to identify the wear mechanisms present in the three different types of PEEK.

There are currently no cervical spinal PEEK-on-PEEK implants on the market. The purpose of the present thesis is to determine if PEEK is a competitive alternative to the conventional cervical disc implant materials.

3.0 WEAR TESTING OF PEEK

3.1. Test Apparatus

Wear testing is performed using a multi-station pin-on-plate Ortho-POD™ (AMTI, Watertown, MA). The pin-on-plate apparatus differs from a simulator in that it does not attempt to replicate in vivo conditions, it applies similar sliding speeds and contact stresses to material combinations that may be experienced in the body [95]. Simulator testing, often completed after the implant is designed, can be both costly and time consuming, therefore pin-on-plate machines are a useful tool for initial evaluation of different material combinations prior to completion of implant design.

The present study subjects the materials to normal and adverse conditions. The adverse loading conditions assess the behaviour of the materials under extreme loading conditions and articulate three versions of PEEK against themselves. Polymer-on-polymer pin-on-plate testing is unconventional, as are polymer-on-polymer cervical implants, hence the need for further research in this area.

3.1.1 Pin-on-Disc Apparatus

The OrthoPOD™ (AMTI, Watertown, MA) pin-on-disc apparatus, shown in Fig. 21, is a six station pin-on-disc machine developed for orthopaedic material screening [108].

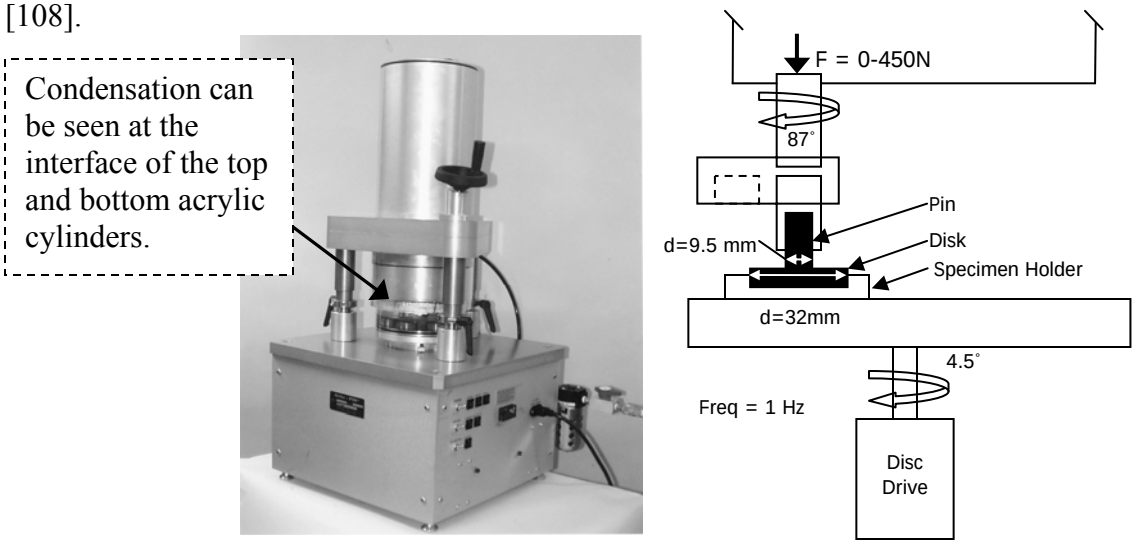

Fig. 21: Schematic of OrthoPOD™ [108]

The machine is made of two parts: the top portion contains six independent pin actuators and the bottom portion contains a single disc drive axis with specimens mounted on the main drive disc. The six pin drive axes are centered on a planet gear that is driven by a backlash-free harmonic drive gearhead, which is driven by a brushless DC motor causing all the pins to have the same rotary motion. The pins are attached to graphite pistons that are loaded with air pressure and slide through Pyrex® bores. The load range for the pins is 0 - 450 N. Pin rotation, plate rotation and load are dynamically controlled by a microprocessor.

The OrthoPOD™ performs reciprocating rotation of both pin, through an angle of 87˚, and disc through an angle of 4.5˚. The combined motion is applied to create crossing-path motion which has been shown to occur in vivo from explant analyses [95].

3.1.2 Temperature

The Ortho-POD™ is considered a pin-on-plate test apparatus however it has many features that mimic in vivo conditions more so than conventional pin-on-plate machines. One feature is the recirculating temperature controller. An external bath of de-ionized water is held at a 44˚C and circulates below the base plate to which the specimen chambers are fastened. Thus, the base plate of the apparatus is held at 44˚C, but the temperature drops as the heat moves through the polyurethane specimen holders and the specimen resulting in a specimen chamber lubricant temperature of 37˚C, the in vivo body temperature. Polymers are sensitive to fluid uptake, which is temperature sensitive. Therefore, it is crucial to maintain in vivo temperature during testing to obtain accurate and clinically relevant wear results.

3.1.3 Chamber Sealing

An acrylic cylindrical cover slides over an o-ring seated around the top portion of the POD that holds the pins. A second cylindrical cover slides over an o-ring on the disc plate and holds de-ionized water. The individual disc specimen holders have acrylic covers that slide over o-rings that separate the lubricant from the water bath. The pins are lowered to meet the discs resulting in an overlap of the top cover over the bottom cover.

There is an approximate 22 mm vertical overlap and a 7.5 mm horizontal gap between the two acrylic cylinders. Condensation forms within the gap during the course of a test.

Fig. 22 shows the fluid levels of the lubricant chambers after 0.2 Mc. The chambers are numbered in the diagram for future reference.

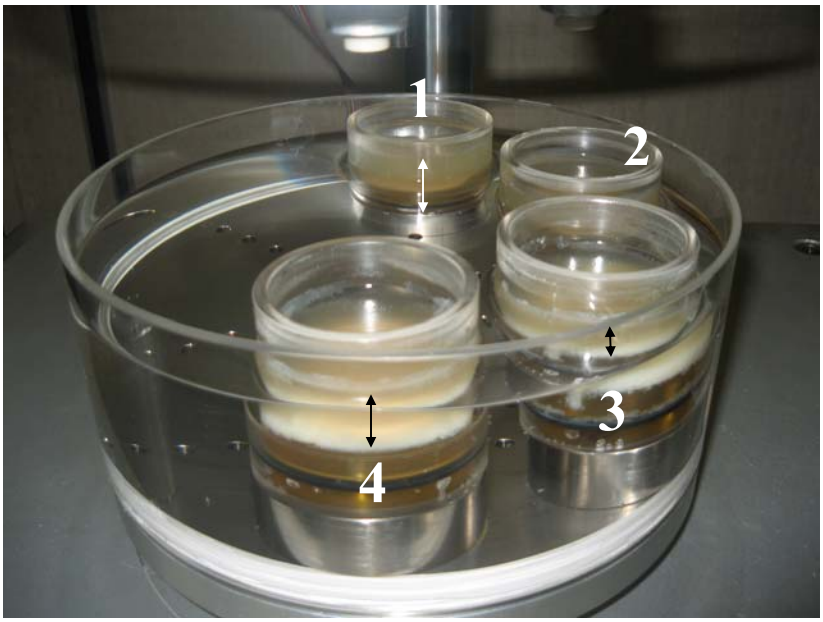

Fig. 22: OrthoPOD lubricant levels after 0.2 Mc cycles

Upon completion of a 0.2 Mc test, it is noted that the lubricant level varies depending on chamber location. Chamber 4, located at the front of the POD, consistently loses more fluid by evaporation, than does the adjacent chamber 3. Similarly, chamber 3, loses more than chamber 2 and the fluid level in chamber 1 experiences minimal change. The difference in fluid lost to evaporation and protein degradation (indicated by the clarity of the serum) between chambers 1 and 4 are displayed in Fig. 23.

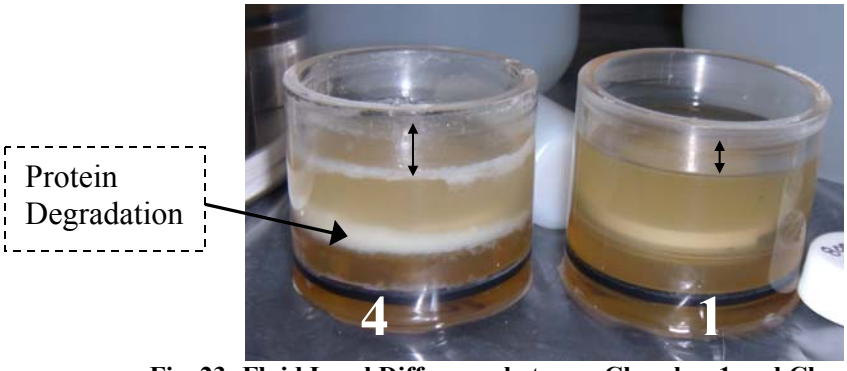

Fig. 23: Fluid Level Difference between Chamber 1 and Chamber 4

The specimens located in the load soak apparatus, used to monitor fluid uptake, display similar fluid levels to chamber 1. Fig. 24 is a graph showing the actual loss of fluid in the POD compared to the load soak chambers over the course of a 0.2 Mc test, during which the chambers were refilled once after 93.25 hours. There are only 7 specimens so the number in each location is not equal.

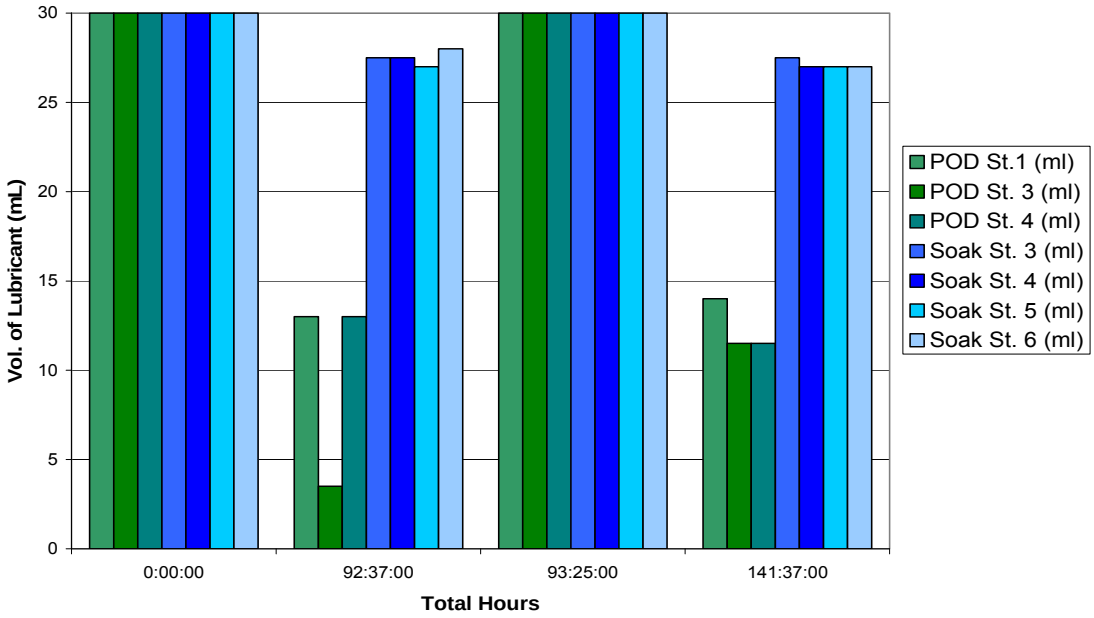

Fig. 24: Volume of lubricant in the OrthoPOD™ and Load Soak

The load soak specimen holders and the OrthoPOD™ specimen holders are identical. The load soak specimen holders are dropped into a capped cylindrical ¼" acrylic tube that separates the specimens from the surrounding de-ionized water held at 37˚C. The tubes are longer than the height of the specimen holders providing room to insert steel bars that fit snuggly above the specimen holders and apply an 80 N load. The load soak chambers are essentially sealed and the majority of the evaporation that takes place condenses back into the lubricant. The above graph illustrates an experiment performed twice producing similar results. The chambers are filled with lubricant and the test runs for 0.2 Mc. The volume of lubricant is measured after the test is complete. The load soak lubricant levels, shown in blue in Fig. 24, indicate approximately the same amount of lubricant lost in the load soak chambers. The OrthoPOD™ lubricant levels, shown in green, drop almost twice as much as the load soak lubricant levels. This indicates the load soak's sealed chambers produce consistent minimal lubricant loss in

comparison to those of the OrthoPOD™. Therefore a modification is added to the test protocol to minimize the effect of diminished fluid levels: the top and bottom components of the OrthoPOD™ are wrapped in Saran™ wrap to reduce the effect of air flow over the chambers. Lubricant loss is noted as minimal in the OrthoPOD™ after this modification.

3.1.4 Hardware and Software

Both hardware and software difficulties were encountered with the OrthoPOD™ during the course of testing. The first issues concerned the interface between the hardware and software. The OrthoPOD™ has a "home" position and a "rest" position. The "home" position is native to the machine and cannot be altered by the user. The "rest" position is selected by the user and describes the position that the plate and pins will return to after the test is complete. The "home" position is indicated by two green LED lights located on the side of the machine, one for the pins, one for the plate. When the components are in "home" position, the manual mode controls indicate the position of the plate and pins to be (0˚,0˚). There are magnets in the disc, the pistons holding the pins and just below the disc in the bottom of the apparatus. The button "Home" initiates turning of both the plate and pins and the magnets signal the machine when "home" position is reached by each of the components. However, when the "Home" button is selected, the disc continues to rotate, approximately 6 times, past the magnetic signal and eventually settles on a position that is 97.4˚ offset from the correct (0˚,0˚) "home" position. This process was repeated several times producing the same result. The pin LED "home" light is illuminated indicating the pins are the true home position. The disc LED "home" light is not illuminated indicating the disc is not in true home position. The disc can be rotated manually to a position that appears to be in the approximate region of "home" and the disc LED "home" light then illuminates.

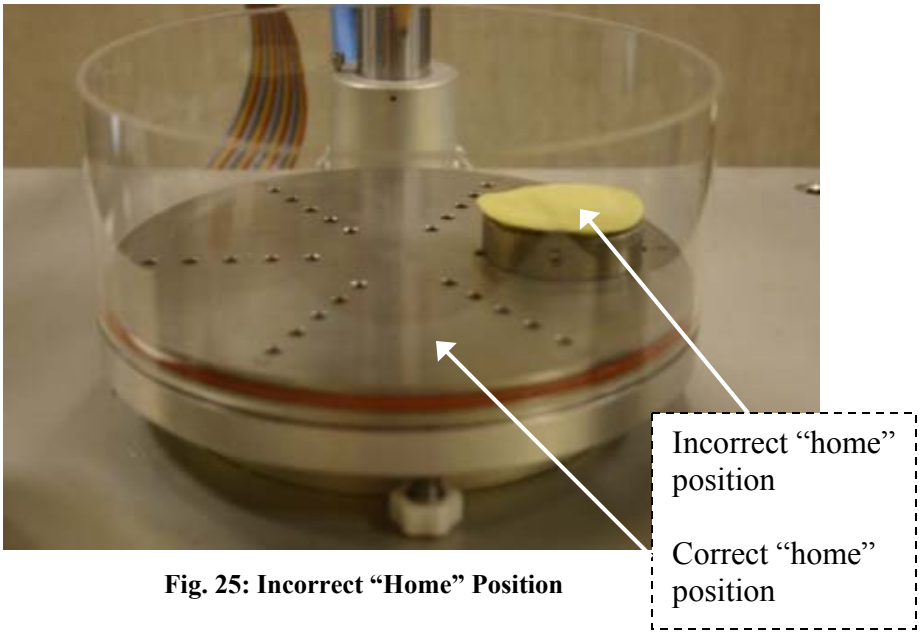

Fig. 25: Incorrect “Home” Position

The machine indicates the disc is at -97.4˚ even though the disc is in true “home” position which is indicated by the LED lights. Consequently, the rest position is set to -97.4˚ to ensure the final resting position after completion of the test is (0˚, 0˚). This modification results in both LED lights illuminating, indicating the machine is in true “home” position. Issues that arose from these countermeasures included the inability to turn the machine off as it would force the machine into the wrong home position. Once the machine completes a test, it moves to the specified rest position until the user specifies a new position. If the machine ends up at 97.4˚ after being “homed” and then is manually moved to the correct “home”, it will attempt to move back to what it thinks is “home” if the machine is manually stopped, shut off and then restarted. This is disastrous as the pins ram into the side of the chambers causing the acrylic lubricant holders to come off the specimen holders, spilling lubricant into the water bath and contaminating the test specimens. The specimen holders and specimens can then be damaged. Any hard contact of the pin with the acrylic chamber holder has the potential to remove material from the pin, affecting the wear results. The most difficult issue with this error is the unpredictability of the machine as the software indicates the machine is in the correct position and the hardware is consistently in the incorrect position. This issue was brought to the attention of both the technicians who previously worked with this specific OrthoPOD^{TM} and the manufacturers of the OrthoPOD^{TM}. No solution was reached and

the 97.4˚ offset is currently the modification in place to allow relatively normal operation of the machine.

An additional software issue was encountered that involves the machine shutting off in the middle of a test for no apparent reason. The offset issue mentioned above comes into play here in addition to there not being any record of the cycles the test completed prior to the machine turning off. This is a major concern as wear is tracked by the number of cycles. The test runs without constant supervision for 0.25 Mc and, in the event the machine shuts off at some point during the test, the number of unknown cycles can be upwards of +/- 0.1 Mc. This is a serious concern and jeopardizes the accuracy of the wear results, especially if this occurs more than once during the course of a test. This error occurred during the CFR PEEK test; fortunately it occurred early in the test and so the number of undetermined cycles was minimal.

Cleaning and weighing is performed at different points in the test for CFR PEEK and PEEK OPT as a result of the machine shutting off and the number of cycles per interval changing. Direct numerical comparison is difficult between the two materials at specified points as wear readings are obtained at different points in the test. The overall effect of this error is minimal as comparison is easily made at the 2.0 Mc mark.

5.1.1. Motion

Crossing path motion occurs due to the combination of axial rotation, flexion-extension and lateral bending motions presented in Table 1. It is difficult to select pin-on-disc input parameters that represent in vivo conditions exactly. The design of the implant was not specified at the time the pin-on-disc tests were completed. Different implant designs impose different amounts of crossing path motion making it even more difficult to specify parameters for pin-on-disc tests. The current thesis selected a rotation value with the intention of exaggerating the in vivo conditions. There might be some merit in reducing the angle of rotation in future studies to see how sensitive wear is to crossing path motion with PEEK materials.

The 8.5 mm sliding distance used in the present project was somewhat similar to the sliding when both flexion-extension and lateral bending occurred simultaneously (at ASTM or ISO levels). It is worth noting that the geometry of an implant may incorporate

a sliding distance equal to or greater to the sliding distance used in the present project. This value is crucial in Archard's law calculation that uses load, sliding distance and volumetric wear to establish a wear factor that is used to compare wear results.

The top and bottom portion on any implant are fastened to the surrounding vertebral bodies which, of course remain aligned with each other and move within specific ranges of motion. It is noted that other studies utilize continuous motion which would simulate the head continually turning with respect to the body.

3.1.6 Load

The present thesis includes a "baseline test" of 2.0 Mc. The baseline test for PEEK OPTIMA, CFR PEEK and CNF PEEK are completed under an 80 N axial compressive load which results in a contact stress of 1.129 MPa. A load of 80 N is selected because it is a representative of the weight of the head on the cervical spine. The standard upright position of the head imposes 75 N on each level of the cervical spine according to Hattori and Moroney et al. suggests a value of 73.6 N represents the weight of the head [36, 38].

The "adverse condition" test involves increasing the load until material failure is evident. The load values for each 0.15 Mc interval after the baseline test are: 120N, 180N, 210N, 250N, 300N, 350N & 400N. The failure point of the material is unknown and the load increase for each interval is dependent on the wear seen over the previous interval.

The present thesis uses load as an experimental parameter rather than contact stress. This is done to allow comparison with the literature, where load is specified more frequently than contact stress. The second rationale behind is to do with the contact area continually changing as a function of the wear. The exact rate at which the contact stress changes is undetermined in the present thesis. Creep experienced by the polymer also distorts the relationship between wear and contact area.

The loads used in the adverse condition test are drastically higher than ASTM and ISO standards and are not necessarily a representation of what might be experienced by an implant in vivo.

3.2 Load-Soak Apparatus

A load soak apparatus is required by the ASTM and ISO standards when testing any material that may absorb lubricant [32, 34, 106]. The load soak is generally an external machine separate from the wear test apparatus that replicates the conditions the wear test specimens are subjected to as closely as possible without subjecting the load soak specimens to any motion. The fluid uptake for all the load soak specimens is averaged and that value is subtracted from the wear value of each of the wear test specimens. The most prominent concern with wear testing polymers is that the fluid uptake may mask the wear of the material in materials that already experience very low wear. The load soak attempts to remove this factor from the results and ensures more accurate wear values.

3.2.1 Design & Fabrication

The load soak apparatus, shown below in Fig. 26, is constructed out of an existing viscometer. The water circulator/heater is attached to a newly fabricated foam insulated stainless steel bath. A ¼" thick aluminum cover is placed over top of the bath and has holes cut in the top for the tubes that hold the specimens, thermometer and circulator/heater. Acrylic tubes, ½" thick, are capped on the bottom and have a slightly larger diameter lip added on the top to allow the chamber to slide through the aluminum top cover and have the top lip support the load. The chambers that hold the disc specimens, identical to those used in the OrthoPOD™, are slid into the tube and a plastic piece that holds the pin specimens in the same fashion as the OrthoPOD™ is slid in on top of the disc specimen holder. The chamber and pin holder slide to the bottom of the acrylic tube and sit below the water line in the bath. The water circulator/heater ensures the lubricant in the chamber is held at a 37˚C constant temperature. An 80 N constant load is applied to the load soak specimens using ~18 lb steel bars. The bars fit snuggly in the tubes above the pin holder eliminating any air flow and cause any evaporation to condense back into the chamber. This reduces the chance of elevated protein concentration due to water evaporating out of the lubricant.

A limitation of the load soak is its inability to apply higher loads in accordance with the adverse conditions test load values. Steel bars that could apply loads as high as

400 N, the final load value for the CFR adverse conditions test, would not physically fit into the load soak apparatus.

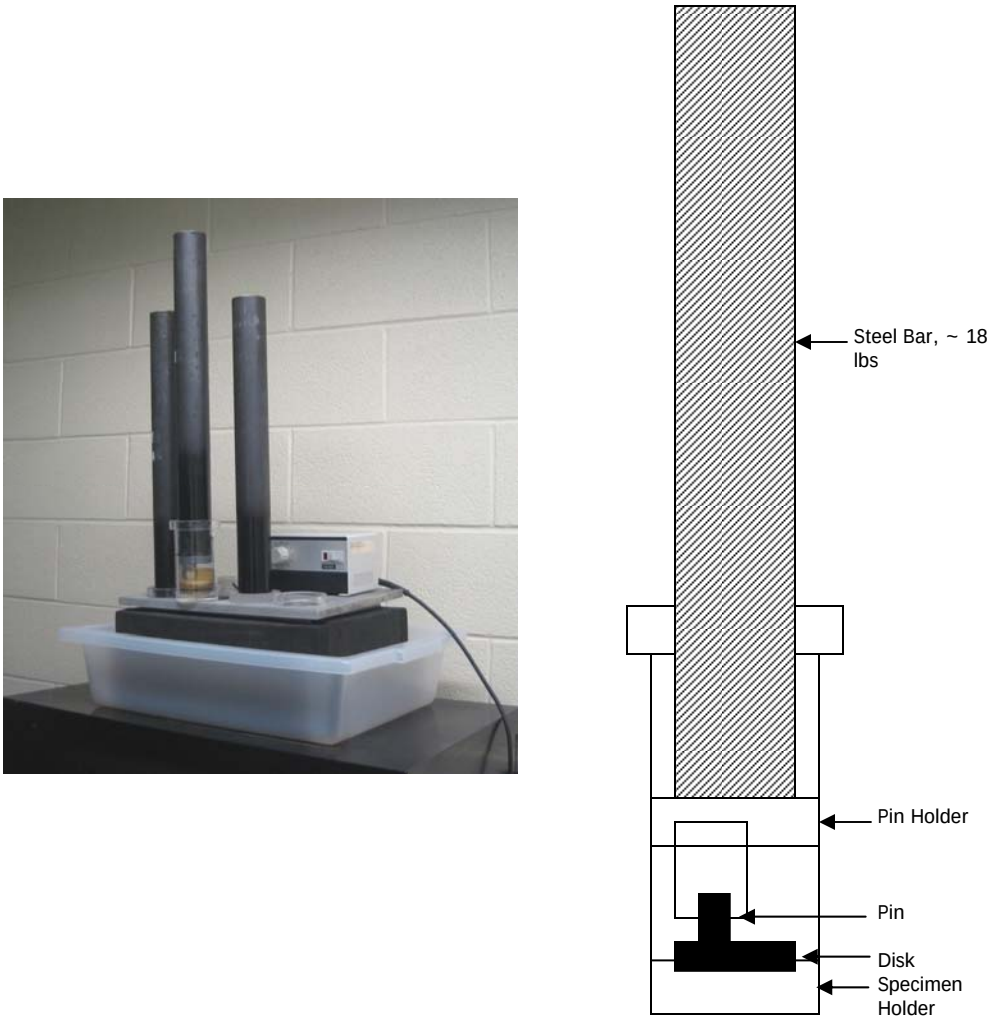

Fig. 26: Load Soak Apparatus

.

4.0 MATERIALS AND METHODS

4.1. Specimens

All specimens were provided by Medtronic Spinal and Biologics (Memphis, TN). These consisted of three versions of PEEK (manufactured by Invibio Ltd, Thornton Cleveleys, UK) in Optima (OPT), Carbon Fiber Reinforced (CFR) and Carbon Nano-Fiber reinforced (CNF) versions were cut from bar stock, engraved with numbers and sent to the present author. The test pairs were chosen arbitrarily by the present author. Alignment markings were engraved on the pins just above the wear surface end of the pin in order to ensure the orientation of the pin and plate remained the same throughout the course of the tests. The rationale was to replicate in vivo conditions as closely as possible.

Each pin is 9.5 mm in diameter and is manufactured to have a 100 mm radius spherical tip. The pin size gave a contact area that was a little smaller than that likely to occur in an implant. The pins are articulated against flat plates. The radius is included to avoid edge contact with abnormal stress concentrations. The geometry of an implant would likely be a ball-in-socket articulation with the ball smaller than the socket to also avoid edge contact. The pin and plate specimens are shown in Fig. 27 A & B.

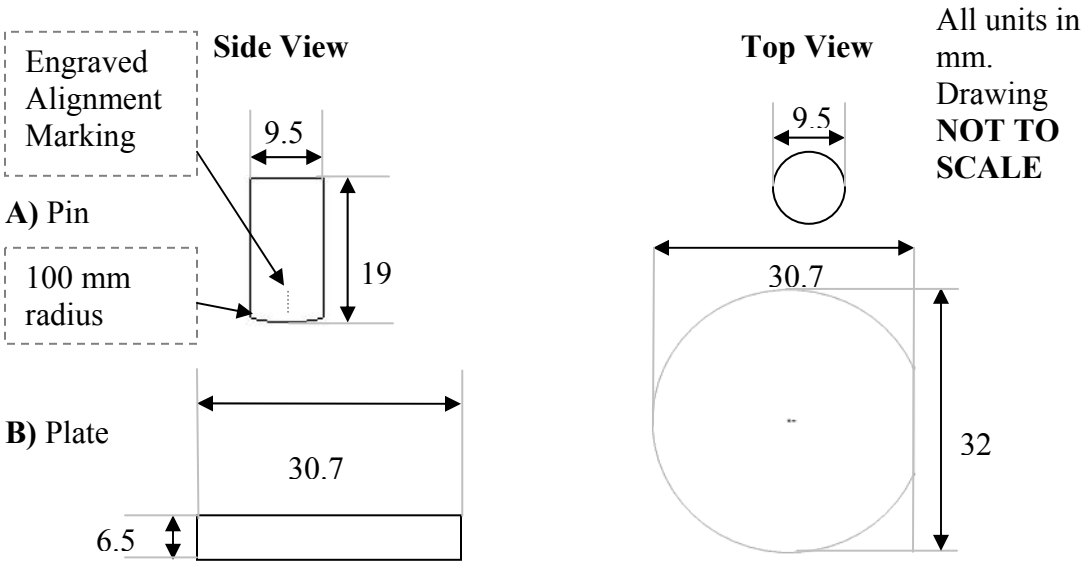

Fig. 27: Specimens A) Pin B) Plate

The radius on the pins is shown in Fig. 28. The image shows the PEEK OPTIMA specimens after the preliminary test. The pins illustrate clearly a smaller contact area than the surface area of the pin. There is a non-contact area ring approximately 1 mm in thickness between the edge of the pin and the edge of the polished contact area. Similar rings were noted on the CFR PEEK and CNF PEEK specimens after the first test interval.

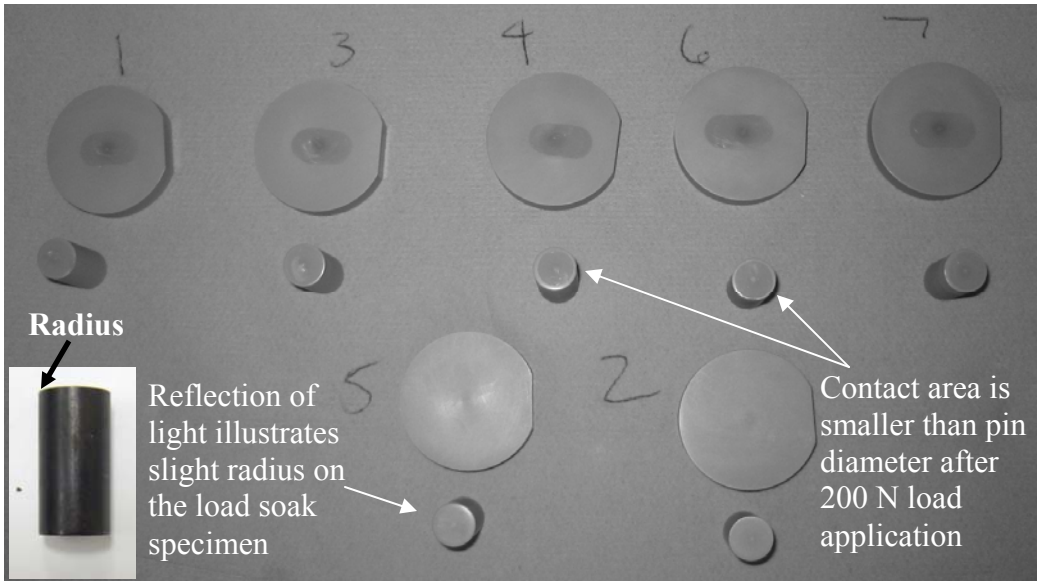

Fig. 28: Confirm of Radius on Pins (PEEK OPT)

The assigned pin and plate pairings are listed below in Table 8 for the three different material combinations.

Table 8: Specimen Pairings

	PEEK OPTIMA		CFR PEEK		CNF PEEK	
	Plate #	Pin #	Plate #	Pin #	Plate #	Pin #
Wear Test Specimens	1	1	1	10	1	1
	2	2	2	2	2	2
	3	3	3	8	4	3
	4	4	5	4	5	4
Load Soak Specimens	5	5	6	9	6	5
	6	6	7	7	7	6
	7	7	(only 6 specimens)		8	7

The numbering schemes for the stations in the OrthoPOD™ and load soak are shown in Fig. 29.

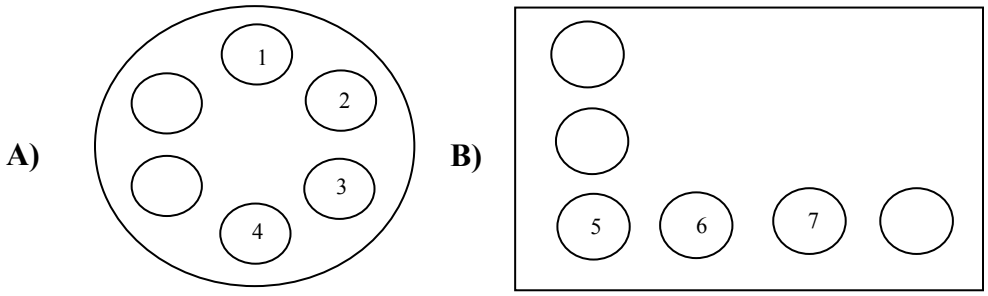

Fig. 29: Numbering Scheme for A) OrthoPOD™ B) Load Soak

Certain stations were not used in both apparatus due to the number of test samples. There were between 6-7 specimens of each material and load soak controls are essential and usually take up 2-3 of the specimens. Therefore both the OrthoPOD™ and load soak were not completely full.

4.2. Protocols

All PEEK specimens were supplied in sealed containers, submerged in lubricant. The preliminary test used a 25% bovine serum lubricant. The details of the two lubricants are found in Section 4.2.1. The protocols changed over the course of the tests and the lubricant was switched from 25% bovine serum lubricant to a 12g/L alpha calf fraction based lubricant as described in Section 4.2.1.

Four wear tests were performed. The first test, performed on PEEK OPTIMA, was a preliminary test to evaluate the effect of load increase. The test is performed quickly and determines if a load increase is worth investigating further. The preliminary test performed on PEEK OPTIMA, raised the load from 80 N to 200 N after only 0.01 Mc at the lower load level.

Details of the preliminary test can be found in Table 9. The intervals, both time and cycles, are shown in addition to the processes that took place. Further details include the temperature, load, and lubricant. The cleaning and weighing process are described in Sections 4.2.2.and 4.2.3, respectively

.

Table 9: Preliminary Test Protocol

PEEK OPTIMA						
Test	**Process**	**Time (Hours)**	**Cycles (Mc)**	**Temp (˚C)**	**Load (N)**	**Lubricant**
Conditioning	Clean and Weigh	~ (4 months)	0	20	0	Bovine
Preliminary	Clean and Weigh	44	0	20	0	Bovine
	"	54	0	37	0	Bovine
	"	~ 3	0.01	37	80	Bovine
	"	~ 6	0.02	37	200	Bovine

The PEEK OPTIMA 'baseline' test was completed several months after the preliminary test using the same specimen. A new wear path was chosen to ensure the results of the new test were on mostly new unworn material. The two wear paths on the PEEK OPTIMA specimen are shown in Fig. 30. The same pin was used, however, since weight measurements are taken at the beginning of the test, volumetric wear is still accurate. The onset set of adverse conditions may be slightly premature from the pin having been previously worn for a short interval.

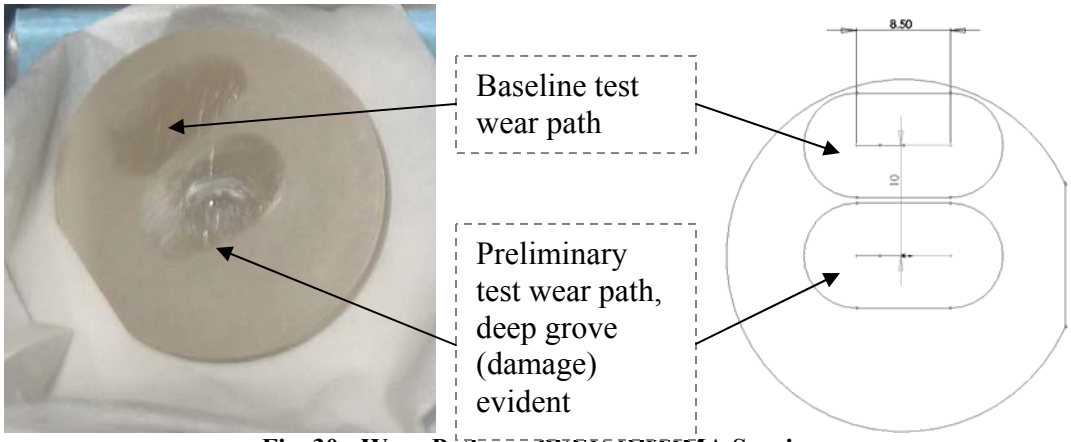

Fig. 30: Wear Paths on PEEK OPTIMA Specimen

The decision to switch lubricants was made at the beginning of the normal conditions tests for PEEK OPT. All tests completed after that point were completed with alpha calf fraction serum rather than 25% bovine serum. A 'baseline' prep test was performed using the new lubricant to determine if the weight of the specimen changed under the following conditions; room temperature vs. 37˚C in vivo temperature, and with or without an 80 N load.

The cleaning and weighing is performed much more frequently at the beginning of the PEEK OPT normal conditions test as a result of the uncertainty surrounding the wear behaviour of PEEK. It was deemed necessary to obtain adequate data points at the beginning of the test to formulate an appropriate test interval length. It was decided after

the first 0.2 Mc to perform the cleaning and weighing process every 0.2 Mc. The protocol for the 'baseline' test and the subsequent 'adverse' conditions test is shown in Table 10.

Table 10: PEEK OPTIMA Test Protocol

PEEK OPTIMA						
Test	**Process**	**Time (Hours)**	**Cycles (Mc)**	**Temp (˚C)**	**Load (N)**	**Lubricant**
Conditioning	Clean and Weigh	0	0	20	0	De-Ionized H_20
	"	21	0	37	0	Alpha
	"	48	0		80	
	Add Pin Engraving Marks + Clean and Weigh	72	0			
Normal	Clean and Weigh	191	0.01			
	"	215	0.05			
	"	238	0.10			
	"	334	0.20			
	"	402	0.40			
	"	476	0.60			
	"	551	0.80			
	"	669	1.00			
	"	907	1.20			
	"	1004	1.40			
	"	1075	1.60			
	"	1131	1.78			
	Clean, Weigh, Increase Load	1222	2.00			
Adverse	Clean and Weigh	1535	2.05		120	
	"	1560	2.10			
	Clean, Weigh, Increase Load	1655	2.15			
	Clean and Weigh	1702	2.20		180	
	Clean, Weigh, Increase Load	1822	2.30			
	"	3019	2.45		210	
	"	3067	2.60		240	
	Clean and Weigh	4052	2.75		300	

Specimens were cleaned and weighed every 0.05 Mc at the beginning of the 'adverse' condition tests and the load was increased as indicated in Table 10. It became apparent during the PEEK OPTIMA testing, that longer test intervals and significantly higher loads were required to induce failure. The low wear of the material seen at early stages of the test indicated cleaning and weighing was not necessary every 0.05 Mc and was subsequently performed only when the load was increased. A general guideline was used to indicate the value of the load at each interval, however, the point at which the material will fail is unknown and the load increase for each interval is dependent on the wear measured over the previous interval. On the basis of this experience, the protocols for CFR PEEK and CNF PEEK were modified to those shown in Tables 11 & 12.

Table 11: CFR PEEK Protocol

CFR PEEK						
Test	**Process**	**Time (Hours)**	**Cycles (Mc)**	**Temp (˚C)**	**Load (N)**	**Lubricant**
Normal	Clean and Weigh	0	0.00	37	80	Alpha
		69	0.25			
		163	0.59			
		233	0.84			
		302	1.09			
		372	1.34			
		441	1.59			
	Clean, Weigh, Increase Load	556	2.00			
Adverse	"	597	2.15		120	
	"	639	2.30		180	
	"	681	2.45		210	
	"	722	2.60		250	
	"	764	2.75		300	
	"	804	2.90		350	
	"	847	3.05		400	

The lower wear exhibited early in the CFR PEEK test caused the author to extend the test interval length to 0.25 Mc vs. 0.20 used in the PEEK OPTIMA tests.

Table 12: CNF PEEK Protocol

CNF PEEK						
Test	**Process**	**Time (Hours)**	**Cycles (Mc)**	**Temp (˚C)**	**Load (N)**	**Lubricant**
Baseline	Clean and Weigh	0	0.00	37	80	Alpha
	"	93	0.25			
	"	165	0.50			
	"	262	0.75			
	"	333	1.00			
	"	429	1.25			
	"	506	1.50			
	"	598	1.75			
	Clean, Weigh, Increase Load	671	2.00			
Adverse	"	765	2.15		120	
	"	822	2.30		180	
	"	864	2.45		210	
	"	905	2.60		250	
	"	949	2.75		300	
	"	989	2.90		350	
	"	1032	3.05		400	

4.2.1. Lubricant

Preliminary tests performed on PEEK OPTIMA utilized a 25% bovine solution. The bovine calf serum (Fisher Scientific, Whitby, ON) was diluted with de-ionized water. Fungizone and Streptomycin (Invitrogen Canada Inc., Burlington, ON) are added to inhibit fungal and bacterial growth. Ethylenediaminetetra-acetic acid, EDTA (EM

Science, Gibbstown, NJ) is added to inhibit calcium precipitation onto the surfaces. The quantities of the above additives are shown in Table 14. A certificate of analysis is issued from the serum supplier which contains the total protein concentration in a bottle from a specific batch. This concentration can potentially vary from batch to batch resulting in the need to recalculate the quantities listed in Table 13 and 14 if the batch number is different on new serum to maintain a protein concentration of 12g/L.

Table 13: Bovine Lubricant

Additive	Quantity
Bovine Serum	500 ml
EDTA	20 ml
Fungizone	5 ml
Streptomycin	3 ml
De-ionized H_20	1472 ml

The conventionally used sodium azide has shown inability to kill bacteria in certain hospital environments raising the need for other regimes of antibiotics to be used in serum [104, 105]. The lubricant used in the present thesis utilizes anti-mycotic antibiotic to kill bacteria rather than sodium azide.

Wear tests performed in the present thesis were primarily conducted in alpha serum with the exception of the preliminary tests performed on PEEK OPTIMA outlined above. The alpha lubricant consists of non-iron supplemented alpha calf fraction serum (Fisher Scientific, Whitby, ON) diluted with phosphate buffer solution (PBS) in the form of blood bank saline (VWR International, Mississauga, ON), to a protein concentration of 12g/L. A general antibiotic called Antimycotic (Invitrogen Canada Inc., Burlington, ON), was added to reduce the bacterial growth in the lubricant during testing. Table 14 lists the additives and quantities of the components of the lubricant.

Table 14: Alpha Lubricant

Additive	Quantity
Alpha Calf Fraction Serum	500 ml
Blood Bank Saline - PBS	1650 ml
Antibiotic - Antimycotic	5 ml

The alpha calf fraction serum and antibiotic are kept frozen until 12 hours before mixing. The PBS fluid is sealed and kept at room temperature. The components are mixed according to the solution proportions outlined in Table 14 and then separated into 250 ml containers. The containers are frozen and a single container is thawed individually before using the lubricant for wear testing.

The 12g/L protein concentration differs from the ASTM's [34] recommendation of 20g/L and the ISO's [32, 34] recommendation of 30g/L +/- 2 g. The lower protein concentration is thought to better reflect the situation in the cervical spine. It also reduces the possibility of distorted wear results due to protein degradation, which occurs most often in high protein concentration lubricant and is thought to mask the actual wear of certain materials [109].

4.2.2. Dis-assembly and Cleaning

In the present thesis protocols, lubricant was removed from each individual chamber prior to cleaning the specimens. The lubricant, especially in the latter stages of testing, can provide insight into the type of wear mechanisms taking place. Lubricant analysis examines protein degradation, bacteria levels and wear particles, however, this was not done in the present study. Lubricant from each individual was frozen and stored for potential examination in the future.

The pin and plate specimens were removed from the OrthoPOD^{TM} and cleaned at the end of every test interval. The specimens were initially rinsed with de-ionized water to remove anything weakly attached. This process helped to remove any degraded proteins that are floating in the lubricant and often adhere to the specimens after the lubricant is removed from the chambers. The specimens were then scrubbed with a soft bristled, clean tooth brush and rinsed again in de-ionized water. They were placed in individual jars filled with de-ionized water and then placed in an ultrasonic cleaner for 5 minutes. The ultrasonicator vibrated the specimens, which was done to help to detach any substances adhered to the surfaces. A 2% Liqui-Nox (a strong cleaning agent) was diluted with de-ionized water and then distributed into containers. Liqui-Nox is a strong cleaning solution that is diluted with de-ionized water.

The specimens were removed from the de-ionized water containers, rinsed again in de-ionized water, and ultrasonically cleaned in the Liqui-Nox solution for 10 minutes. The specimens are scrubbed with a soft bristled, clean toothbrush and antibacterial soap, rinsed in de-ionized water and returned to containers with de-ionized water to be ultrasonically cleaned for an additional 10 min.

The drying process involves rinsing the specimens with de-ionized water and then placing them in isopropanol alcohol for 5 minutes. They are then removed from the isopropanol and dried under a jet of nitrogen gas. The specimens are then carefully placed in a vacuum desiccator, and held in at 16 inches Hg for 1 hour.

4.2.3. Weighing and Re-assembly

PEEK wear was measured gravimetrically using an analytical balance (AX 205, Mettler-Toledo, Columbus, OH) with a precision of 0.01 mg and converted to volumetric wear in mm^3 using the densities of the different versions of PEEK. Volumetric wear calculations are described further in Section 4.2.4.

The balance was leveled prior to taking measurements by ensuring the air bubble was in the center of the indicator. The adjustable legs were used to level the balance if necessary. The balance was calibrated at the beginning of each weighing interval using an internal calibration command that provided a temperature value.

Ultra class standard weights (Troemner LLC, Thorofare, NJ) 1 g and 10 g were weighed one after the other for a total of three measurements each. The same process was repeated after the wear test and load soak specimens had been weighed. This process checked whether the balance had shifted over the course of the weighing process.

The pin and plate specimens were weighed 3 times sequentially to obtain 3 measurements per specimen. If the measurement for any particular pin or plate had a difference higher than 0.0001g, that particular specimen was re-weighed until the deviation specification was met.

The specimens were re-loaded back into the machine upon completion of the weighing process. New lubricant was used to fill each individual specimen chamber and the water bath that surrounds the lubricant filled specimen holders was replenished with

de-ionized water with addition of Clear Bath Algicide (VWR International, Mississauga, ON) to reduce the chance of bacterial growth in the actual specimen chamber.

The pins and plates were moved to the home location using the 'home' command on the OrthoPOD^{TM} software, and the position corrected as previously discussed in Section 3.1.4. The pins were lowered to a distance approximately 4 mm from the plates and the top portion of the OrthoPOD^{TM} was locked in place with the three locking post mechanisms. The rest load, previously set to 80 N, was applied to the specimens. The rest load was the load that would be applied to the specimens once a test was complete. The balance command was selected and applied for all wear tests performed for this project. The OrthoPOD^{TM} was started and run for the specified number of cycles.

4.2.4. Wear Measurements

Volumetric wear measurements involved subtracting the average fluid uptake value for the load soak specimen from the weight obtained for each wear test specimen. The ASTM [106] standard outlines a calculation method used to take fluid absorption into account during a test interval. Eqn. 3 is used to calculate the "fluid uptake" adjusted wear. The average mass gain of soak control specimens is expressed as S_{avg}. The mass of a specimen at the end of the test interval is W_2 and the mass of a specimen at the beginning of the test interval is W_1.

$$W = W_1 - (W_2 + S_{avg})$$

Eqn. 3: Wear in mg

The volumetric wear (Δ V) was calculated using Eqn. 4 for a test interval where ρ is the density of PEEK.

$$\Delta V = \frac{W}{\rho}$$

Eqn. 4: Volumetric Wear

The density of PEEK OPTIMA is 1.265 mg/mm^3 [12] while that of PAN CFR PEEK 30 wt% is 1.4 mg/mm^3 [12] and CNF PEEK is 2.0 +/- 0.4 mg/mm^3 [88].

A wear factor is often used to compare results of different wear test studies. Archard's law [44], previously stated in Eqn. 2, can be simplified to the form expressed in Eqn. 5. The wear factor is denoted by K, is expressed in $mm^3\ N^{-1}\ m^{-1}\ 10^{-6}$. The change in volume, ΔV , is the change in volume over a specified test interval. The applied load, F, is the applied load expressed in Newtons. The sliding distance, x, is expressed in meters.

$$K = \frac{\Delta V}{F \bullet x}$$

Eqn. 5: Wear Factor

The volumetric wear vs. no. of cycles is plotted for all the specimens of the same material. A slope is then obtained from a trend line plotted over the specified interval for each specimen. The individual slopes are used to calculate a K value for each specimen and finally the K values are average to obtain an average wear factor. Wear results generally depict a run-in period with a significantly steeper slope, and therefore the slope selected for wear factor calculations is usually the steady-state region following the run-in region. The simplified version of Archard's law shown in Eqn. 5, implies wear increases linearly and is proportional to applied load, F, and the sliding distance, x. The slope obtained from the selected interval is expressed in mm^3/Mc. The slope is used as the Δ V value in Equation 4.

The sliding distance entered into the equation is simply twice the stroke length. The rotation the pin goes through adds lateral sliding distance to the x value. This value is small compared with the "longitudinal" sliding and is not included in the present thesis in the x value used in the wear factor calculations.

4.2.5. Contact Stress

Polymeric material pairs, articulated against each other, experience wear and the surfaces can become smooth and thus the apparent area of contact may be about the same as the real area of contact, assuming perfectly smooth surfaces. However, if the surfaces are wear resistant and roughen as they wear, the real area of contact can be significantly smaller than the apparent area of contact because it is the sum of the contact areas at the

asperity tips. If the real area of contact equals the apparent area of contact, local frictional forces are related to contact stress. In this situation the contact stress is calculated from Eqn. 6. Wear is influenced by the way in which the material accommodates local frictional forces.

Sub-surface fatigue wear mechanisms can take place and are dependent on sub-surface shear stresses as well. A given material pair and configuration can have related surface shear stress and contact stress. Contact is therefore an important tribological parameter.

Average contact (σ_{avg}) stress is useful when attempting to compare the present thesis pin-on-plate results to the results of other pin-on-plate tests provided the real and apparent areas of contact are about the same as discussed previously. Contact stress is calculated using Eqn. 6, where a is the radius of the contact area for the pin surface and F is the applied load in Newtons.

$$\sigma = \frac{F}{\pi * a^2}$$

Eqn. 6: Contact Stress Formula [110]

At the start of the wear test, the contact radius area (a) can be predicted using Hertzian theory shown in Eqn. 7, where R is the pin tip radius.

$$a = \left(\frac{1.5\ F\ R}{E'} \right)^{1/3}$$

Eqn. 7: Hertzian Theory

It can be useful to consider the intial contact stress when considering wear. A calculation is included in Appendix D that determines how much wear has to occur on the pin to flatten it's tip. The volume of the tip of the pin should equate to the volume lost due to wear, assuming the pin is entirely flat at the end of the wear test and has only lost the height of the spherical tip. The wear results for PEEK OPTIMA are most similar to the volume of the spherical tip. The CFR PEEK wear value is much less than the volume of the tip which correlates with the appearance of the CFR PIN, a radius is apparent at the

end of the wear test. The CNF PEEK has a wear value much higher than the volume of the tip indicating the spherical tip is worn down completely as well as additional material. The diameter of the contact area at the end of the wear test is the same as the original diameter of the pin.

4.2.6. Microscopy

Surface analysis was performed using a JSM-6460 (JEOL, Peabody, MA) scanning electron microscope (SEM). It reveals damage that could not be quantified using conventional volumetric wear.

Images were taken of PEEK OPT, CFR PEEK and CNF PEEK at various stages during the wear tests but, in particular just before or just after the material began to exhibit significant surface damage.

The PEEK OPT pin and plate specimen were coated after 2.75 Mc because the test was complete. The surface damage seen with the naked eye on the pin and plate specimens indicated no further wear testing was necessary. SEM images are taken of the CFR PEEK at 2.90 Mc and 3.05 Mc. In this case, a coating was unnecessary because the carbon in the sample limits the electron charging. However, bright white areas are noted on the CFR PEEK images, shown in Section 5.5 where the electrons charge the surface, suggesting the coating would have allowed better analysis/imaging.

4.3. Concluding Remarks

The geometry of test specimens, pairing schemes, lubricant details, cleaning and weighing procedures are described in the present chapter. Calculation methods are explained for volumetric wear, wear factors and contact stress. Finally, the details of processes, load used and temperatures maintained are described at different intervals of the preliminary, normal and adverse conditions tests.

5.0 RESULTS AND DISCUSSION

The following section contains the results of the preliminary tests used to assess the influence of temperature, lubricant and load on fluid uptake. Tests were conducted to confirm the influence of location on fluid uptake. The specimens were evaluated in their original locations, specimens 1, 2, 3 and 4 in the OrthoPOD^{TM} and specimens 5 and 6 in the load soak. The location of each specimen is reversed to determine if it is the specimens that govern the amount of fluid uptake or the location of the specimens. The wear results are presented for both the normal conditions tests, i.e. applying 80 N of load for 2.0 Mc, and also for the adverse conditions tests, increasing the load every 0.15 Mc until failure is noted. The wear rates calculated for these tests are compared to those published in the literature for different contacts. Different contacts refer to different materials, loads, motions and lubricant. Finally, microscopy is presented to highlight the failure mechanisms seen on the each of the materials.

5.1. Preliminary Tests

A considerable amount of effort was spent to determine the effect of temperature and load on fluid uptake. The load soak specimens were used to account for fluid uptake in the wear test specimens as was shown in Eqn. 3. Checking of the load soak apparatus was necessary to ensure correct adjustments were made to the wear test specimens because accurate results depended on the fluid uptake of the wear test specimens being very close to the fluid uptake of the load soak control specimens. The load and temperature of the load soak specimens should be the same as the wear test specimens.

5.1.1. Effect of Fluid Composition, Temperature and Load on Fluid Uptake

The effect of temperature and load was evaluated in two separate studies performed on the OPTIMA version of PEEK. It is assumed that any major fluid uptake fluctuations apparent in the OPTIMA version of PEEK, would also be an issue in both the CFR and CNF versions of PEEK.

The tests began with the specimens being soaked in either de-ionized water or lubricant at room temperature, 20˚C. They were then placed in the holders used for wear testing and soaked in lubricant held at 37˚C. Fig. 31 shows the impact of temperature and

load in the first study. This test was performed on unworn specimens. The graph indicates the specimens do not show any significant change when the temperature was raised. Application of an 80 N static load did not result in a significant change in mass.

The scale on the graph below was selected to illustrate the temperature and load effect on fluid uptake in comparison to the change in mass due to wear testing. Wear test specimens experienced a change in mass up to 4 mg.

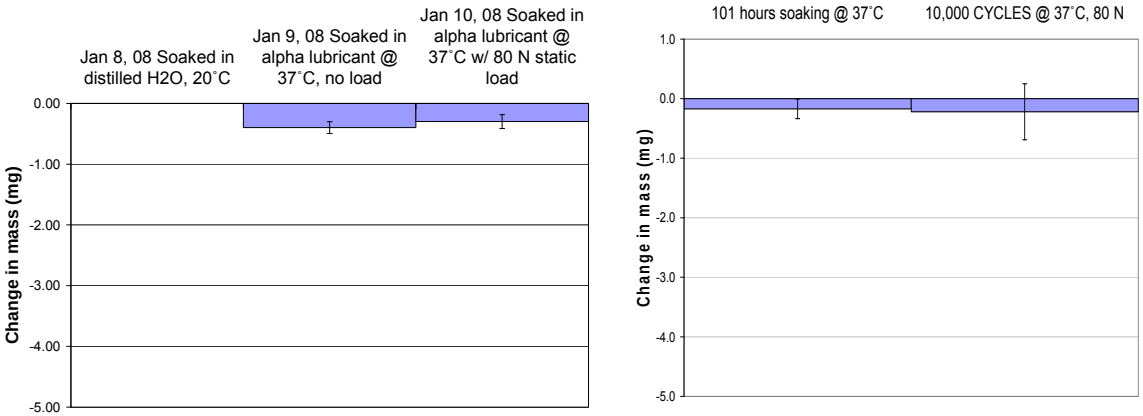

Fig. 31: Effect of Temperature (Above Left) & Load (Above Right) on Fluid Uptake – Study 1

The second study was performed before the PEEK OPTIMA normal conditions test. The specimens were soaked in bovine serum for several weeks after the preliminary test and the commencement of the following test marks the point where the new alpha serum was adopted. The results of the second study are shown in Fig. 32.

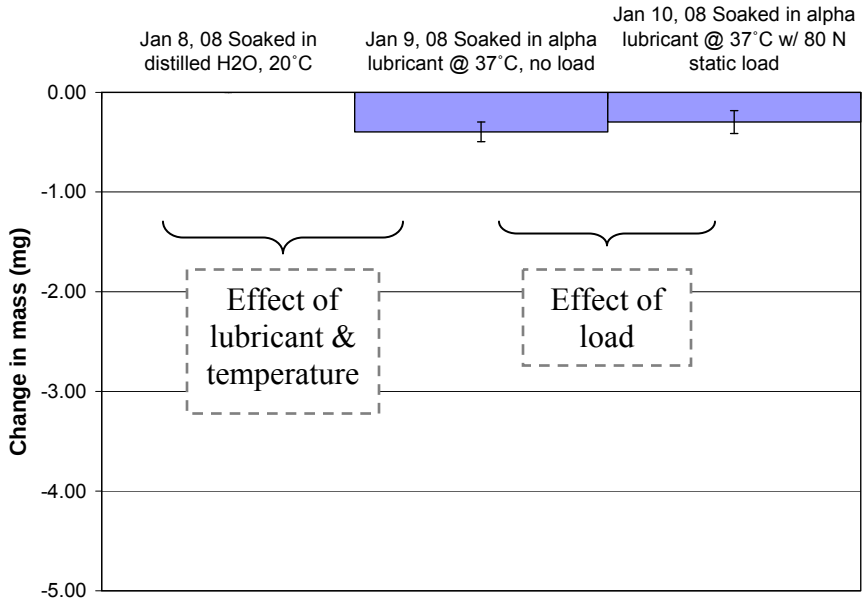

Fig. 32: Effect of Temperature and Load - Study 2

The above is shown on the same scale as Fig. 31 and 33 to emphasize the minimal effect of transferring specimens from de-ionized water to alpha lubricant, increasing the temperature and adding an 80 N static load. The above graph is put in context of the entire wear test in Fig. 33, as it compares the fluctuations seen above with those experienced over a 2.0 Mc wear test.

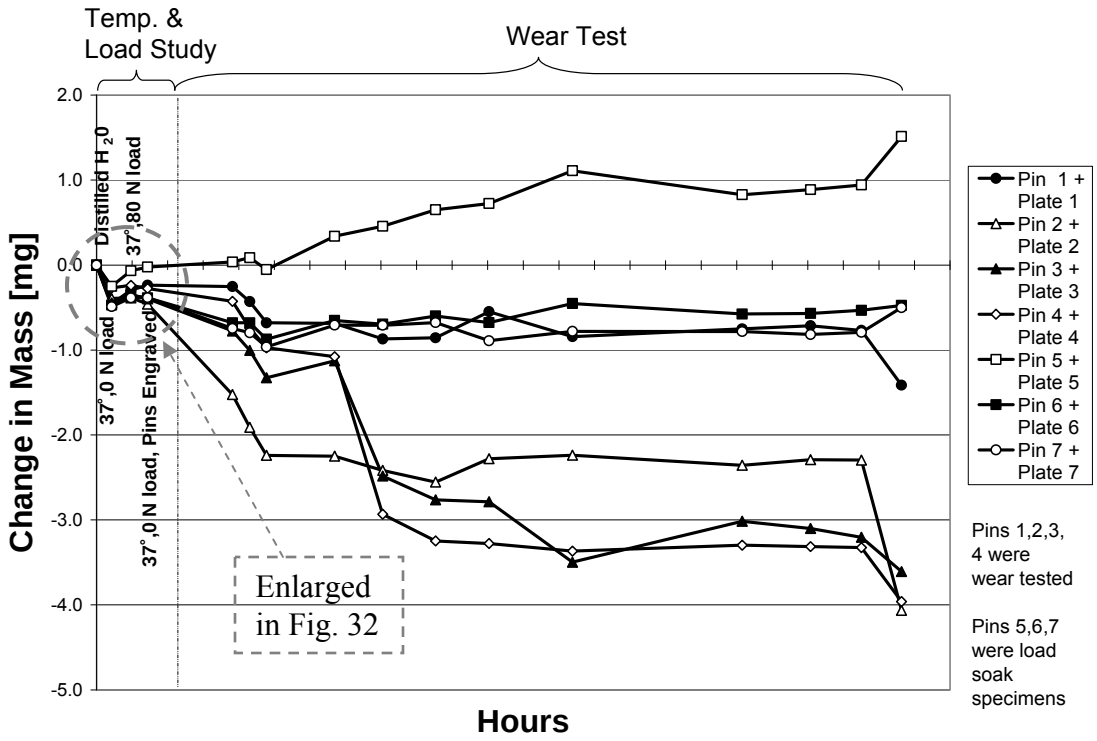

Fig. 33: Change in Mass (mg) for PEEK OPTIMA pairs (plate+pin)

Fig. 33 illustrates the unusual behaviour of load soak specimen 5. Appendix E examines this in more detail. The load soak specimens must behave in a similar manner to be credible. Plate 5 of the PEEK OPT specimen exhibits behaviour uncharacteristic of the rest of the load soak controls. Generally, as seen in Appendix E, the load soak specimens experience similar changes in weight.

5.1.2. Fluid Uptake – Load Soak vs. OrthoPOD^{TM}

The original location of the specimen pairs in both the OrthoPOD^{TM} and the load soak are shown in Fig. 34. The fluid uptake test is performed to investigate the fluid uptake behaviour of the specimens when placed in the load soak vs. the OrthoPOD^{TM}.

The diagram below shows the location of the specimen pairs before and after their locations are reversed.

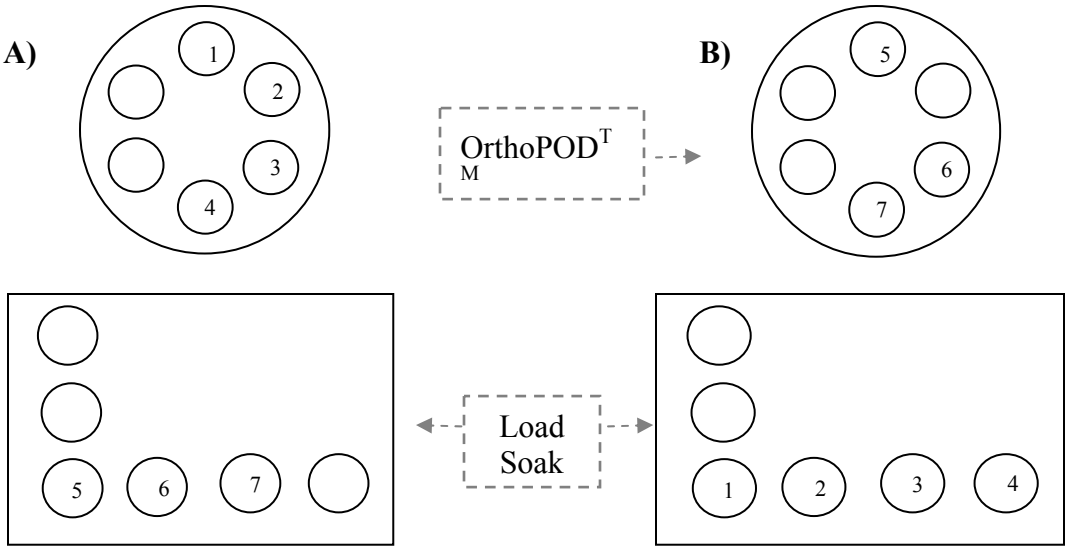

Fig. 34: Fluid Uptake Test A) Original Location B) Reversed Location

The graphs shown in Fig. 35 indicate the load soak specimens experience very similar fluid uptake to those in the OrthoPOD™.

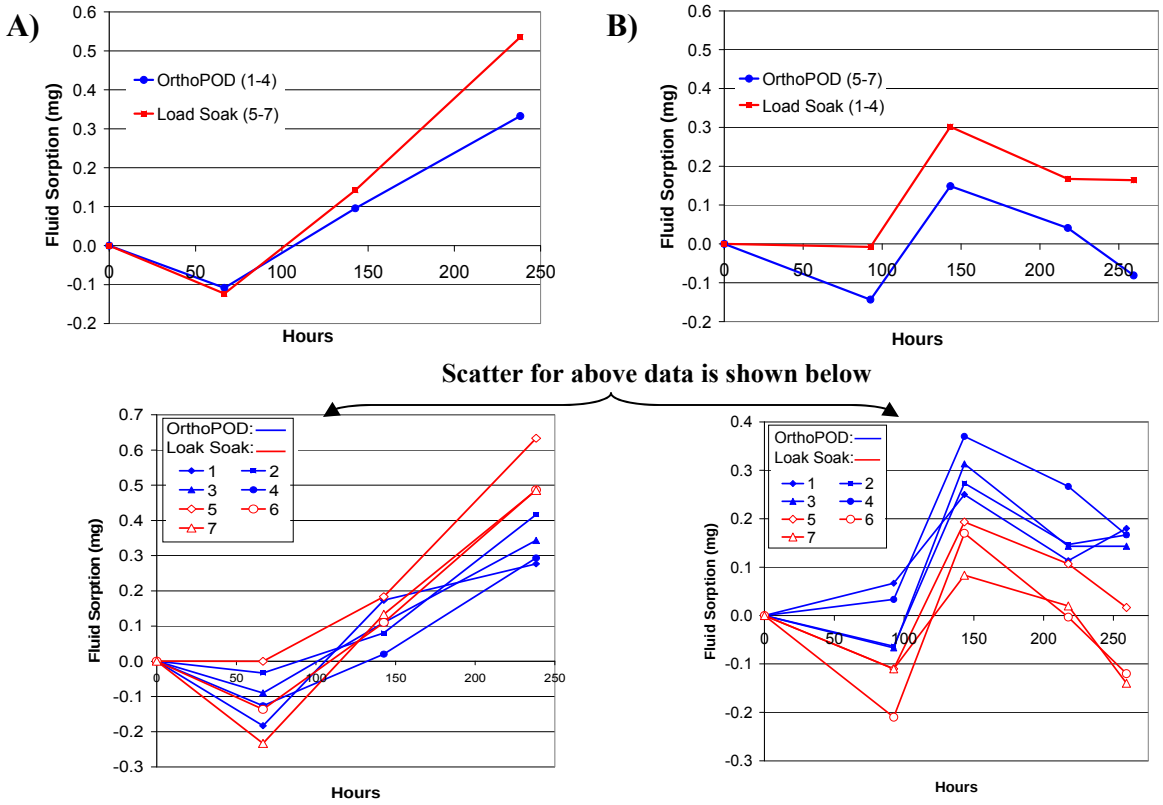

Fig. 35: Average Fluid Uptake Study A) Original Locations B) Locations Reversed

The tests also indicate fluid uptake is not significantly affected by the location of the specimens. The two lines represent averages of the fluid uptake of the 3-4 specimens in each location and indicate the specimens exhibit the same trend in fluid uptake regardless of location. The conditions remain the same and the change in fluid uptake from one reading to another is much more significant than the difference between the two locations. It is possible the fluctuations are due to changes in the environment, i.e. uncontrolled humidity in the lab, or slight fluctuations in cleaning and weighing protocols.

Materials that exhibit low wear require accurate load soak controls. Using a separate, external load soak apparatus is not ideal. A pin-on-plate machine that permits independent pin control would result in very accurate load soak control values. An apparatus with independent pin control would entail rotation and loading in some stations, and simply loading in others. The current apparatus rotates all pins and therefore load soak controls are placed in a separate apparatus that only applies load. It was not possible to maintain exactly the same conditions in two separate apparatuses given the environment factors of the current study.

5.2. Normal Conditions

Normal conditions refer to reciprocating motion between the pin and plate. The pin moves at a frequency of 1 Hz, through an 86˚ angle and a load of 80 N is applied. The wear test runs for 2.0 Mc and then the load is increased as the adverse conditions test begins. This test is performed on all three versions of PEEK and is presented graphically in the next section.

5.2.1. PEEK OPTIMA

The normal conditions test wear curves are shown in Fig. 36. Trendlines are also plotted to highlight the interval the slope was taken over to calculate the wear factors. The load soak specimens were averaged and that weight was subtracted off each of the weight of each of the wear test specimens. The net fluid adjusted weight is divided by the density of the material to obtain volumetric wear.

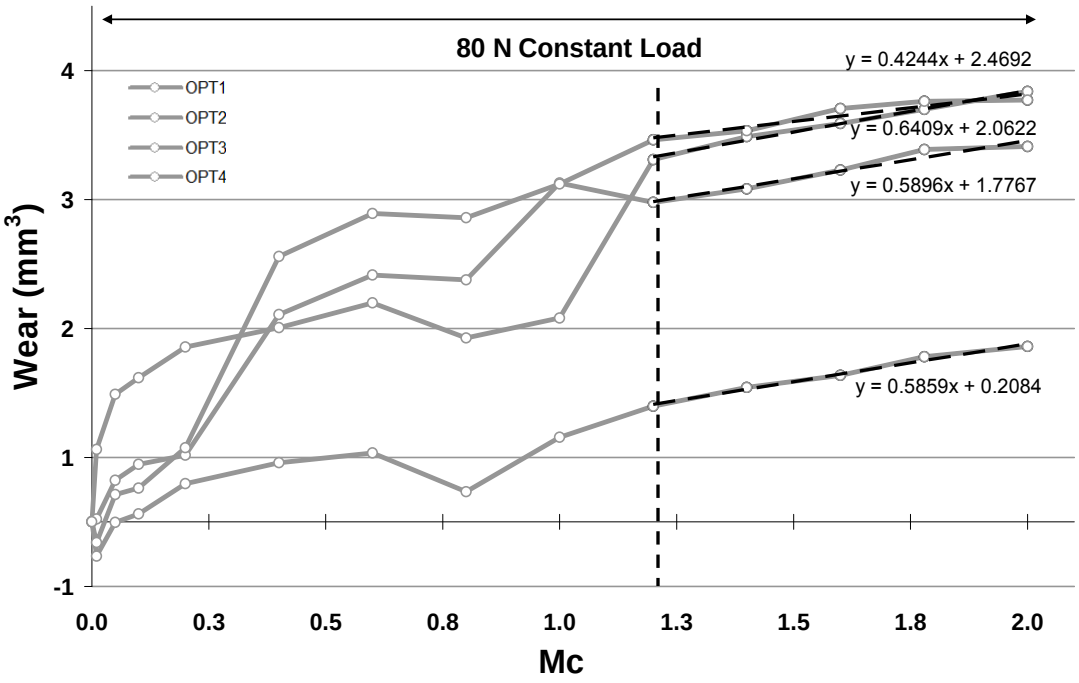

Fig. 36: PEEK OPTIMA Wear Curves

The above wear curves are presented to illustrate the overall range of wear. An average wear value can be misleading because one particular specimen exhibits higher or lower wear than the others. The volumetric wear curves are shown above and the wear factors are calculated from the trend lines plotted over the 1.2 – 2.0 Mc range in which the curves are fairly linear and are, therefore, considered steady state. Wear factors are calculated using the slopes of these trend lines mm^3 vs. Mc. Each slope is divided by twice the stroke length in m, the applied load in N and the number of cycles in the interval over which the slope is calculated to give the wear factor. The values for the stroke length and applied load are 0.085 m and 80 N respectively. Table 15 presents the results for PEEK OPTIMA obtained from Fig. 36.

Table 15: Volumetric Wear & Wear Factors for PEEK OPTIMA - Normal Conditions

Range of Volumetric Wear (mm^3)	**1.36 - 3.34**
Average Volumetric Wear (mm^3)	**2.72** ±0.93
Range of Wear Factors (mm^3/Nm x 10^{-7})	**3.12 – 4.71**
Average Wear Factor (mm^3/Nm x 10^{-7})	**4.12** ±0.69

5.2.2. CFR PEEK

The CFR PEEK samples present wear results in the negative region. This is due to the weight of absorbed fluid being greater than the weight of material lost due to wear. A detailed examination of the load soak specimen in relation to the wear test specimens is included in Appendix E. The wear curves of the CFR PEEK wear tests specimens are very similar to the load soak specimens, indicating virtually no wear.

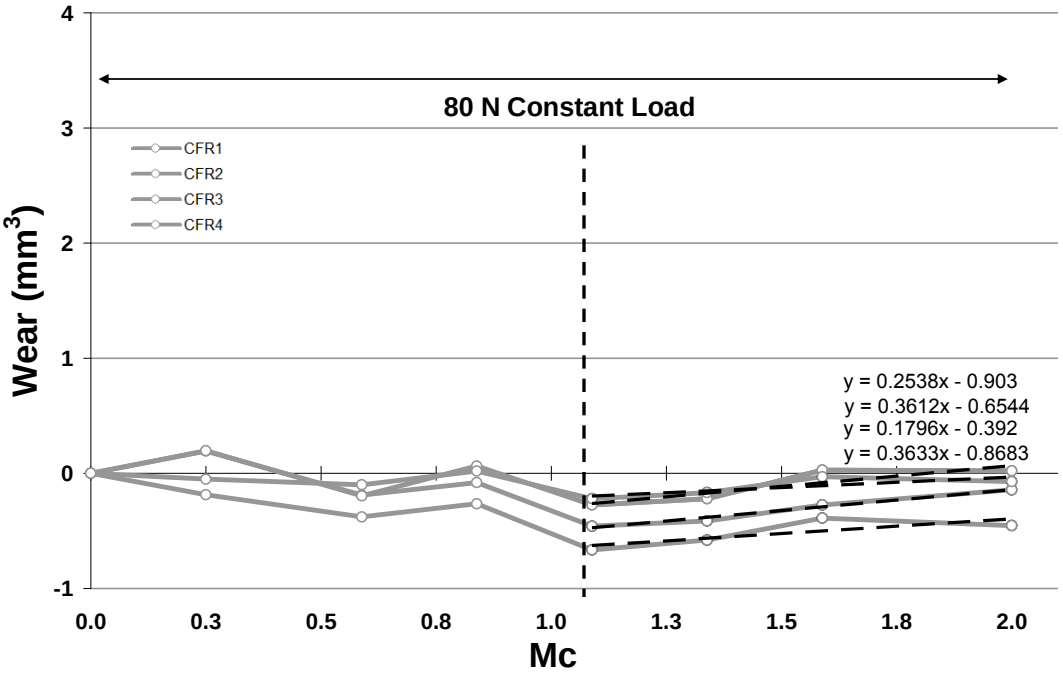

Fig. 37: CFR PEEK Wear Curves

The wear factors for CFR PEEK are determined over the 1.09 – 2.0 Mc range shown in Fig. 37. The trend line equations are included to illustrate the slope values used to calculate the wear factors. It is important to differentiate between the wear presented in Fig. 37 and the PEEK OPTIMA wear shown in Fig. 36. The PEEK OPTIMA wear factors are calculated once steady state wear is reached. The run-in wear factors would be much higher than the wear factors calculated in the steady state region. The CFR PEEK wear factors are calculated over the only region that would produce a positive slope for the trend line introducing a lack of precision into the results. The significance of this is that the wear factors for PEEK OPTIMA are reported over the region with the lowest wear rate, i.e. most gradual slope. The CFR PEEK wear factors are reported over

the region with the highest occurring wear rate because that is the only region that produces realistic values. The above wear curves are summarized in Table 16.

Table 16: Volumetric Wear and Wear Factors for CFR PEEK - Normal Conditions

Range of Volumetric Wear (mm^3)	**-0.45 – 0.02**
Average Volumetric Wear (mm^3)	**-0.16** ± 0.21
Range of Wear Factors ($mm^3/Nm \times 10^{-7}$)	**1.32 - 2.67**
Average Wear Factor ($mm^3/Nm \times 10^{-7}$)	**2.13** ± 0.66

The wear factors calculated for CFR PEEK are unlikely to be accurate. The change in wear over the linear region is less than the precision of the wear measurements themselves. Therefore, the calculated wear factors are essentially meaningless however they are presented in Table 16 in an effort to provide a likely upper limit for the CFR PEEK wear.

5.2.3. CNF PEEK Wear Curves

Wear curves for CNF PEEK are shown in Fig. 38.

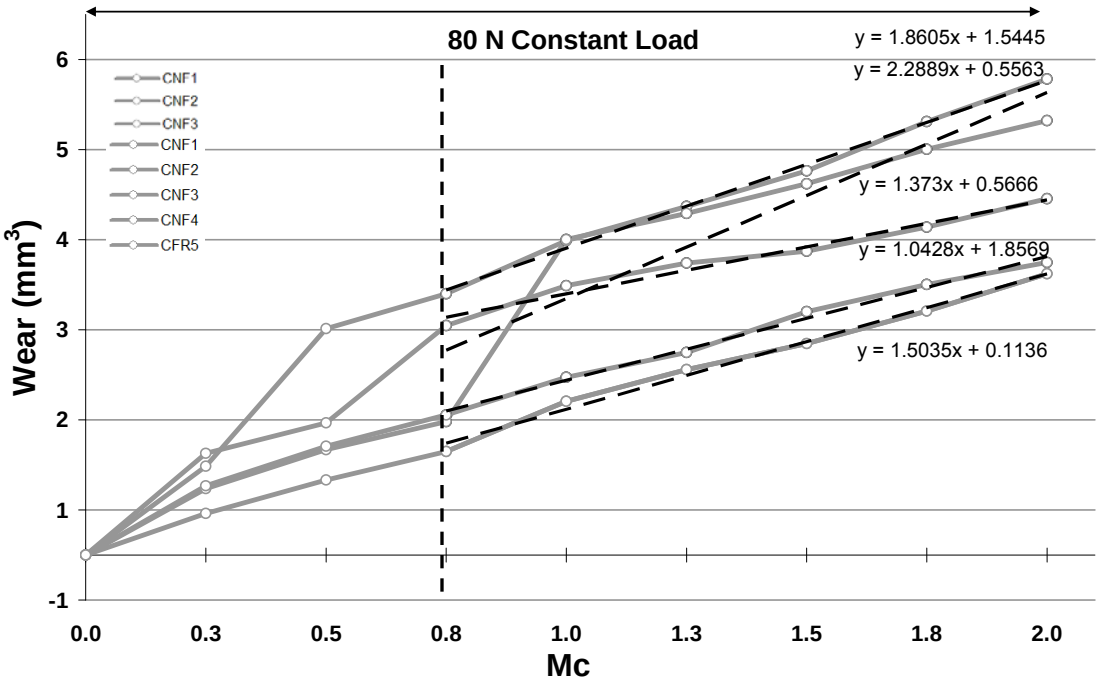

Fig. 38: CNF Wear Curves

CNF PEEK cleaning and weighing procedures were completed by Dan Langohr, University of Waterloo M.A.Sc. Candidate

The wear factors for CNF PEEK are calculated over the steady state range of 0.8 – 2.0 Mc. The CNF PEEK specimens appear polished before the wear test begins. Whereas the polishing process occurs early on in the PEEK OPTIMA and CFR PEEK wear tests. This may have caused more adhesive wear and/or friction heating in CNF PEEK in comparison to the other versions of PEEK. The wear data for CNF are summarized in Table 17.

Table 17: Volumetric Wear and Wear Factor for CNF PEEK - Normal Conditions

Range of Volumetric Wear (mm^3)	**3.12 – 5.28**
Average Volumetric Wear (mm^3)	**4.09** ± 1.11
Range of Wear Factors ($mm^3/Nm \times 10^{-7}$)	**7.67 – 16.83**
Average Wear Factor ($mm^3/Nm \times 10^{-7}$)	**11.87** ± 3.51

These CNF PEEK results contradict the findings of Werner et al. [86] for a ball-on-prism test using commercial grade CNF PEEK and PEEK OPT. The specimens were held in a metallic prism and pressed against a 100Cr6 steel ball. The applied force, sliding speed, frequency and contact stress ranges were 21.2 N, 2.82 m/s, 1 Hz and 3-27 MPa respectively. Werner firmly concluded the addition of carbon nanofibres "significantly" reduces the wear rate of PEEK in these tests.

5.2.4. Comparison of PEEK OPTIMA, CFR PEEK and CNF PEEK

The results of the normal conditions tests for all three materials are presented in Fig. 39. The lowest wear values occur when articulating CFR PEEK against itself.

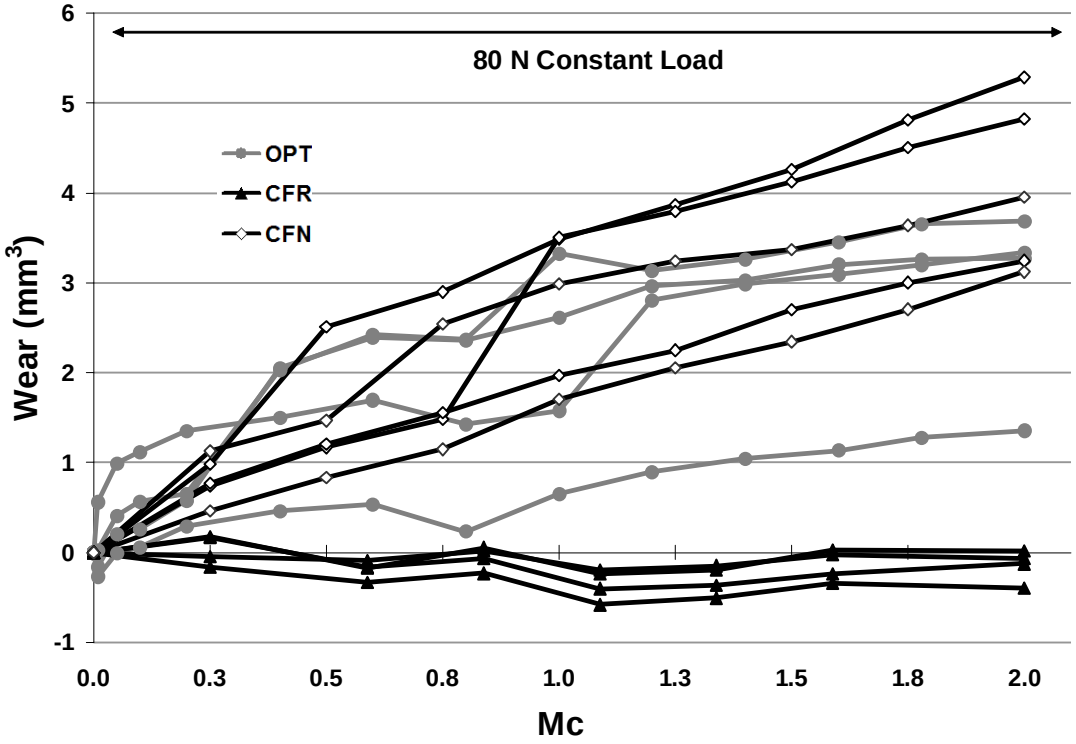

Fig. 39: Normal Conditions Wear Curves

The individual wear curves are shown above rather than the average of the wear test specimens to indicate the repeatability of the results. The present author suggests that the steady-state wear rates of CFR PEEK specimens show very little variation between specimens. PEEK OPT and CNF PEEK show more variation; however, the specimens illustrate similar wear rates and wear behaviour. The average volumetric wear values are compared for the three versions of PEEK in Table 18.

Table 18: Average Volumetric Wear Values after 2.0 Mc for PEEK OPT, CFR PEEK & CNF PEEK

Material	Average Volumetric Wear (mm^3)	Average Wear Factor ($mm^3/Nm \times 10^{-7}$)
PEEK OPTIMA	2.72 ± 0.93	4.12 ± 0.69
CFR PEEK (30wt% PAN)	-0.16 ± 0.21	2.13 ± 0.65
CNF PEEK	4.09 ± 0.95	11.87 ± 3.5

The wear of CFR PEEK is the lowest of three materials tested. The wear is so low that the average volumetric wear value is negative. This phenomenon is not completely understood, however it is possible the worn surface could absorb more protein. A negative wear value is generally the result of a higher mass gained due to fluid uptake, than actual mass lost due to wear. However, the fluid uptake calculations

explained in Eqn. 3 should remove the fluid uptake influence from the wear values. There exists a possibility that the behaviour of the wear test specimens is different from the load soak control specimens with respect to fluid uptake. Preliminary tests determined the PEEK OPTIMA fluid uptake to be very similar in the both the OrthoPOD^{TM} and the load soak as illustrated in Fig. 35. The largest difference in fluid uptake experienced by specimens in the OrthoPOD^{TM} versus the specimens in the load soak is 0.25 mg. It is not possible to convert this value directly to a mm^3 unit because it is a measurement of fluid rather than wear material. Nevertheless this fluid uptake difference, 0.25 mg, is much larger than the maximum wear experienced by CFR PEEK, 0.03 mg. This leads to the conclusion that what was once initially believed insignificant considering the significantly higher wear of PEEK OPTIMA is now believed to be very significant considering the extremely low wear experienced by CFR PEEK. It quite possible that the difference in fluid uptake between the two apparatus' could push the wear values of CFR PEEK into the negative region, meaning the mass gained by the fluid uptake is greater than that lost by wear.

5.2.4.1. Comparison of Wear Rates for Different Contacts

The results shown in Table 18 are compared to wear rates from the literature. The results are for different contacts, tested on pin-on-plate machines. Table 7 provides further details on the studies presented in the graph below. The significance of Fig. 40 is to illustrate how the materials tested in the present thesis compare to material currently in use in orthopaedic applications. Studies that reported factors higher than 20 $mm^3N^{-1}m^{-1}10^{-7}$ are omitted from the graph below to better depict the comparison of the current results to material combinations that produced similar wear rates. A comprehensive comparison of all pin-on-plate studies presented in the literature, and the present results, can be found in Appendix B.

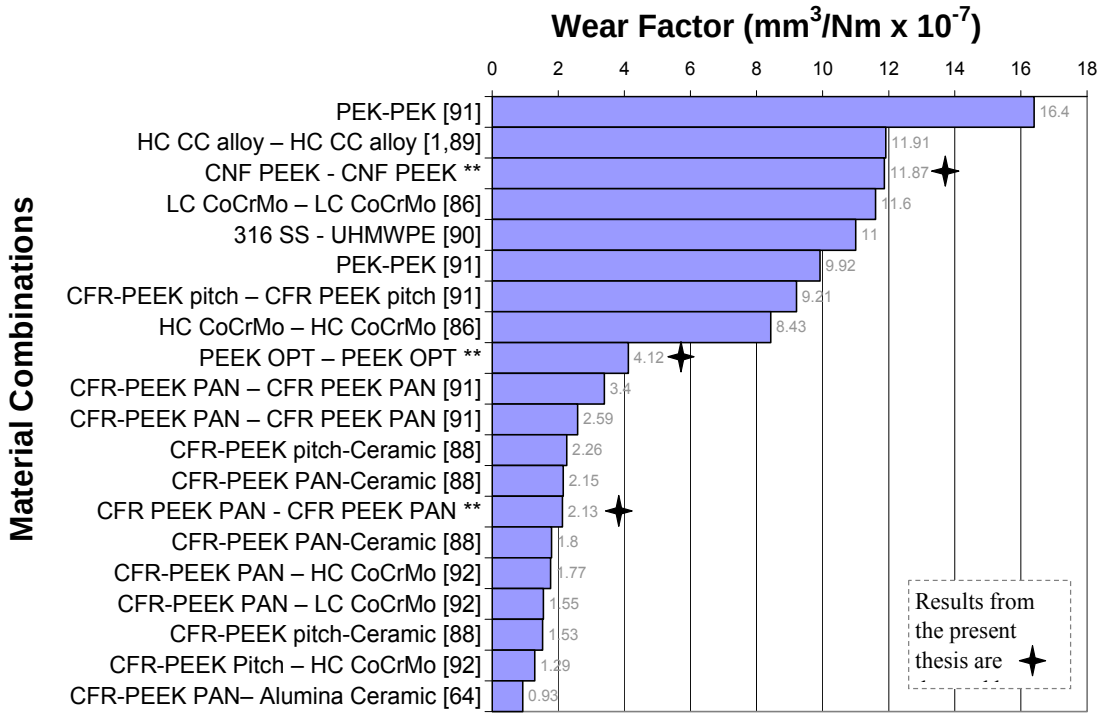

Fig. 40: Comparison of Results and Studies from the Literature (wear rates < 20 mm^3/Nm x 10^{-7})

The wear rate of CNF PEEK is most similar to that reported for HC(0.2%) CC alloy [49, 98] articulating against itself and LC(0.06%) CoCrMo [95] articulating against itself. A review of the wear rates and the studies that produced them reveals a significantly different contact stress for each study. The HC(0.2%) CC [49, 98], the present data and the LC(0.06%) CoCrMo [95] had contact stress values of 10 MPa [49, 98], 1.1 MPa [14], and 2 MPa [95], respectively.

The wear rate of PEEK OPTIMA in the present study, with a contact stress of 1.1 MPa, is most similar to the reported [100] wear rate for CFR-PEEK PAN articulating against itself for which the contact stress was 2 MPa.

The wear rate of CFR PEEK is most similar to the wear rate reported for CFR-PEEK OPT PAN articulating against a ceramic based material [97]. Again the average contact stress exhibited in the present study is half the magnitude of the average contact stress exhibited in the CFR-PEEK OPT PAN-ceramic study [97].

5.2.4.2. Comparison of Wear Rates for Various PEEK pin-on-plate Studies

The wear rates calculated in the current study are compared to wear rates reported in the literature for PEEK materials articulating against either themselves or another material. Details of the studies chosen from the literature can be found in Table 7.

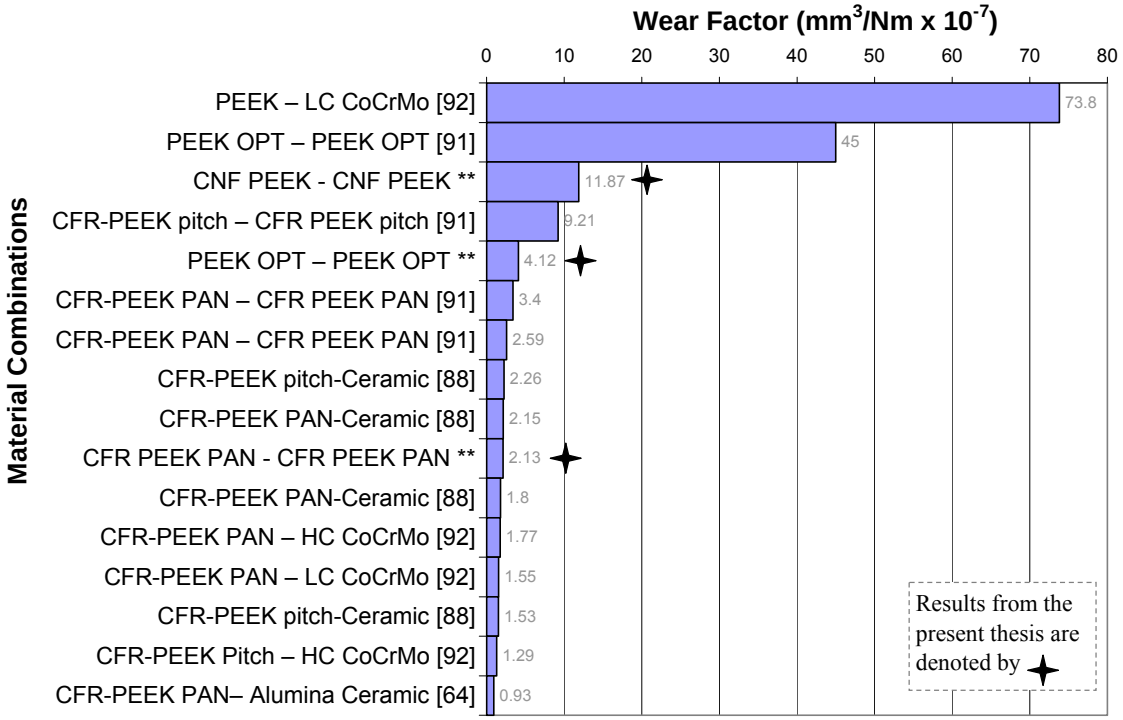

Fig. 41: Comparison of PEEK Wear Rates

The studies are displayed in order of highest to lowest wear rate. It is very interesting that a wear rate of 45 $mm^3N^{-1}m^{-1}10^{-7}$ is reported by Scholes [100] for PEEK OPTIMA articulating itself compared with that of the present study of 4.12 $mm^3N^{-1}m^{-1}10^{-7}$ for materials from the same source. The source of the difference between results for the same articulating material is unknown. The materials used for Scholes' [100] study are manufactured by the same company that supplied the materials for the present thesis studies. The contact stress reported for Scholes' study [100] is twice that used in the present study. ,

The wear rate calculated for CFR PEEK articulating against itself is very similar to wear rates reported in the literature for the same material.

In contrast, the wear rate of CNF PEEK articulating against itself is almost an order of magnitude higher than the majority of wear rates reported for CFR PEEK. This indicates addition of nanofibers do not improve the wear characteristics of PEEK.

A wear rate of 73.8 $mm^3N^{-1}m^{-1}10^{-7}$ obtained from PEEK OPTIMA articulating against LC CoCrMo, reported by Scholes [101], is considerably higher than the wear rates reported for other PEEK studies. This value, in addition to another reported [100] wear rate of 45 $mm^3N^{-1}m^{-1}10^{-7}$ for PEEK OPTIMA articulating itself, are omitted from Fig. 42 because they are considerably higher than both the current study and the remainder of the studies in the literature.

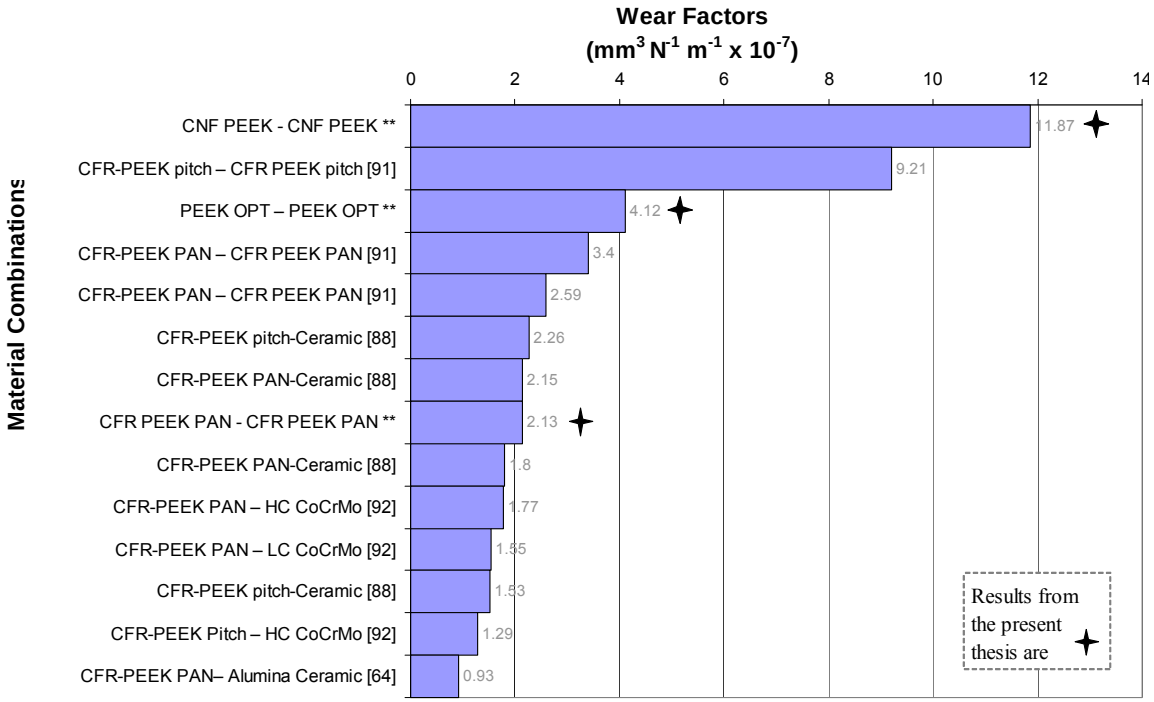

Fig. 42: Comparison of Results to PEEK studies from the literature (2 studies not shown in graph)

5.3. Observations on the Effect of Protein Degradation on Wear

Protein degradation is discussed in section 3.1.3 and is depicted in Fig. 43. As the surface temperature and loads are increased, proteins begin to die. The death of the protein, referred to as protein degradation is noted by the white deposits sitting in the bottom of the specimen holder, shown at the top of Fig. 43. The effect of protein degradation on wear behaviour is not entirely understood. However, a multi-laboratory simulator study [109], performed on PTFE cups and CoCr heads, reported a 200% wear

rate increase as the protein concentration was raised from 17 g/L to 69g/L. The relevance of this study to the current project is the relationship found between protein degradation and wear. Protein degradation can result in higher levels of wear. This is interesting due to the change in parameters between the PEEK OPT and CFR PEEK tests. The protein degradation appeared to be significantly reduced by isolating the chambers from air flow after the PEEK OPTIMA tests were completed. It is possible that the protein degradation increased the wear values of PEEK OPTIMA in some specimens. The wear curves for PEEK OPTIMA are shown along side images of the protein degradation in Fig. 43. Protein degradation of this magnitude was not seen in any of the specimens for the other two versions of PEEK.

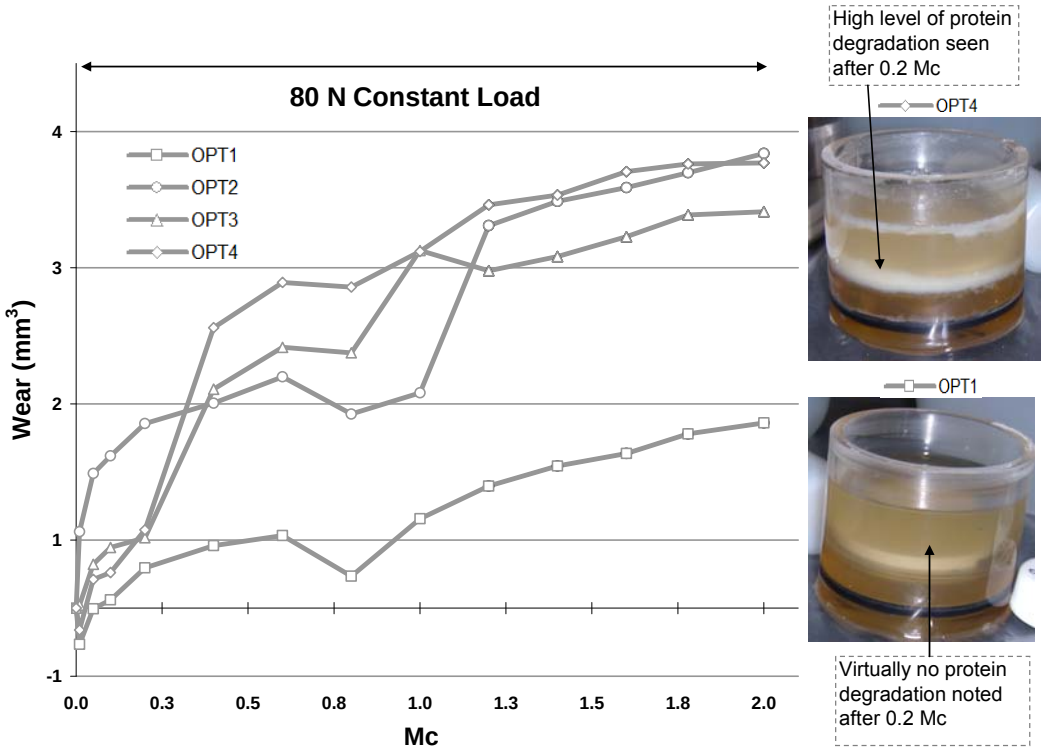

Fig. 43: Protein Degradation and Wear Curves for PEEK OPTIMA Normal Condtions

The protein degradation is most extreme in chamber 4, yet the wear rate is the highest in chamber 4. It is possible that the wear rate would have been even higher in chamber 4 without the protein degradation, however, the results shown in Fig. 43 do not correspond with the finding of Clarke[109].

It is worth noting that the chambers were not sealed during the tests performed on PEEK OPTIMA and, therefore, the protein degradation was significantly higher than the that seen in subsequent tests on both CNF PEEK and CFR PEEK which are performed in sealed chambers. The wear of PEEK OPTIMA is significantly higher than CFR PEEK which could indicate the protein degradation had the reverse effect on the wear than that in Clarke's studies.

5.4. Adverse Conditions

Adverse condition tests are intended to offer insight into the type of wear mechanisms taking place at the onset of small scale failure and also to obtain information on the magnitude of load that causes material failure. The load is first increased to 120 N and the wear test is run for 0.15 Mc. The specimens are cleaned, weighed and reloaded into the OrthoPOD^{TM}. The load is increased again and the test is run for another 0.15 Mc. This process continues until any of the specimens reveal any indication of failure, such as: large scuff marks, large amounts of material removal, pitting and/or a ripped appearance on the surface. The specimen with failure markings, both pins and plates are then examined in the SEM for further evaluation. The sequence of the loads applied to the materials is noted in Fig. 44.

5.4.1. Wear Curves for PEEK OPTIMA, CFR PEEK and CNF PEEK

The adverse conditions test for PEEK OPTIMA reveals significant surface damage at a load level of 300 N. The contact stress calculated at the time of failure is 4.24 MPa. CFR PEEK indicates failure on one specimen at a load level of 400 N, resulting in a contact stress of 5.64 MPa. CNF PEEK was in unique in that it started to shows surface damage due to abrasive wear after the first interval of testing under normal conditions. Both CFR PEEK and PEEK OPTIMA appeared smooth and polished until 0.25 Mc before failure. The surface damage on the CNF PEEK specimens gradually increased and the overall wear at the last interval testing, 400 N with a contact stress of 5.64 MPa, was considerably higher than CFR PEEK and slightly higher than the PEEK OPTIMA. Fig.44 shows results for all three versions of PEEK.

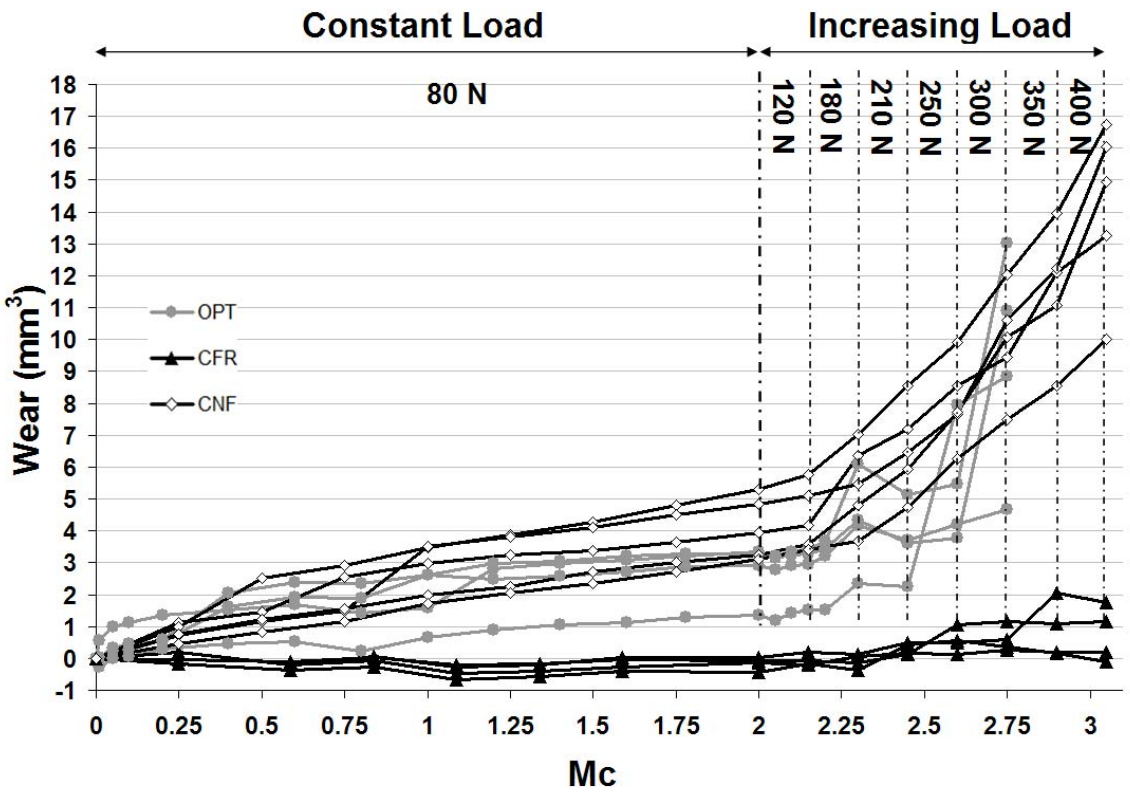

Fig. 44: Wear Curves for Adverse Condition Tests

Wear ranges and averages are presented for CNF PEEK, PEEK OPTIMA and CFR PEEK at the last interval of testing in Table 19.

Table 19: Adverse Conditions Wear Results

Material	Range of Volumetric Wear (mm^3)	Average of Volumetric Wear (mm^3)
CNF PEEK	**10.00-16.74**	**14.20** ± 4.75
PEEK OPT	**4.67 – 13.03**	**9.36** ± 3.56
CFR PEEK	**-0.10 – 1.74**	**0.75** ± 0.85

The three versions of PEEK are compared below in Fig. 45. The first bar indicates the volumetric wear at end of the normal condition tests and the second bar indicates the wear at the end of the adverse conditions test. The standard deviation is notably higher for both PEEK OPTIMA and CNF PEEK after the adverse conditions test.

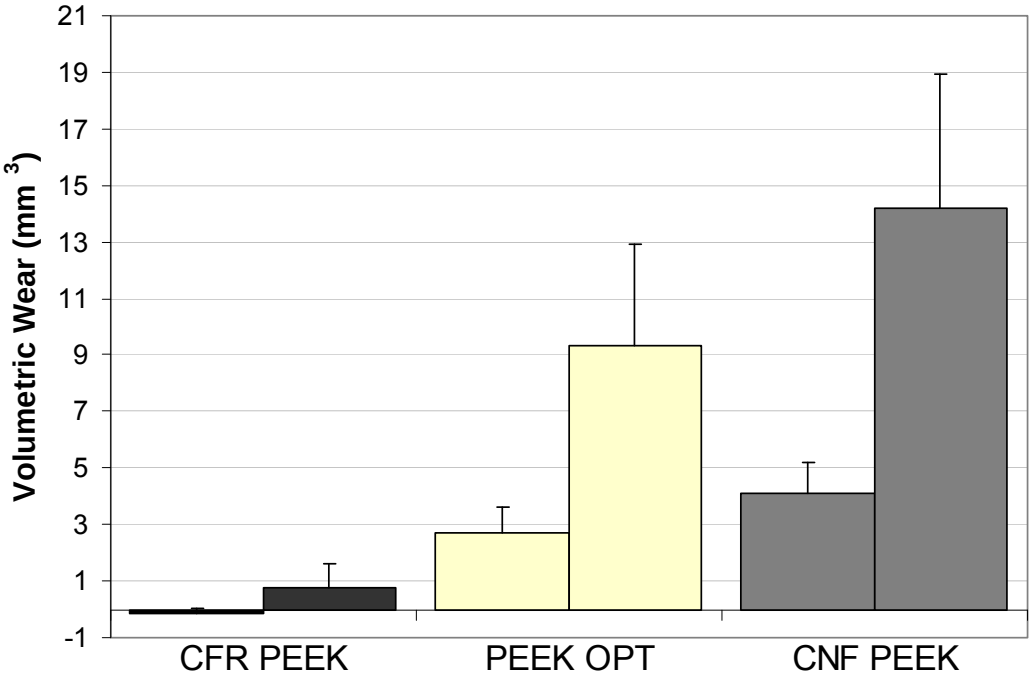

Fig. 45: Volumetric Wear of All Versions of PEEK after Normal and Adverse Conditions

The wear of PEEK OPTIMA is approximately 12.5 higher than CFR PEEK at the onset of failure. It is interesting to note the difference in wear values from the end of the normal conditions test to the onset of failure. At the end of the normal conditions test, the average wear of all the CFR PEEK specimens is negative, most likely due to the weight of the absorbed fluid being higher than the weight of the material lost due to wear. The highest individual specimen wear value is 0.02 mm^3. This indicates the average wear value at the onset of failure is much higher than the highest individual specimen wear after the normal conditions test. Even though the CFR PEEK specimen exhibits very low wear at the failure point, it is still considerably higher than the wear value obtained at the end of the normal conditions test. The wear value obtained at the onset of failure for PEEK OPTIMA is only 3.4 times higher than the wear value obtained at the end of the normal conditions test.

There are two main conclusions drawn from the data presented in Table 18 and 19. The first is; CNF PEEK shows more wear than PEEK OPTIMA at the end of the adverse conditions test which could indicate a much higher wear value at the onset of failure if CNF PEEK exhibits the same wear behaviour as PEEK OPTIMA. The wear

behaviour displayed for 3 of the 4 PEEK OPTIMA specimens includes a linear increase in wear and then sudden failure causing the wear value to jump approximately 6 to 7.5 mm^3.

The second conclusion is that CNF PEEK may not experience a sudden increase in wear. The wear curves over the 0 – 3.05 Mc range are quite linear. A gradual increase in wear rate is seen rather than the run-in and subsequent linear steady state wear behaviour see in PEEK OPTIMA over the same range. Thus it is possible CNF PEEK won't experience a sudden increase in wear.

5.4.2. Modes of Failure

Failure is indicated by significant surface damage that would be a concern clinically. The failure occurred suddenly with the PEEK OPTIMA and CFR PEEK specimens. The specimens obtained a polished appearance after the first interval of wear testing and the specimens continued to appear polished until approximately 0.15 Mc before failure. The material in the centre of the wear track on the PEEK OPTIMA specimens appeared melted, likely due to plastic deformation, during the last interval of wear testing. The depth of the scuff marks were noted to increase during the final 0.15 Mc of testing. An image of a damaged PEEK OPTIMA specimen, as described above, is shown in Fig. 45. The contact area is elliptical as a result of a circular pin moving through relatively linear 8.5 mm stroke length.

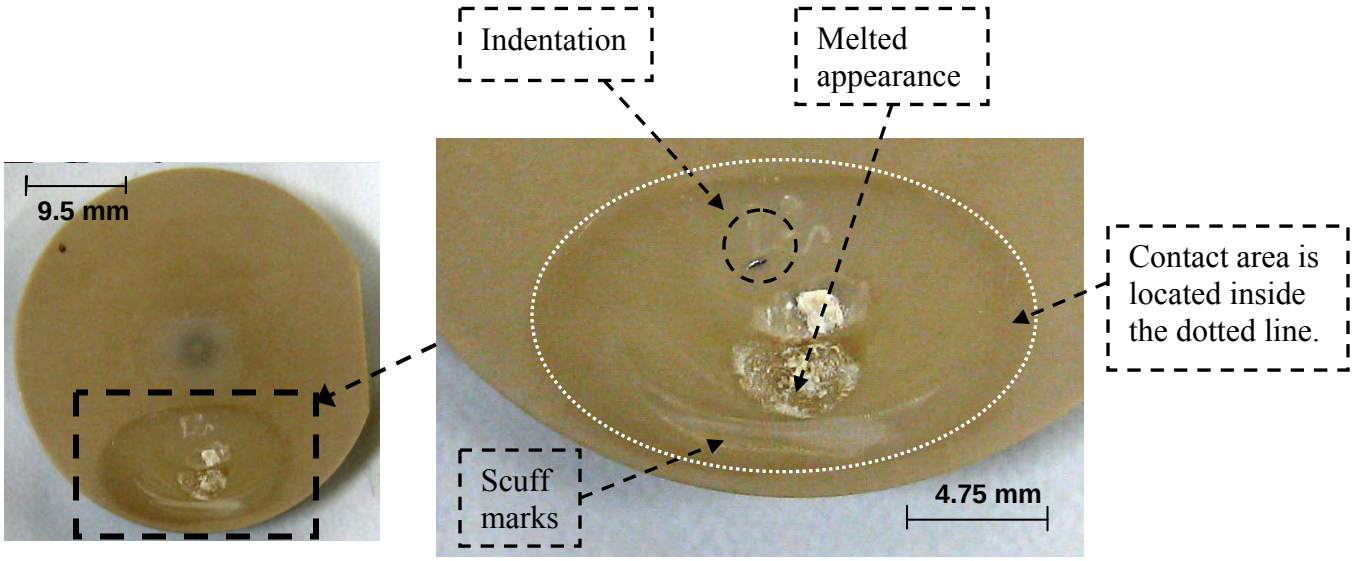

Fig. 46: PEEK OPTIMA – Plate 2 at the 300 N load level of the Adverse Conditions Test

Pitts, shown in Fig. 46, are also noted in the wear track of the CFR PEEK specimens just before failure.

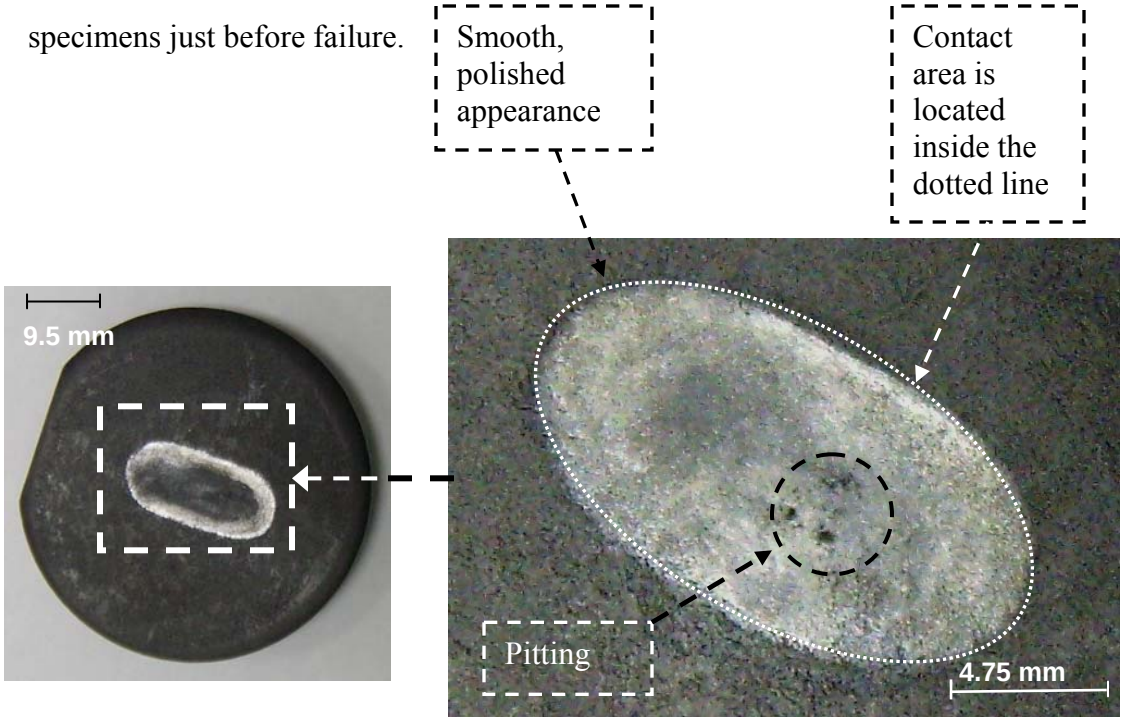

Fig. 47: CFR PEEK – Plate 2 at the 400N load level of the Adverse Conditions Test

The contact areas shown in Fig. 45 and Fig. 46 are smooth, with the exception of the surface damage, similar to those seen on the pins.

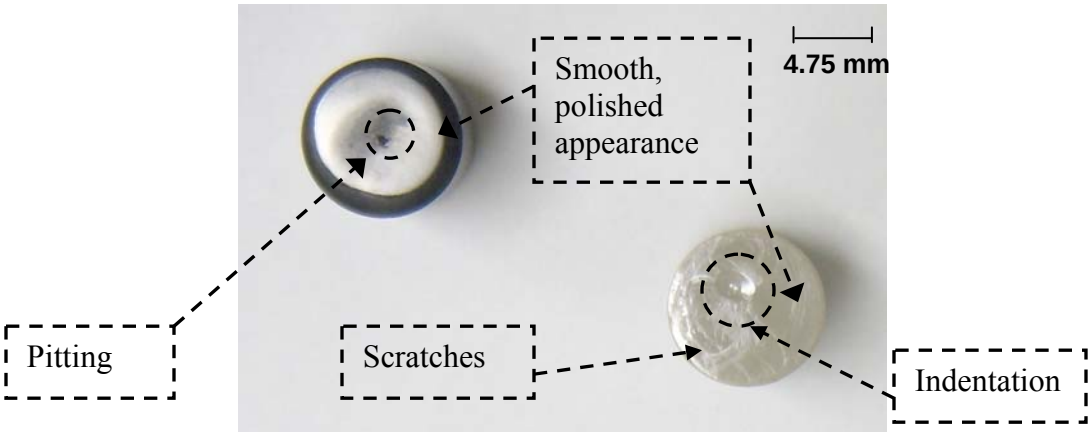

Fig. 48: Worn End of CFR Pin 1 and OPT Pin 2

5.5. Microscopy of Surface Failure

Failures are observed on the surface prior to significant changes in volumetric wear values. Microscope of specimens revealed potential surface damage mechanisms.

The size of both flakes from the PEEK OPTIMA specimens and broken fibers from the CFR PEEK specimens is attainable at a magnification nominally set at 500 X on the microscopic dial. The micrographs have been modified from their original version therefore reference can be made to the scale indicated on the actual image which is accurate.

5.5.1. PEEK OPTIMA

PEEK OPT specimens exhibit signs of material failure during the 300 N load interval of the adverse conditions test. Plates 2 and 4, shown in Fig. 47, reflect the most obvious wear. Plate 1, not shown, has indentations that suggest plastic deformation and plate 3, also not shown, with the exception of a polished appearance that developed early on in the wear test, has absolutely no sign of failure (whatsoever). The level of damage apparent to the naked eye correlates with volumetric wear values which are confirmed in Fig. 48.

Fig. 48 shows the visual damage on plates 2 and 4. These specimens have significantly higher volumetric wear than the other two test samples that do not display the magnitude of damage shown below.

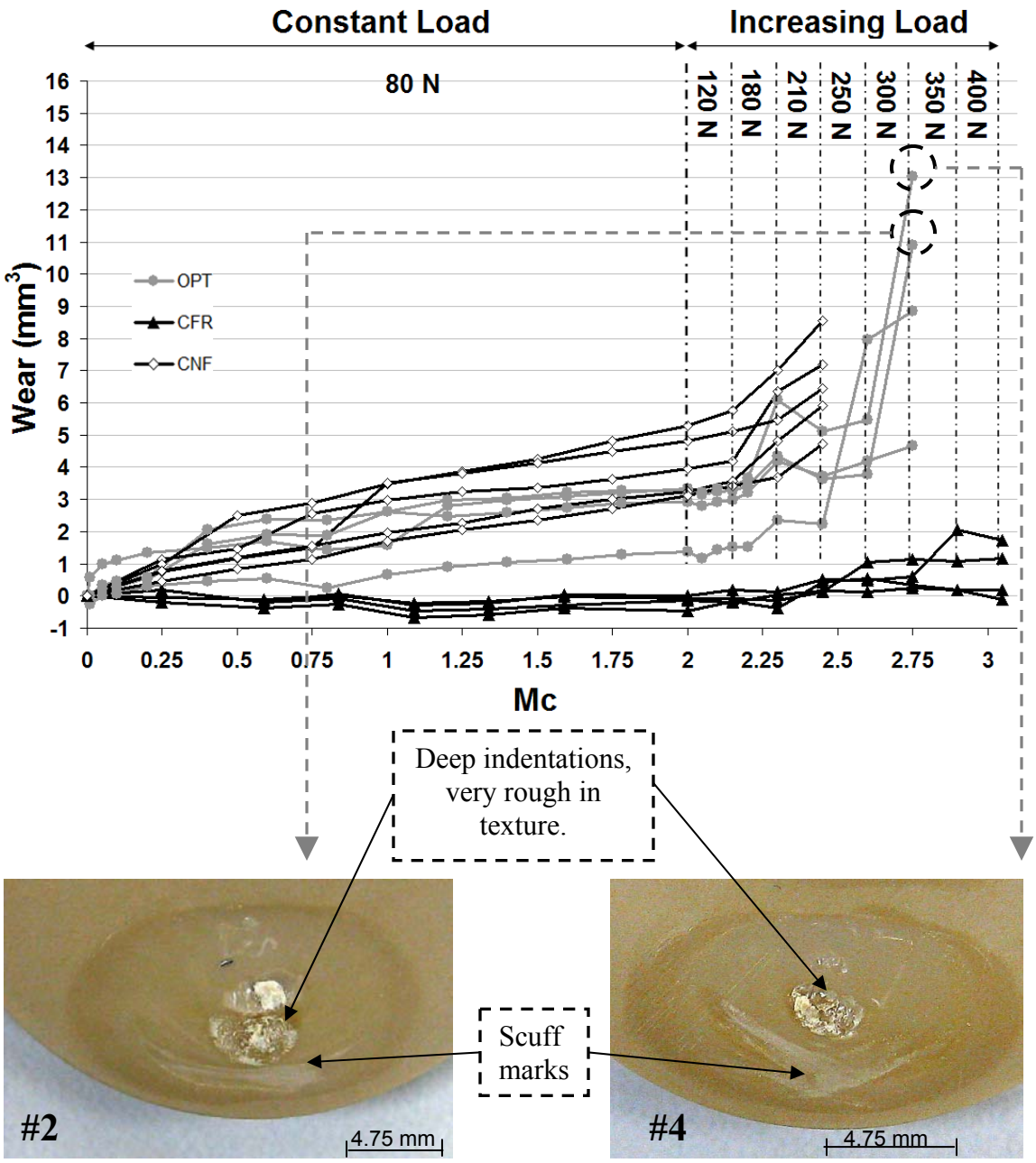

Fig. 49: Macrographs of PEEK OPT Plates 2 & 4 after Adverse Conditions Test (300N, 2.75 Mc)

5.5.1.1. SEM

The SEM was used to further investigate the damaged region on plate 2. Gold coating of the specimen was possible because the test was complete. Images are presented in Fig. 49.

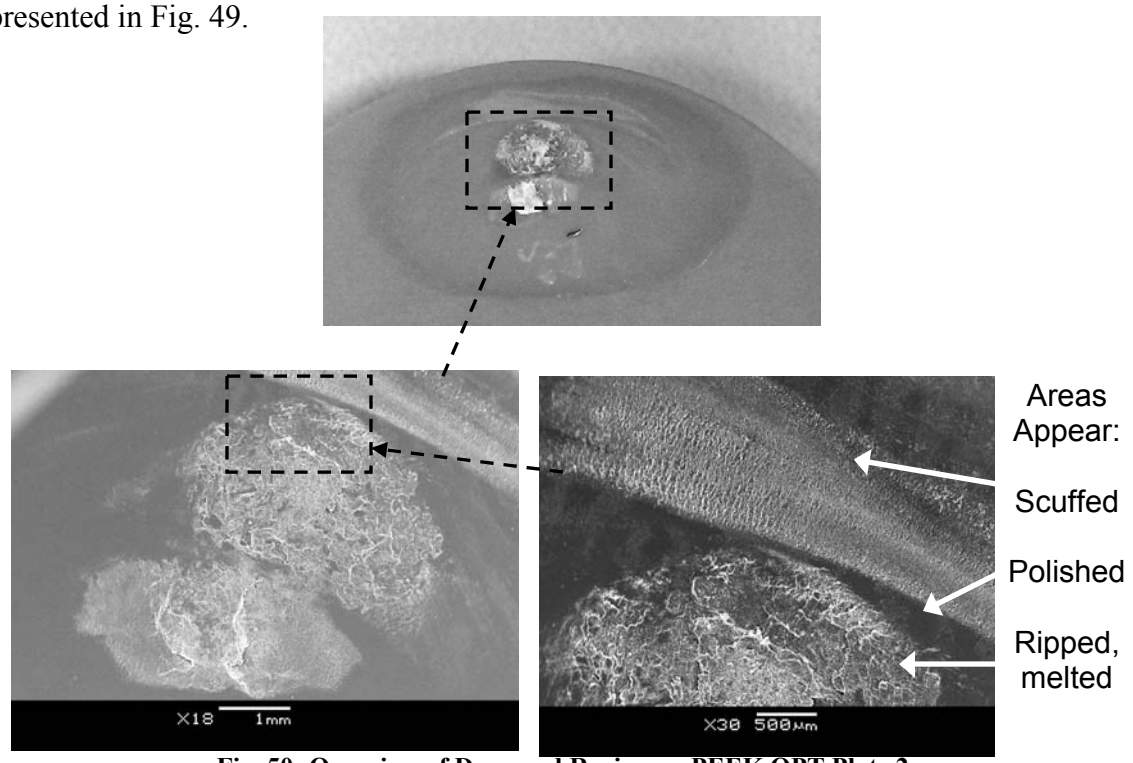

Fig. 50: Overview of Damaged Region on PEEK OPT Plate 2

The damaged region results from different mechanisms. Fig. 50 shows higher magnification images of the different regions in the damaged zone to illustrate the various stages of wear. Particles are released from the surface in a form that corresponds to the degree of wear. Fig. 50 A represents the region of the specimen that appears scuffed and slightly indented. This damage is less severe than in locations B and C. The scuffing is an indication of plastic deformation. Fig. 50 B is located at the interface of the polished region and the melted/ripped zone. It is believed that the rapid increase in wear, seen in the last interval of the adverse conditions test, is related to the polished zone transforming into a melted/ripped zone. The wear rises rapidly as flakes of the matrix are dislodged. Fig. 50 C is located in the centre of the most severe damage. Friction induced fatigue tearing and localized melting are probably responsible for the shredded appearance of the surface. Many flakes have been dislodged completely, unlike the interface image which displays partial attachment of flakes. The detached flakes are also

smaller in this zone, most likely due to further breakdown once loose in the contact zone. The adhesive/fatigue wear mechanisms responsible for the damage are possibly enhanced by elevated surface temperatures.

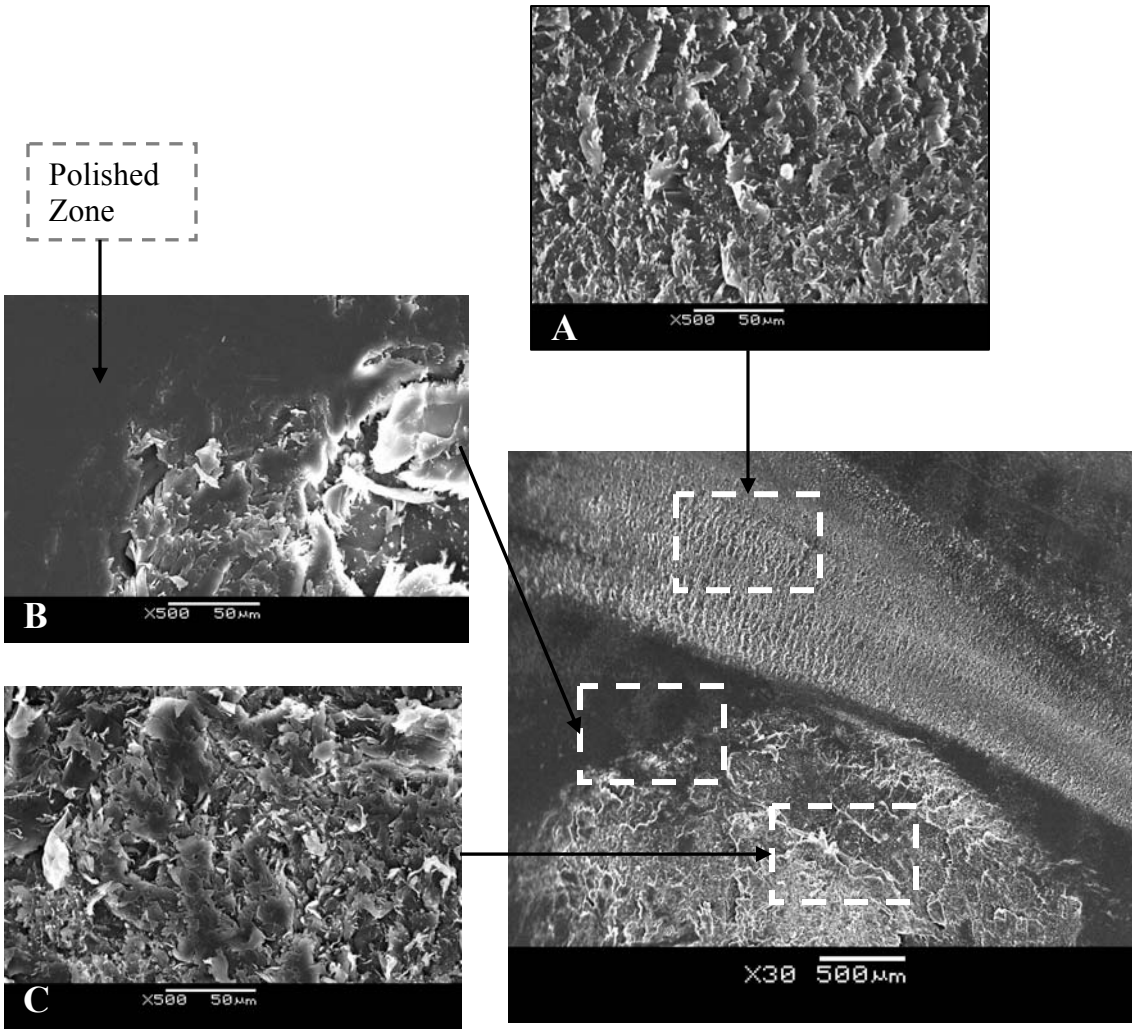

Fig. 51: Different Locations in the Damaged Zone – PEEK OPT (plate 4)

An image of unworn PEEK OPT is compared, in Fig. 51, to an image obtained from the centre of the damaged region. Fig. 51 A depicts machining marks from the original process of cutting the specimens from bar stock material.

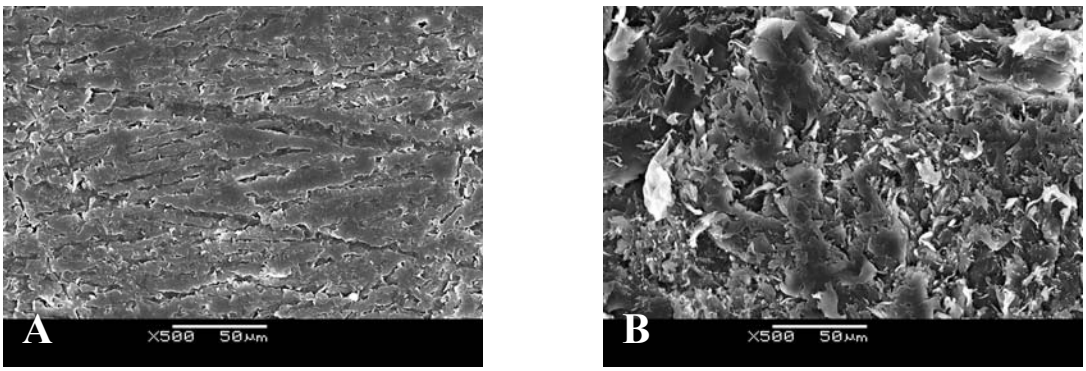

Fig. 52: Microscopy of Plate 5 - Unworn (A) and Plate 4 - Severely Damaged (B) PEEK OPT

It is interesting to note the difference between the polished zones, shown in Fig. 50 B and the unworn zones, shown in Fig. 51 A. The machining marks noted on the original unworn specimens have been burnished, resulting in a polished appearance.

Fig. 52 shows the articulating surface on the pin. The damage appears as indentations and groves to the naked eye. A magnified view of the damage zone reveals similar wear patterns to those seen on the plate. Shredding is apparent, however, it is not nearly as prominent as that seen on the plate specimens.

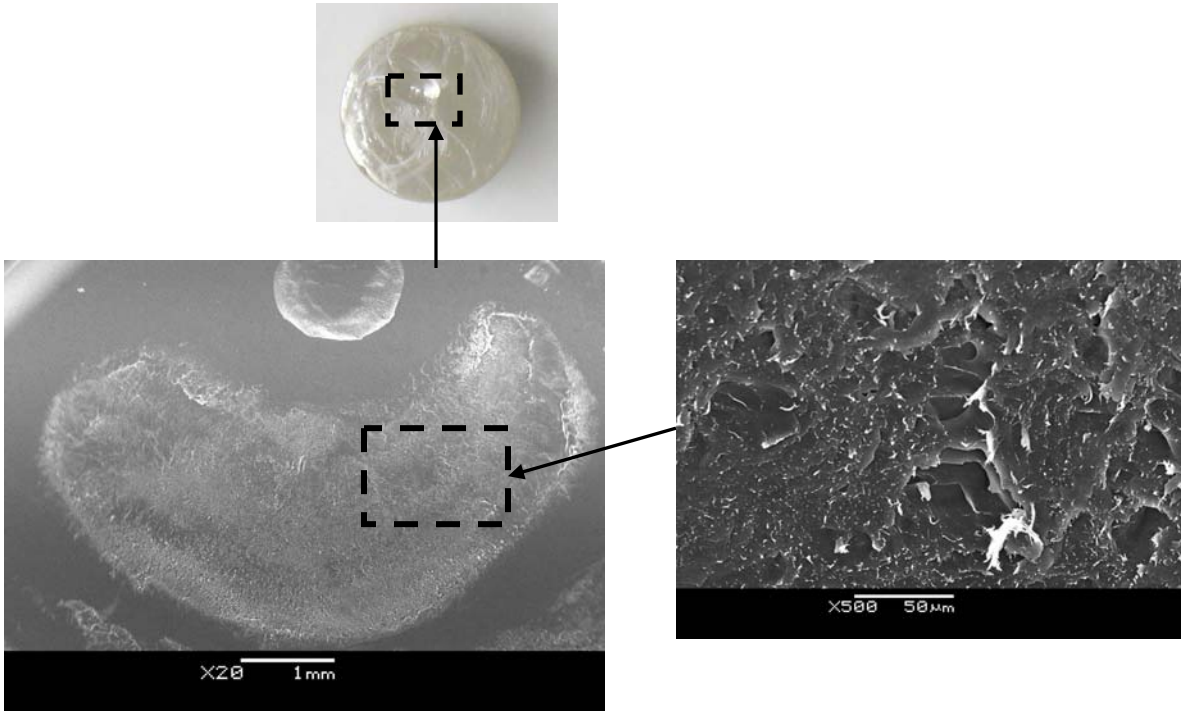

Fig. 53: Pin 4 after Adverse Conditions (300N, 2.75 Mc)

5.5.2. CFR PEEK

The CFR PEEK specimens indicate some level of failure after 2.90 Mc and 350 N applied load. The surface damage is less pronounced than that seen on PEEK OPT. Wear testing was continued and more notable failure was seen after 3.05 Mc and 400 N applied load. The damage, shown previously in Fig. 46, is not as severe as that seen on the PEEK OPT specimens. The surface appears pitted and mildly scuffed. There is no evidence of melting or significant tearing of the material.

5.5.2.1. Scanning Electron Microscopy

Minimal volumetric wear is displayed in some instances and yet under 500 x magnification, fiber breakdown is clearly visible and the size of the fiber particulates is measurable. The focus is on interface locations between them in an attempt to display the contrast between worn and unworn surfaces and polished and damaged surfaces. Gold or carbon coating is considered necessary with electron microscopy of non-conducting materials [48]. However, coating the current specimens may affect the future wear properties and since images are taking at various intervals during the test, coating was not possible. This results in over exposed sections of the image where the polymer matrix has become charged by the electrons (bright white appearance).

A small hole, shown in Fig. 53 A, appears on the surfaces of both a pin and plate after 2.9 Mc and 350 N. The SEM images reveal interesting detail on the surface. The centre of the hole appears to contain whole fibers, shown Fig. 53 B. The region that appears polished to the naked eye, Fig. 53 C, contains fibers broken into segments in the size range of 5-45 μm. The fibers are intact in the damaged region but visible, probably as a result of a delamination. The carbon fibers help the matrix resist surface adhesion/abrasion but delamination occurs eventually as a result of sub-surface fatigue.

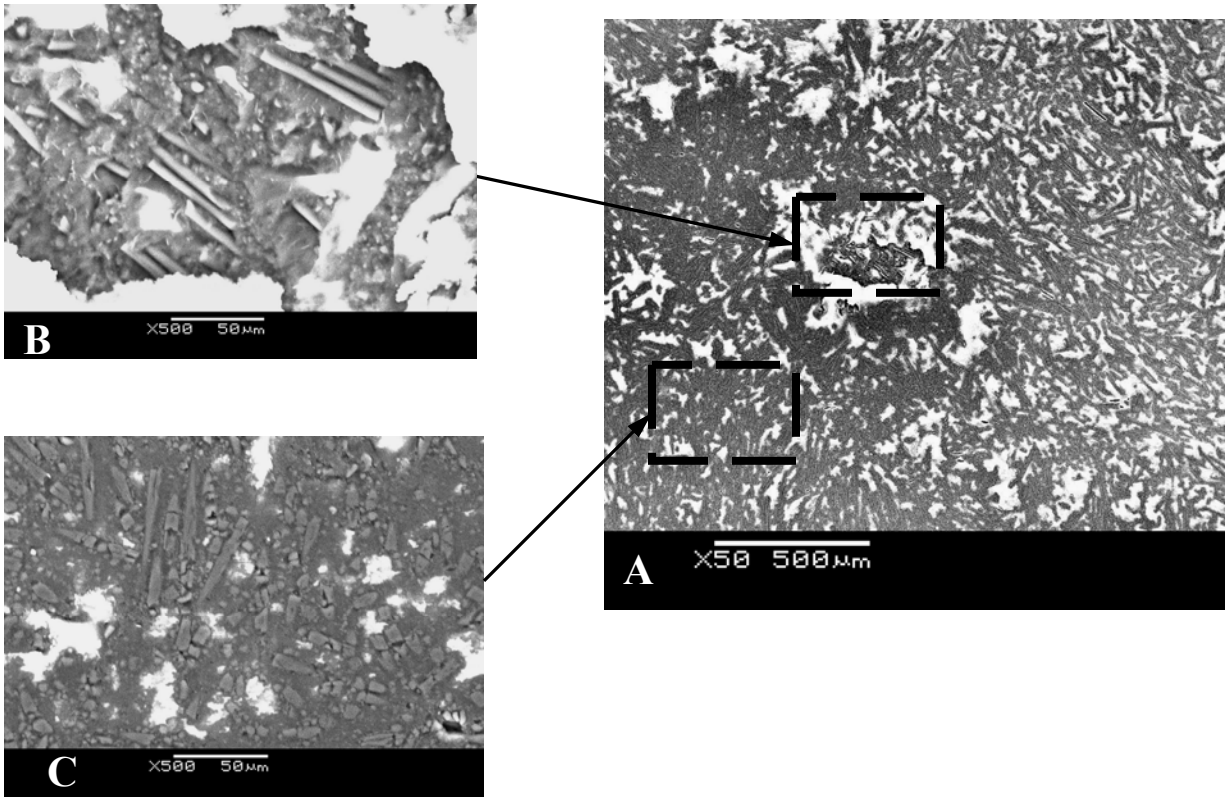

Fig. 54: Damage seen at 2.90 Mc and 350 N - CFR PEEK Plate 2 A) Centre of hole B) Polished wear track

CFR PEEK is compared in its unworn, original form and just after the onset of failure. Initially, the matrix partially covers the carbon fibers, shown in Fig. 54 A. The second image, Fig 54 B indicates the matrix is worn down over the course of the test and fibers are broken into many segments. The segments are still embedded in the matrix which is most likely the reason for CFR PEEK low wear results, even after damage is apparent on the surface.

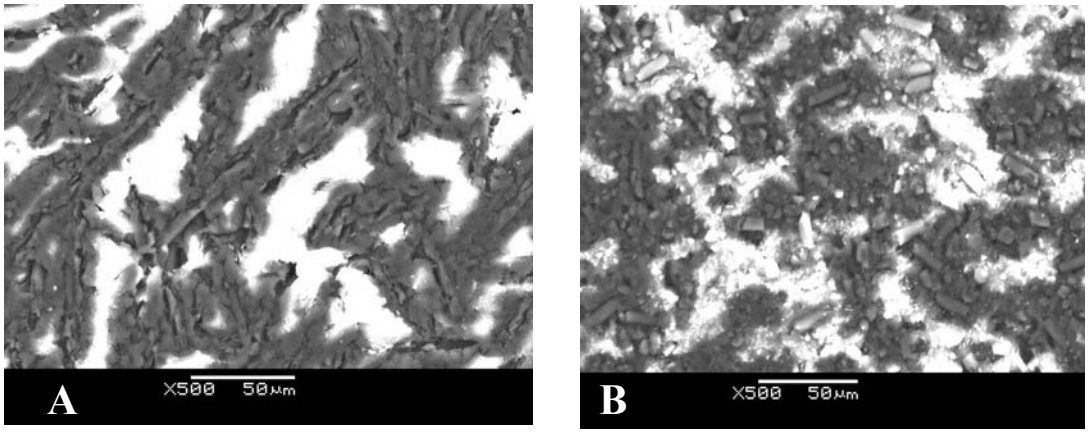

Fig. 55: Images of Unworn (A) and Severely Damaged (B) CFR PEEK Plate 3

The most severe wear seen on a PEEK OPT specimen and a CFR PEEK specimen is shown below, Fig. 55. The PEEK OPT specimen shreds while the CFR PEEK remains relatively smooth. The carbon fibers stop the matrix from pulling off the matrix in large fragments. Such fragments are very apparent on the PEEK OPT specimen.

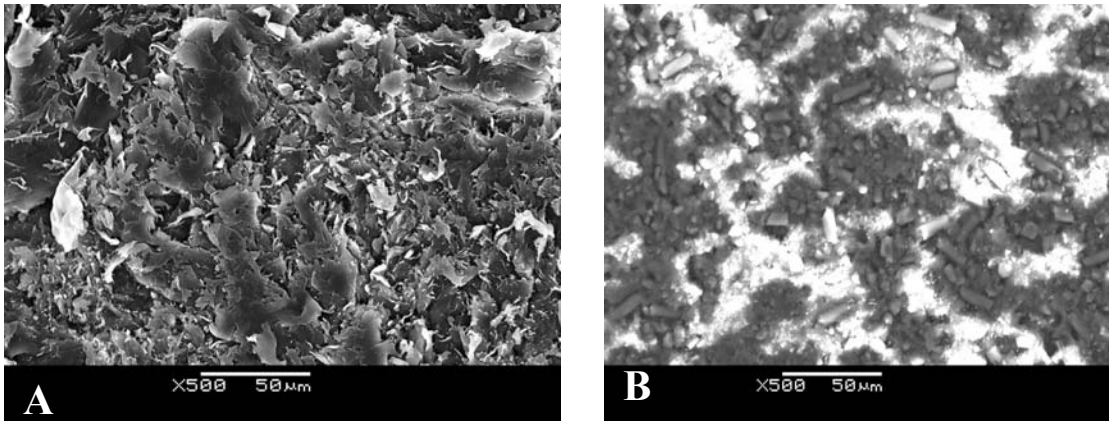

Fig. 56: Max Damage in A) PEEK OPT – Plate 2 @ 2.75 Mc, 300N and in B) CFR PEEK – Plate 2 @ 3.05 Mc, 400 N

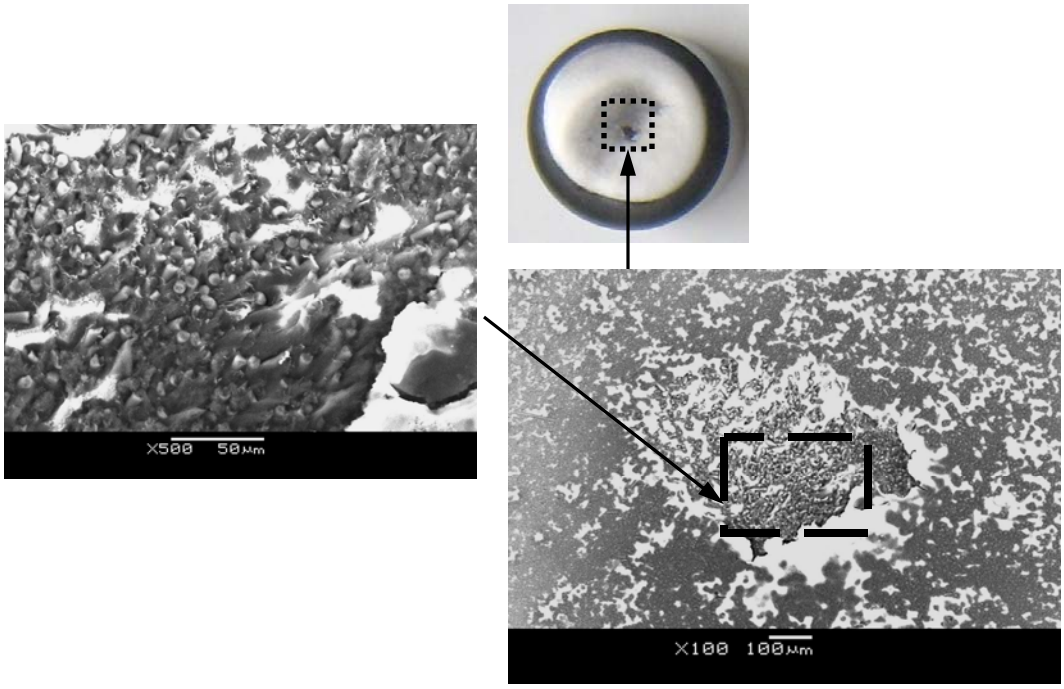

Fig. 57: Pin hole damage on a CFR PEEK pin specimen after 2.9 Mc and 350 N

Carbon fiber orientation appears to be different in the pin and plate specimens. The carbon fibers are lying parallel to the surface in the plate specimens and as the matrix wears away, many intact fibers are seen on the surface. A close examination of damage, Fig. 56, on the pin surface, reveals a fiber orientation opposite to the plates. The ends of the fibers are seen in Fig. 56. A schematic diagram of the pin and plate fiber orientation during testing is shown below in Fig. 57. The significantly lower wear experienced by CFR PEEK could be related to perpendicular fiber orientation between the pin and the plate. The pin experienced significantly less wear than the plate in the CFR PEEK specimens compared to the other materials.

Fig. 58: Carbon Fiber Orientation in Pin and Plate Specimens

The percentage of wear experienced by the pin and plate with respect to the total wear is shown in Table 21.

Table 20: Percentage of Wear Experienced by the Pin and the Plate

Material	% of Wear – Plate	% of Wear - Pin	SD
PEEK OPT	~ 42 %	~58 %	6 % N=4
CFR PEEK	~ 85 %	~ 15 %	35 % N=4
CNF PEEK	~ 55 %	~ 45 %	1 % N=5

5.5.3. CNF PEEK

Microscopic evaluation of wear was performed on CNF PEEK early on in the wear tests. The specimens, both pin and plate, show evidence of extensive third body abrasive wear damage. It is possible that third bodies form which are rich in carbon nano-fibers. The wear of CNF PEEK is evaluated with volumetric measurements and indicates the material is not ideal for all-polymer articulation. The micrograph of the specimens, shown in Fig. 58, taken early on in the wear tests, show it is this damage that probably resulted in the poor performance of CNF PEEK.

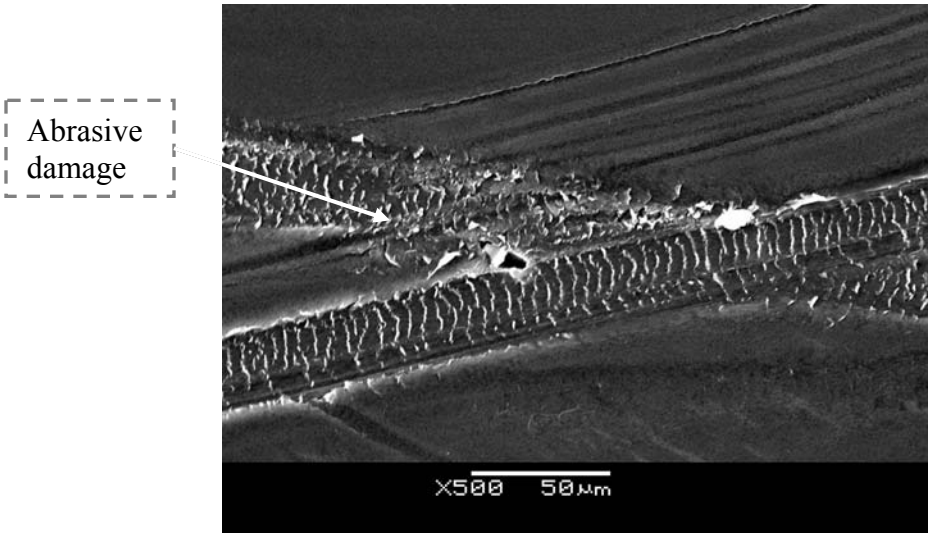

Fig. 59: CNF PEEK plate @ 0.25 Mc, 80 N

5.6. Concluding Remarks

The overall results of the present thesis indicate CFR PEEK has the overall lowest wear. Though surface damage was seen in the form of pitting after the adverse conditions test, volumetric wear did not indicate a rise in wear. The PEEK OPT experienced lower wear than CNF, however, surface damage was significant after the adverse conditions test and the volumetric wear increased significantly as a result of this.

The CNF PEEK did not complete the adverse condition tests but exhibited higher wear than the two other versions of PEEK in its last wear test interval. Overall it did not exhibit tribological behaviour suitable for an implant.

The microscopy study revealed torn and ripped surfaces on PEEK OPT after adverse condition testing. The damage is probably caused by adhesive and fatigue wear mechanisms. The damage on the CFR PEEK is much less than PEEK OPT and suggests delamination due to sub-surface fatigue. The CNF PEEK showed early evidence of third body wear damage.

5.7. Clinical Implications

The majority of implants in use today consist of a metal surface adjacent to the bone. The metal can block x-rays and distorts MRI images. A major clinical advantage of PEEK is its radiolucent property and that it does not distort MRI images [11]. Spinal surgeons rely on imaging tools to perform postoperative assessment of cervical arthroplasty. These assessments are crucial in the cervical spine [11] to ensure the implant has not migrated toward neural tissues, whereas in other joints, such as the hip or knee, the consequences of misalignment are not as severe.

The biocompatibility of CFR PEEK was proven over two decades ago [12]. There is clinical use of PEEK for implants in non-articulating applications. CFR PEEK materials are in the clinical stage for use in isoelastic femoral hip stems. There is an abundance of materials that have a proven history in hip applications requiring the advantages of PEEK to be quite significant [18].

PEEK materials have had the greatest clinical success in the area of spinal implants [18] and have a 15 year history of success in spinal fusion applications [18]. Fusion devices, similar to femoral hips stems do not involve articulation.

Articulation of PEEK against either CoCr alloy, zirconia or alumina ceramic has some clinical history. Acetabular CFR-PEEK cup inserts have been in development for the last decade. PEEK has been under investigation to replace UHMWPE in knee implants for almost 20 years.

The articulation of PEEK OPT-on-PEEK OPT, an all polymer bearing surface, exists to a limited extent as a clinical application. The PEEK OPT-on-PEEK OPT

lumbar nucleus replacement, the NUBAC® (Pioneer Surgical Technology, Marquette, Mich), has shown no evidence of proinflammatory response. The device was implanted in 100 patients and monitored for 24 months. The wear amount calculated for PEEK OPT after 2.0 Mc in the current study is very similar to the wear calculated for the NUBAC after 10.35 Mc [103]. It is noted that the loads applied in the lumbar spine simulator are significantly higher than the loads applied in the current study.

The parameters selected for the current study can be related to clinical practice. An angle of 86˚ was selected to ensure crossing-path motion, a phenomenon noted to produce results closer to those seen in metal-on-metal combinations [95]. The adverse condition loads were applied to assess the surface damage and identify different wear mechanisms. The maximum load applied in the adverse conditions test was 400 N for the CFR PEEK and 350 N for PEEK OPT. Moroney et al. [39] reports loads as high as 1,164 N, at the C4-C5 level, for the extension motion in the neck. The study involved patients exerting maximum voluntary strength against a load cell. This would imply the loads applied in the adverse conditions test of the current study are within a region that may be experienced in vivo.

It is true that maximum exertion is not necessarily a daily living activity for the majority of patients. However, there could be a population group that does exert maximum extension on a daily basis. This population could include certain athletes, for instance, competitive weight lifers.

The results of the current study indicate PEEK-on-PEEK combinations are suitable for individuals carrying out normal daily activities. However, individuals who might impose high loads on the spine on a regular basis may be at risk of implant damage with all polymer PEEK implant.

6.0 CONCLUSIONS AND RECOMMENDATIONS

Cervical disc arthroplasty currently utilizes metal-polymer, ceramic-ceramic or metal-metal implant materials. All metallic materials impair the clarity of medical images to some extent making evaluation of the impact on surrounding bone and tissue very difficult. PEEK is considered for use in cervical disc implants due to its high wear resistance, high strength, radiolucent properties and lack of magnetic interference in MRI images. The present thesis has examined the wear of material pairs made from each of the three versions of PEEK; OPT, CFR and CNF. The specimens were subjected to normal and adverse conditions in a pin-on-plate apparatus that includes both rotation and translation. Normal conditions involved the application of an 80 N load with a reciprocating rotation of both the pin through an angle of 90˚ and the disc through an angle of 4.5˚. The tests ran for 2.0 Mc and created an 8.5 mm wear path. The adverse conditions involved the same rotation values, however, the load was increased every 0.15 Mc until the material shows signs of failure. The intention of the adverse conditions test was to locate a point at which the material begins to fail and to observe the wear mechanisms occurring at such high loads. PEEK has been tested in both pin-on-plate machines and hip simulators. The findings of the current study are compared to those in the literature.

6.1. Conclusions

1) The articulation of CFR PEEK-on-CFR PEEK produced the lowest wear of all three versions of PEEK and, therefore, shows the most promise for application in cervical disc arthroplasty. The wear results are noted to be very similar to pin-on-plate studies articulating different material combinations including; CFR PEEK-on-ceramic [97]and CFR PEEK-on-HC CoCrMo [101]. A study reporting the wear rates of 30 wt% PAN CFR PEEK and PEEK OPT in relation to each other [85] appears to be similar to the difference between CFR PEEK-on-CFR PEEK and PEEK OPT-on-PEEK OPT wear rates found in the current study. CFR PEEK demonstrates significantly lower wear rates than PEEK OPT in both cases. It is impossible to compare results quantitatively

due to the fact that wear depends on specimen geometry, load, motion, lubricant and surface temperature that can vary between studies. Many results are presented in different units and/or omit information essential to comparing all the data in the same units, however, qualitative comparisons can be made to some extent.

2) The wear amount found for PEEK OPT-on-PEEK OPT at 2.0 Mc under a load of 80 N is very similar to those reported [103]for a PEEK OPT-on-PEEK OPT device tested in a spine simulator for 10.35 Mc. However, the latter bearing is intended for lumbar spine application and was, therefore, subjected to loads approximately 7.5 times higher than cervical load values used in the current study. There is no exact correlation between simulator wear and pin-on-plate wear, but the 80 N baseline test conducted on PEEK OPT did produce similar results to the above mentioned PEEK OPT simulator study [103] performed for 2.0 Mc. This implies the baseline test may have some clinical relevance.

3) The adverse conditions test produced severe surface damage in the PEEK OPT material in addition to a marked increase in wear. The same test, performed on the CFR PEEK, did produce obvious indications of failure, including pitting and plastic deformation. It did not, however, produce a marked increase in the amount of wear. The CFR PEEK appears to be very wear resistance, even under extreme loads, most likely due to the carbon fibers embedded in the PEEK matrix. The matrix is intertwined with carbon fibers and therefore removal of large pieces of material is much more difficult. The microscopy images of both the PEEK OPT and CFR PEEK at the end of the adverse conditions test support this view.

4) The clinical significance of the extreme loads used in this thesis is not clear. The loads experienced in the cervical spine from daily living activities are significantly lower than the loads applied in the pin-on-plate studies. The load experienced in the cervical is highest during the extension motion. Studies have reported values of 155N [25] and 1,164 N [38] with a standard deviation

of 494. This could imply that the loads used in extreme testing are in the range of maximum loads reported in the cervical spine. Since the geometry of the potential implant is unknown, it is difficult to equate maximum load values to loads experienced by the implant and subsequent damage experienced by the implant at elevated loads.

5) An all polymer PEEK implant would be appropriate for application in cervical arthroplasty in terms of its wear resistance, imaging capability, and biocompatibility. However, the present study suggests there are some issues with PEEK including the surface damage seen at high load levels. Once an implant design is developed, simulator studies could assess tribological risks more accurately than pin-on-plate tests.

6.2. Recommendations

1) Future research efforts should be directed primarily towards CFR PEEK and secondarily PEEK OPT. These two materials are competitive alternatives to the materials in used in cervical disc implants today. CNF PEEK shows higher wear than the PEEK OPT and CFR PEEK in the current study, in addition to showing higher wear than the majority of PEEK pairings published in the literature. However, it should be noted that all PEEK pairings, including CNF PEEK, show wear considerably lower than materials that are already in use in FDA approval cervical spine implants, i.e. stainless steel.

2) Low wear materials identified with a pin-on-plate machine should be investigated further using a spine simulator. Flexion, extension, lateral bending and sinusoidal loads can be applied in a simulator and allow for better estimation of the performance of the material in vivo. Longer term testing is required to accurately evaluate the suitability of a material for implantation. Pin-on-plate testing is a method to evaluate new materials quickly and cost effectively. Therefore, the number of pin-on-plate cycles is nowhere near the

number of cycles an implant experiences in its lifetime, in vivo. Longer term testing is required to determine the wear of an implant over a lifetime of implantation.

3) The clinical significance of CFR PEEK and PEEK OPT wear debris in the cervical spine should be investigated. Macrophagic response to wear particles and the possibility of osteolysis should be evaluated.

4) Currently ASTM and ISO standards include test conditions that replicate daily living activities for the cervical spine. PEEK has been suggested endurance and athletic applications. Assessment of a PEEK implants under extreme conditions would offer insight into how the implant wears in high activity patients.

References

[1] Kokubun, S., and Tanaka, Y., 1995, "Types of Cervical Disc Herniation and Relation to Myelopathy and Radiculopathy," Journal of Back and Musculoskeletal Rehabilitation, **5**pp. 145-154.

[2] Sasso MD., Rick C., Smucker MD., Joseph D., Hacker MD., Robert J., 2007, "A Prospective, Randomized Study with 2-Year Follow-Up on 99 Patients," Spine, **32**(26) pp. 2933-2940.

[3] Oskouian, R. J., Whitehill, R., Samii, A., 2004, "The Future of Spinal Arthroplasty: A Biomaterial Perspective," Neurosurgical FOCUS, **17**(3) pp. 1-14.

[4] Bryan Jr, Vincent E., 2002, "Cervical Motion Segment Replacement," European Spine Journal, **11**(Suppl.2) pp. S92-S97.

[5] Scient'x, "Product Information - Non Fusion - Discocerv," **2008**(12/2) pp. 1.

[6] Medtronic Sofamor Danek, 2008, "Prestige® Cervical Disc ," **2008**(December/2) pp. 1.

[7] Anderson, P. A., Rouleau, J. P., Bryan Jr, Vincent E., 2003, "Wear Analysis of the Bryan Cervical Disc Prosthesis," Spine, **28**(20S) pp. 186-194.

[8] Harris, W. H., 1995, "The Problem is Osteolysis," Clinical Orthopaedics and Related Research, (311) pp. 46-53.

[9] Amstutz, H. C., Campbell, P., Kossovsky, N., 1992, "Mechanism and Clinical Significance of Wear Debris-Induced Osteolysis," Clinical Orthopaedics and Related Research, **276**pp. 7-18.

[10] Anderson, P. A., Rouleau, J. P., Toth, J. M., 2004, "A Comparison of Simulator-Tested and -Retrieved Cervical Disc Prostheses," Journal of Neurosurgery, **2**pp. 202-210.

[11] Sekhon, L. H. S., Duggal, N., Lynch, J. J., 2007, "Magnetic Resonance Imaging Clarity of the Bryan, Prodisc-C, Prestige LP, and PCM Cervical Arthroplasty Devices," Spine, **32**(6) pp. 673-680.

[12] Kurtz, S. M., and Devine, J. N., 2007, "PEEK Biomaterials in Trauma, Orthopedic, and Spinal Implants," Biomaterials, **28**(32) pp. 4845-4869.

[13] Invibio, "PEEK OPTIMA: Image Contrast Grades," .

[14] Austin, H., Harper, M., and Medley, J. B., 2008, "PEEK-on-PEEK for Application in Cervical Arthroplasty?" Anonymous .

[15] Nordin, M., and Frankel, V.H.(.H., 2001, "Basic biomechanics of the musculoskeletal system," Lippincott Williams & Wilkins, Philadelphia, .

[16] Seaside Data Systems, 2007, "Westborough Spine Center - Back Anatomy," **2008**(12/12) pp. 1.

[17] Medical MultiMEDIA Group, LLC, "EOrtho*Pod*," **2008**(12/12) pp. 1.

[18] Kurtz, S.M., and Edidin, A.A., 2006, "Spine technology handbook," Elsevier Academic Press, Amsterdam ; Boston, .

[19] Panjabi, M. M., Summers, D. J., Pelker, R. R., 1986, "Three-Dimensional Load-Displacement Curves due to Forces on the Cervical Spine," Journal of Orthopedic Research, **4**(2) pp. 152-161.

[20] U.S. Food and Drug Administration - Center for Devices and Radiological Health, 2007, "Summary of Safety and Effectiveness Data - Summary of Nonclinical Laboratory Studies (ProDiscTM-C)," P070001, .

[21] U.S. Food and Drug Administration - Center for Devices and Radiological Health, 2006, "Summary of Safety and Effectiveness Data - Summary of Nonclinical Laboratory Studies (Prestige)," P060018, .

[22] Dvorak, J., Hayek, J., and Zehnder, R., 1987, "CT-Functional Diagnostics of the Rotatory Instability of the Upper Cervical Spine. Part 2. an Evaluation on Healthy Adults and Patients with Suspected Instability," Spine, **12**(8) pp. 726.

[23] Penning, L., and Wilmink, J. T., 1987, "Rotation of the Cervical Spine," Spine, **12**(8) pp. 732.

[24] Panjabi, M. M., Crisco, J. J., Vasavada, A., 2001, "Mechanical Properties of the Human Cervical Spine as shown by Three-Dimensional Load-Displacement Curves," Spine, **26**(24) pp. 2692-2700.

[25] White, A.A., and Panjabi, M.M., 1990, "Clinical biomechanics of the spine," Lippincott, Philadelphia, .

[26] White, A.A., and Panjabi, M., 1978, "Clinical Biomechanics of the Spine," Lippincott, Philadelphia ; Toronto, .

[27] Dvorak, J., Froehlich, D., Penning, L., 1988, "Functional Radiographic Diagnosis of the Cervical Spine: Flexion/Extension," Spine, **13**(7) pp. 748-755.

[28] Dvorak, J., Panjabi, M., Grob, D., 1993, "Clinical Validation of Functional Flexion/Extension Radiographs of the Cervical Spine," Spine, **18**(1) pp. 120-127.

[29] Penning, L., 1978, "Normal Movement of the Cervical Spine," AJR Am J Roentgenol, **130**(2) pp. 317-326.

[30] Ordway, N., Seymour, R., Donelson , R., 1999, "Cervical Flexion, Extension, Protrusion, and Retraction: A Radiographic Segmental Analysis," Spine, **24**(3) pp. 240-247.

[31] Holmes, A., Wang, C., Hui Han, Z., 1994, "The Range and Nature of Flexion-Extension Motion in the Cervical Spine," Spine, **19**(22) pp. 2505-2510.

[32] International Organization for Standardization, 2005, "Implants for surgery - Wear of total intervertebral spinal disc prostheses - Part 1: Loading and displacement parameters for wear testing and corresponding environmental conditions for test," ISO 18192-1, .

[33] American Society for Testing and Materials, 2000, "Standard Practice for In-Vitro Environmental Conditioning for Polymer Matrix Composite Materials and Implant Devices," ASTM F 1634 -95, .

[34] American Society for Testing and Materials, 2006, "Standard Guide for Functional, Kinematic, and Wear Assessment of Total Disc Prostheses," American Society for Testing and Materials, ASTM F 2423 -05, PA, United States.

[35] Pare, P. E., Chan, F. W., Buchholz, P., 2006, "Surface Texture Analysis of Artificial Disks Wear-Tested Under Different Conditions and Comparison to a Retrieved Implant," Journal of ASTM International, **3**(4) pp. 1-8.

[36] Hattori, S., Oda, H., Kawai, S., 1981, "Cervical Intradiscal Pressure in Movements and Traction of the Cervical Spine," Zeitschrift Fur Orthopadie, **119**pp. 568-569.

[37] Nachemson, A. L., 1981, "Disc Pressure Measurements," Spine, **6**pp. 93-97.

[38] Moroney, S. P., Schultz, A. B., Miller, J. A. A., 1988, "Load-Displacement Properties of Lower Cervical Spine Motion Segments," Journal of Biomechanics, **21**(9) pp. 769-779.

[39] Moroney, S. P., , S., A.B., and Miller, J. A. A., 1988, "Analysis and Measurement of Neck Loads," Journal of Orthopedic Research, **6**pp. 713-720.

[40] Cripton, P. A., Dumas, G. A., and Nolte, L. -., 2001, "A Minimally Disruptive Technique for Measuring Intervertebral Disc Pressure in Vitro: Application to the Cervical Spine," Journal of Biomechanics, **34**(4) pp. 545-549.

[41] Ghosh, P.(., 1988, "Biology of the intervertebral disc," CRC Press, Boca Raton, FL, .

[42] Buckwalter, J., 1995, "Aging and Degeneration of the Human Intervertebral Disc," Spine, **20**(11) pp. 1307-1314.

[43] Roughley, Peter J. PhD., 2004, "Biology of Intervertebral Disc Aging and Degeneration: Involvement of the Extracellular Matrix," Spine, **29**(23) pp. 2691-2699.

[44] Williams, J.A., 1994, "Engineering Tribology," Oxford University Press, New York, pp. 487.

[45] Flöck, J., Friedrich, K., and Yuan, Q., 1999, "On the Friction and Wear Behaviour of PAN- and Pitch-Carbon Fiber Reinforced PEEK Composites," Wear, **225-229**(Part 1) pp. 304-311.

[46] Davim, J. P., Marques, N., and Baptista, A. M., 2001, "Effect of Carbon Fibre Reinforcement in the Frictional Behaviour of PEEK in a Water Lubricated Environment," Wear, **251**(1-12) pp. 1100-1104.

[47] Stachowiak, G.W.(.W.)., and Batchelor, A.W.(.W., 2000, "Engineering tribology," Butterworth-Heinemann, Boston, pp. xxiii, 744 p.

[48] Bhushan, B., 2002, "Introduction to tribology," John Wiley, New York, pp. xix, 732 p.

[49] Powell, M.L., 2005, "Investigtion into wear of materials for metal-on-metal cervical disc implants," University of Waterloo, Waterloo, Ont., .

[50] Halling, J., 1976, "Introduction to tribology," Wykeham Publications ; Springer Verlag, London ; Winchester : New York, .

[51] Bartenev, G.M., Lavrentév, V.V.(.V., Lee, L., 1981, "Friction and wear of polymers," Elsevier Scientific Pub. Co., Amsterdam, .

[52] Bowden, F.P., and Tabor, D., 2001, "Friction and lubrication of solids," Clarendon, Oxford, .

[53] Auerbach, MD, Joshua D., Jones, MD, Kristofer J., Fras, MD, Christian I., 2008, "The Prevalence of Indications and Contraindications to Cervical Total Disc Replacement," The Spine Journal, **8**pp. 711-716.

[54] Ishihara, H., Kanamori, M., Kawaguchi, Y., 2004, "Adjacent Segment Disease After Anterior Cervical Interbody Fusion," The Spine Journal, **4**(6) pp. 624-628.

[55] Hedman, T., Kostuik, J., Fernie, G., 1991, "Design of an Intervertebral Disc Prosthesis," Spine, **16**(6 Supp) pp. S256-S259.

[56] Le, H., Thongtrangan, I., and Kim, D. H., 2004, "Historical Review of Cervical Arthroplasty," Neurosurgical FOCUS, **17**(3) pp. 1-9.

[57] Cummins, B., ROBERTSON, J. T., and GILL, S. S., 1998, "Surgical Experience with an Implanted Artificial Cervical Joint," Journal of Neurosurgery, **88**(6) pp. 943-8.

[58] Wigfield, C., Gill, S., Nelson, R., 2002, "The New Frenchay Artificial Cervical Joint," Spine, **27**(22) pp. 2446-52.

[59] Traynelis, V. C., 2004, "The Prestige Cervical Disc Replacement," The Spine Journal, **4**(6, Supplement 1) pp. S310-S314.

[60] Synthes Spine, 2006, "ProDisc Cervical," **2008**(Nov/12) pp. 1.

[61] Nabhan MD., A., Ahlhelm MD., F., Shariat MD., K., 2007, "The ProDisc-C Prothesis - Clinical and Radiological Experience 1 Year After Surgery," Spine, **32**(18) pp. 1935-1941.

[62] DiAngelo, D. J., Foley, K. T., Morrow, B. R., 2004, "In Vitro Biomechanics of Cervical Disc Arthroplasty with the ProDisc-C Total Disc Implant," Neurosurgical FOCUS, **17**(3) pp. 44-54.

[63] Smith, H. E., Wimberley, D. W., and Vaccaro, A. R., 2004, "Cervical Arthroplasty: Material Properties," Neurosurgical FOCUS, **17**(3) pp. 1-21.

[64] Lind, B., Zoega, B., and Anderson, P. A., 2007, "A Radiosteriometric Analysis of the Bryan Cervical Disc Prosthesis," Spine, **32**(8) pp. 885-890.

[65] Anderson, P. A., Sasso, R. C., Rouleau, J. P., 2004, "The Bryan Cervical Disc: Wear Properties and Early Clinical Results," The Spine Journal, **4**(6, Supplement 1) pp. S303-S309.

[66] Taksali, S., Grauer, J. N., and Vaccaro, A. R., 2004, "Material Considerations for Intervertebral Disc Replacement Implants," The Spine Journal, **4**(6, Supplement 1) pp. S231-S238.

[67] Pimenta, L., McAfee, P. C., Cappuccino, A., 2004, "Clinical Experience with the New Artificial Cervical PCM (Cervitech) Disc," The Spine Journal, **4**(6, Supplement 1) pp. S315-S321.

[68] Cervitech Inc., 2008, "PCM® Artificial Cervical Disc," **2008**(Nov/12) pp. 1.

[69] Nianbin, H., Cunningham, B., McAfee, P. C., 2006, "Porous Coated Motion Cervical Disc Replacement: A Biomechanical, Histomorphometric, and Biologic Wear Analysis in a Caprine Model," Spine, **31**(15) pp. 1666-73.

[70] Ingham, E., and Fisher, J., 2000, "Biological Reactions to Wear Debris in Total Joint Replacement," Proc Instn Mech Engrs, **214**(H) pp. 21-37.

[71] Jacobs, J. J., Hallab, N. J., Urban, R. M., 2006, "Wear Particles," The Journal of Bone and Joint Surgery, **88**pp. 99-102.

[72] Hallab, N. J., Cunningham, B. W., and Jacobs, J. J., 2003, "Spinal Implant Debris-Induced Osteolysis," Spine, **28**(20S) pp. S125-S138.

[73] Howling, G. I., Sakoda, H., Antonarulrajah, A., 2003, "Biological Response to Wear Debris Generated in Carbon Based Composites as Potential Bearing Surfaces for Artificial Hip Joints," Biomedical Material Research Part B: Applied Biomaterials, **67-B**(2) pp. 758-64.

[74] Catelas, I., Bobyn, J. D., Medley, J. B., 2001, "Effects of Digestion Protocols on the Isolation and Characterization of Metal-Metal Wear Particles. II. Analysis of Ion Release and Particle Composition," Journal of Biomedical Material Research, **55**(3) pp. 330-7.

[75] Campbell, P., Shen, F. W., and McKellop, H., 2004, "Biological and Tribologic Considerations of Alternative Bearing Surfaces," Clinical Orthopaedics, **418**pp. 98-111.

[76] Santos, E. G., Polly, D. W., Mehbod, A. A., 2004, "Disc Arthroplasty: Lessons Learned from Total Joint Arthroplasty," The Spine Journal, **4**((6Suppl)) pp. 182S-189S.

[77] Kurtz, S. M., De Bruin, T., Cleutjens, J., 2007, "169. Long-Term Periprosthetic Tissue Reactions to Polyethylene Wear Debris in Total Disc Arthroplasty," The Spine Journal, **7**pp. 80S-81S.

[78] Traynelis, V. C., Burkus, K., Gornet, M., 2007, "Prospective Study of Serum Metal Ion Levels in Patients with Stainless Steel Metal-on-Metal Cervical Disc Replacements," The Spine Journal, **7**pp. 54S.

[79] Wichmann, W., Von Ammon, K., Fink, U., 1997, "Aneurysm Clips made of Titanium: Magnetic Characteristics and Artifacts in MR," AJNR American Journal of Neuroradiology, **18**(5) pp. 939-44.

[80] Rupp, R., Ebraheim, N., Savolaine, E. R., 1993, "Magnetic Resonance Imaging Evaluation of the Spine with Metal Implants," Spine, **18**(3) pp. 379-85.

[81] Viano, A., Gronemeyer, S., Haliloglu, M., 2000, "Improved MR Imaging for Patients with Metallic Implants," Magnetic Resonance Imaging, **18**pp. 287-95.

[82] Haramati, N., Staron, R. B., Mazel-Sperling, K., 1994, "CT Scans through Metal Scanning Technique Versus Hardware Composition," Computerized Medical Imaging and Graphics, **18**(6) pp. 429-34.

[83] Scholes, S., and Unsworth, A., 2006, "The Introduction of New Materials for Articulating Implantable Devices," Orthopaedic Product News, (July/August) pp. 22-24.

[84] Green, S., 2005, "Using Implantable-Grade PEEK for in Vivo Devices," Medical Device & Diagnostic Industry, (May) pp. 104.

[85] Wang, A., Lin, R., Polineni, V. K., 1998, "Carbon Fiber Reinforced Polyetherether Ketone Composite as a Bearing Surface for Total Hip Replacement," Tribology International, **31**(11) pp. 661-667.

[86] Werner, P., Altstädt, V., Jaskulka, R., 2004, "Tribological Behaviour of Carbon-Nanofibre-Reinforced Poly(Ether Ether Ketone)," Wear, **257**(9-10) pp. 1006-1014.

[87] Zhang, G., and Schlarb, A. K., "Morphologies of the Wear Debris of Polyetheretherketone Produced Under Dry Sliding Conditions: Correlation with Wear Mechanisms," Wear, **In Press, Corrected Proof**.

[88] Altstaedt, V., Werner, P., and Sandler, J., 2003, "Rheological, Mechanical and Tribological Properties of Carbon-Nanofibre Reinforced Poly (Ether Ether Ketone) Composites," Polimeros: Ciencia e Tecnologia, **13**(4) pp. 218-22.

[89] Green, S., 2006, "
Carbon Fibre Reinforced PEEK-OPTIMA® Composite Materials for use in Surgical Implant Applications," .

[90] The Quandrant Group of Companies, 2008, "Quadrant EPP Ketron® PEEK-CA30 LSG," **2008**(Nov/25) .

[91] Sandler, J., Werner, P., Shaffer, M. S. P., 2002, "Carbon-Nanofibre-Reinforced Poly(Ether Ether Ketone) Composites," Composites Part A: Applied Science and Manufacturing, **33**(8) pp. 1033-1039.

[92] Jones, D. P., Leach, D. C., and Moore, D. R., 1985, "Mechanical Properties of Poly(Ether-Ether-Ketone) for Engineering Applications," Polymer, **26**(9) pp. 1385-1393.

[93] Zhang, G., Latour, R. A., Kennedy, J. M., 1996, "Long-Term Compressive Property Durability of Carbon Fibre-Reinforced Polyetheretherketone Composite in Physiological Saline," Biomaterials, **17**(8) pp. 781-789.

[94] Sagomonyants, K. B., Jarman-Smith, M. L., Devine, J. N., 2008, "The in Vitro Response of Human Osteoblasts to Polyetheretherketone (PEEK) Substrates Compared to Commercially Pure Titanium," Biomaterials, **29**(11) pp. 1563-1572.

[95] Scholes, S., and Unsworth, A., 2001, "Pin-on-Plate Studies on the Effect of Rotation on the Wear of Metal-on-Metal Samples," Journal of Materials Science: Materials in Medicine, **12**pp. 299-303.

[96] Mathews, H. H., LuHuec, J., Friesem, T., 2004, "Design Rotionale and Biomechanics of Maverick Total Disc Arthroplasty with Early Clinical Results," The Spine Journal, **4**(6, Supp 1) pp. 268S-275S.

[97] Scholes, S., and Unsworth, A., 2007, "The Wear Properties of CFR-PEEK-OPTIMA Articulating Against Ceramic Assessed on a Multidirectional Pin-on-Plate Machine," Proceeding of the Institute of Mechanical Engineers. Part H, Journal of Engineering in Medicine, **221**(3) pp. 281-289.

[98] Tipper, J. L., Firkins, P. J., Ingham, E., 1999, "Quantitative Analysis of the Wear and Wear Debris from Low and High Carbon Content Cobalt Chrome Alloys used in Metal on Metal Total Hip Replacements," Journal of Materials Science: Materials in Medicine, **10**(6) pp. 353-362.

[99] Joyce, T. J., Monk, D., Scholes, S., 2000, "A Multi-Directional Wear Screening Device and Preliminary Results of UHMWPE Articulating Against Stainless Steel," Bio-Medical Materials and Engineering, **10**pp. 241-249.

[100] Scholes, S., and Unsworth, A., 2008, "Comparison of PEEK, PEK and CFR-PEEK in self-mating wear couples for use in orthopeadics," Anonymous .

[101] Scholes, S., and Unsworth, A., 2008, "The Likely Wear Performance of CFR-PEEK/CoCrMo for Artificial Joints," Anonymous .

[102] Joyce, T. J., and Unsworth, A., 2004, "Wear Studies of all UHMWPE Couples Under various Bio-Tribological Conditions," Journal of Applied Biomaterials & Biomechanics, **2**pp. 29-34.

[103] Brown, T., Bao, Q., Kilpela, T., 2008, "A Comprehensive Wear Assessment of PEEK-OPTIMA for Disc Arthroplasty Applications," Anonymous .

[104] Brandt, J. -., Charron, K. D., Zhao, L., 2007, "Calf Serum Type Affects Protein Degradation, Bacterial Growth and Polyethylene Wear in Knee Simulator Testing," Anonymous **32,** pp. P1871.

[105] Brandt, J. -., Charron, K. D., Zhao, L., 2008, "Development of a Clinically Relevant Lubricant for In-Vitro Wear Testing of Total Knee Replacements," Anonymous .

[106] American Society for Testing and Materials, 2000, "Standard Practice for Gravimetric Measurement of Polymeric Components for Wear Assessment," American Society of Testing and Materials, ASTM F 2025-00, PA, United States.

[107] MENSITIERI, G., APICELLA, A., KENNY, J. M., 2003, "Water Sorption Kinetics in Poly(Aryl Ether Ether Ketone)," Journal of Applied Polymer Science, **37**(2) pp. 381-92.

[108] Advanced Mechanical Technology Inc. (AMTI), 2004, "AMTI's Ortho-Pod - Friction and Wear Testing Machine Manual," .

[109] Clarke, I. C., Chan, F. W., Essner, A., 2001, "Multi-Laboratory Simulator Studies on Effects of Serum Proteins on PTFE Cup Wear," Wear, **250**(1-12) pp. 188-198.

[110] Shigley, J.E., 19uu, "Mechanical engineering design." McGraw-Hill [c1963], New York, .

APPENDIX A

EXCERPTS FROM:
ISO 18192-1
ASTM 2423-05

Implants for surgery — Wear of total intervertebral spinal disc prostheses — Part 1: Loading and displacement parameters for wear testing and corresponding environmental conditions for tests

1 Scope

This International Standard defines a test procedure for the relative angular movement between articulating components, and specifies the pattern of the applied force, speed and duration of testing, sample configuration and test environment to be used for the wear testing of total intervertebral spinal disc prostheses.

Both lumbar and cervical prostheses are addressed. This standard does not address partial disc replacements, such as nucleus replacements, or facet joint replacements. The test method focuses on wear testing, additional mechanical tests such as fatigue testing and others may be required.

This standard does not reproduce the complex in vivo loads and motions. The wear data obtained with this test method will enable comparison between different types of implants but may differ from the clinical wear performance. The user of this standard may consider running additional wear tests addressing specific safety issues of the individual implant design to be tested.

2 Normative references

The following referenced documents are indispensable for the application of this document. For dated references, only the edition cited applies. For undated references, the latest edition of the referenced document (including any amendments) applies.

ISO 14242-2, *Implants for surgery – Wear of total hip-joint prostheses – Part 2: Methods of measurement*

3 Terms and definitions

For the purposes of this document, the following terms and definitions apply.

3.1
axial rotation
angular movement in the transverse plane around the z-axis

NOTE See figure 1C.

3.2
flexion/extension
angular movement in the sagittal plane around the y-axis

NOTE See figure 1A.

© ISO 2005 – All rights reserved

3.3
functional failure
failure that renders the implant unable to resist the load and/or to enable to move as initially intended by the design of the implant.

3.4
lateral bending
angular movement in the frontal plane around the x-axis

NOTE See figure 1B.

3.5
mechanical failure
onset of a defect in the material

EXAMPLE initiation of fatigue crack.

3.6
origin
centre of the coordinate system is located at the instantaneous centre of rotation at the neutral position of the total disc replacement.

NOTE The nominal centre is specified by the design.

3.7
user defined failure
any failure criterion that is established and controlled by the user considering the specific design of the implant to be tested.

3.8
x-axis
positive x-axis is directed anteriorly

NOTE See figure 1.

3.9
y-axis
positive y-axis is directed laterally to the left

NOTE See figure 1.

3.10
z-axis
positive z-axis is directed superiorly

NOTE See figure 1.

4 Principle

The inferior and superior components of a test specimen are placed in position in the configuration intended for clinical use; the test apparatus transmits a specified time-varying force between the components, together with specified relative angular displacements. A load soak control specimen, if polymers are the object of investigation, is subjected to the same time-varying force to determine the creep of the test specimen and/or the amount of mass change due to fluid transfer. The test takes place in a controlled environment simulating physiological conditions.

© ISO 2005 – All rights reserved

5 Reagents and materials

5.1 Fluid test medium

Calf serum diluted with de-ionized water (balance) to a concentration of 30 g ± 2 g protein/l.

The fluid test medium may be filtered through a 2 µm filter if desired.

To minimize microbial contamination, the fluid test medium should be stored frozen until required for test. An anti-microbial reagent (such as sodium azide) may be added. Such reagents may be potentially hazardous.

Note: The addition of EDTA at 20mM may be recommended to bind calcium in solution and to minimize precipitation of calcium phosphate onto the bearing surfaces. The effect of EDTA will depend on the material combination tested. The addition of EDTA shall be justified by the user.

Routine monitoring of the pH of the fluid test medium should be undertaken. If it is, the values shall be included in the test report [see Clause 8 item k) 6)].

5.2 Test and control specimen

Between the inferior and superior component shall be the articulating surface of the inferior and superior component attached by its normal immediate backing (for example bone cement or a machined replica of the inner surface of the backing) unless this is impractical due to physical features of the implant system. If the component forming the articulating surface is fixed to the backing by a rim/snap-fit system, the machined replica shall provide the same fixation conditions.

If it is not practical to use the normal backing or cement fixation, due to physical features of the implant system, the support system for the inferior and/or superior component should represent normal design features and conditions of use but should allow removal of the component for measurement of wear without destruction.

A recommended minimum sample number of six should be used for wear testing. At least one additional sample must be used to correct weight gain by fluid uptake (load soak control). The load soak control has to be loaded according to the load profile given for the type of implant. The user may decide not to use a soak control when testing materials that do not absorb surrounding fluid (for example metal materials).

NOTE 1 The number of specimens tested may be the subject of national legislation.

NOTE 2 If less than six specimens are tested appropriate justification has to be given.

6 Apparatus

6.1 Testing machine

Capable of producing the angular displacements specified in Table 1 and Figures 2 and 3 in association with the corresponding forces specified in Table 2 and operating at a frequency of (1 ± 0,1) Hz based on one cycle being the shortest repetitive interval for all motions and loads combined.

© ISO 2005 – All rights reserved

Table 1 — Angular displacements of the testing machine

	Angle	Flexion/Extension	Axial rotation	Lateral bending
Cervical	min	-7,5°	-4°	-6°
	max	7,5°	4°	6°
Lumbar	min	-3°	2°	2°
	max	6°	-2°	-2°

NOTE 1 The angular displacements indicated may be varied according to data given by the test requestor.

A defined level of shear loading shall be implemented for lumbar implants being restrained in the transverse plane. Shear loading is achieved by inclining the implant with respect to the axial load axis in the sagittal plane at the reference position (see Fig. 4).

NOTE 2 The user of this document should be aware that a certain amount of shear load is generated by the motion of the device with respect to the axial load. In regard to the implant design the user should give a justification for intended physiological conditions, especially for motion of any articulating surfaces during the load and motion cycle.

NOTE 3 See Annex A for load and motion rationale.

NOTE 4 Certain designs may be sensitive to shear loads. The user may intensify the test conditions by increasing the shear load and/or adding alternating load directions.

All angular displacement curves and load curves are smooth. The curves have to reach the given values at 0, 25, 50 and 75 percent of the motion cycle within the tolerances given in 6.4. Sample data sets are provided in annexes B and C.

The angles are referred to moving coordinate system.

The intended sequence of the angular transformation is – Lateral bending– Flexion/Extension – Axial rotation.

NOTE 5 The sequence of the axial rotations will slightly impact the motion and the final position after each motion step (Euler angles). Due to the small angles applied, Euler sequences differing from the above mentioned one will result in almost identical relative motions. The Euler sequence chosen may be selected according to the mechanical set-up of the wear testing machine.

Table 2 — Load parameters of the testing machine.

		Load [N]
Cervical	Load max	150
	Load min	50
Lumbar	Load max	2000
	Load min	600

NOTE 6 The load parameters indicated may be varied according to data given by the test requestor.

NOTE 7 The load curve is sinusoidal.

© ISO 2005 – All rights reserved

Designation: F 2423 – 05

Standard Guide for Functional, Kinematic, and Wear Assessment of Total Disc Prostheses[1]

This standard is issued under the fixed designation F 2423; the number immediately following the designation indicates the year of original adoption or, in the case of revision, the year of last revision. A number in parentheses indicates the year of last reapproval. A superscript epsilon (ε) indicates an editorial change since the last revision or reapproval.

1. Scope

1.1 This guide is intended to provide guidance for the functional, kinematic, and wear testing of total disc prostheses and, to this end, describes test methods for assessment of the wear or functional characteristics, or both, of total disc prostheses.

1.2 Both lumbar and cervical prostheses are addressed.

1.3 Load and kinematic profiles for lumbar and cervical devices are not identical and, therefore, are addressed separately in the guide.

1.4 Partial disc replacements, such as nucleus replacements or facet joint replacements, are not intended to be addressed.

1.5 Wear is assessed using a weight loss method in a testing medium as defined in this guide.

1.6 This guide is not intended to address any potential failure mode as it relates to the fixation of the implant to its bony interfaces.

1.7 It is the intent of this guide to enable comparison of intervertebral disc (IVD) prostheses with regard to kinematic, functional, and wear characteristics when tested under the specified conditions. It must be recognized, however, that there are many possible variations in the *in vivo* conditions. A single laboratory simulation with a fixed set of parameters may not be universally representative.

1.8 In order that the data be reproducible and comparable within and between laboratories, it is essential that uniform procedures are established. This guide is intended to facilitate uniform methods for testing and reporting of data for total disc replacement prostheses.

1.9 Without a substantial clinical retrieval history of IVD prostheses, actual loading profiles and patterns cannot be delineated at the time of the writing of this guide. It therefore follows that the load and motion conditions specified by this guide do not necessarily accurately reproduce those occurring *in vivo*. Rather, the maximum loads and motions specified in this guide represent a severe and therefore conservative case for testing the wear properties of IVD prostheses. Because of this, a substantially greater rate of wear may be realized than that which may occur during the routine daily activities of a typical patient. It should be noted, however, that a full characterization of a candidate IVD prosthesis should include testing under both typical and extreme conditions.

1.10 The values stated in SI units are to be regarded as the standard with the exception of angular measurements, which may be reported in either degrees or radians.

1.11 This guide is not intended to be a performance standard. It is the responsibility of the user of this guide to characterize the safety and effectiveness of the prosthesis under evaluation.

1.12 *This standard does not purport to address all of the safety concerns, if any, associated with its use. It is the responsibility of the user of this standard to establish appropriate safety and health practices and determine the applicability of regulatory limitations prior to use.*

2. Referenced Documents

2.1 *ASTM Standards:* [2]

F 561 Practice for Retrieval and Analysis of Medical Devices, and Associated Tissues and Fluids

F 1582 Terminology Relating to Spinal Implants

F 1714 Guide for Gravimetric Wear Assessment of Prosthetic Hip-Designs in Simulator Devices

F 1877 Practice for Characterization of Particles

F 2077 Test Methods For Intervertebral Body Fusion Devices

3. Terminology

3.1 *Definitions*—All functional and kinematic testing terminology is consistent with the referenced standards, unless otherwise stated.

3.1.1 *coordinate system/axes, n*—global *XYZ* orthogonal axes are defined following a right-handed Cartesian coordinate system in which the *XY* plane is to bisect the sagittal plane angle between superior and inferior surfaces that are intended to simulate the adjacent vertebral end plates. The global axes are stationary relative to the IVD prostheses' inferior end plate

[1] This guide is under the jurisdiction of ASTM Committee F04 on Medical and Surgical Materials and Devices and is the direct responsibility of Subcommittee F04.25 on Spinal Devices.

Current edition approved Nov. 15, 2005. Published January 2006.

[2] For referenced ASTM standards, visit the ASTM website, www.astm.org, or contact ASTM Customer Service at service@astm.org. For *Annual Book of ASTM Standards* volume information, refer to the standard's Document Summary page on the ASTM website.

Copyright © ASTM International, 100 Barr Harbor Drive, PO Box C700, West Conshohocken, PA 19428-2959, United States.

fixture, which, in this guide, is also considered to be stationary with respect to the test machine's frame. Lower case letters, *xyz*, denote a local, moving orthogonal coordinate system attached to the superior end plate fixturing with directions initially coincident with those of the global *XYZ* axes, respectively. The 3-D motion of the superior relative to inferior end plate fixture is specified and is to be measured in terms of sequential Eulerian angular rotations about the *xyz* axes, respectively (*z*, axial rotation; *x*, lateral bending; and *y*, flexion-extension).

3.1.1.1 *origin, n*—center of the global coordinate system is located at the initial position of the total disc replacement's instantaneous center of rotation (COR). **F 1582**

3.1.1.2 *X-axis, n*—positive *X*-axis is a global fixed axis relative to the testing machine's stationary base and is to be directed anteriorly relative to the specimen's initial unloaded position.

3.1.1.3 *Y-axis, n*—positive *Y*-axis is a global fixed axis relative to the testing machine's stationary base and is directed laterally relative to the specimen's initial unloaded position.

3.1.1.4 *Z-axis, n*—positive *Z*-axis is a global fixed axis relative to the testing machine's stationary base and is to be directed superiorly relative to the specimen's initial unloaded position.

3.1.1.5 *x-axis, n*—positive *x*-axis is a fixed axis relative to the IVD prosthesis and a moving axis relative to the global coordinate system and is directed anteriorly relative to the prosthesis.

3.1.1.6 *y-axis, n*—positive *y*-axis is a fixed axis relative to the IVD prosthesis and a moving axis relative to the global coordinate system and is directed laterally relative to the prosthesis.

3.1.1.7 *z-axis, n*—positive *z*-axis is a fixed axis relative to the IVD prosthesis and a moving axis relative to the global coordinate system and is directed superiorly relative to the prosthesis.

3.1.2 *degradation, n*—loss of material or function or material properties as a result of causes other than that associated with wear.

3.1.3 *fluid absorption, n*—fluid absorbed by the device material during testing or while implanted *in vivo*.

3.1.4 *functional failure, n*—permanent deformation or wear that renders the IVD prosthesis assembly ineffective or unable to resist load/motion or any secondary effects that result in a reduction of clinically relevant motions or the motions intended by the design of the device.

3.1.5 *interval net volumetric wear rate VR_i during cycle interval i (mm³/million cycles), n*—$VR_i = WR_i/\rho$, where ρ = mass density (for example, units of g/mm³) of the wear material.

3.1.6 *interval net wear rate WR_i during cycle interval i (g/million cycles), n*—$WR_i = ((NW_i - NW_{i-1})/(\text{number of cycles in interval } i))*10^6$.

3.1.6.1 *Discussion*—For $i = 1$, $NW_{i-1} = 0$.

3.1.7 *intervertebral disc (IVD) prosthesis, n*—nonbiologic structure intended to restore the support and motion or a portion thereof between adjacent vertebral bodies.

3.1.8 *kinematic profile, n*—relative motion between adjacent vertebral bodies that the IVD prosthesis is subjected to while being tested.

3.1.9 *load profile, n*—loading that the device experiences while being tested under a defined kinematic profile or the loading that the IVD prosthesis is subject to if tested in load control.

3.1.10 *mechanical failure, n*—failure associated with a defect in the material (for example, fatigue crack) or of the bonding between materials that may or may not produce functional failure.

3.1.11 *net wear NW_i of wear specimen (g), n*— $NW_i = (W_0 - W_i) + (S_i - S_0)$; loss in weight of the wear specimen corrected for fluid absorption at end of cycle interval *i*.

3.1.12 *net volumetric wear NV_i of wear specimen (mm³), n*— $NV_i = NW_i/\rho$ at end of cycle interval *i* where ρ = mass density (for example, units of g/mm³) of the wear material.

3.1.13 *preload, n*—The resultant force $F_{preload}$ applied to the superior or inferior fixture-end plate that simulates the *in vivo* load that an IVD prosthesis (original healthy disc) must resist.

3.1.13.1 *Discussion*—Based on a healthy disc, the primary component would be an axial compressive force F_Z in the direction of the negative global *Z* axis, and it would pass through the *in vivo* physiologic instantaneous center of rotation (COR) of the IVD prosthesis. Shear components in the *XY* plane would be F_X and F_Y. Lateral bending moment M_X and flexion/extension moment M_Y components would be created about the initial COR when the preload force does not pass through it.

3.1.14 *run out (cycles), n*—maximum number of cycles that a test needs to be carried to if functional failure has not yet occurred.

3.1.15 *wear, n*—progressive loss of material from the device(s) or device components as a result of relative motion at the surface with another body as measured by the change in mass of the IVD prosthesis or components of the IVD prosthesis. Or in the case of a nonarticulating, compliant IVD prosthesis, wear is defined simply as the loss of material from the prosthesis.

3.1.15.1 *Discussion*—Note that inferior and superior bone interface components are excluded from this definition; see 5.2.2.

3.1.16 *weight S_i of soak control specimen (g), n*—S_0 initial and S_i at end of cycle interval *i*.

3.1.17 *weight W_i of wear specimen (g), n*—W_0 initial and W_i at end of cycle interval *i*.

4. Significance and Use

4.1 This guide can be used to describe the function, kinematics, and wear behavior of IVD prostheses subjected to cyclic loading/motion for relatively large numbers of cycles (for example, various designs of IVD prostheses, as well as the effects of materials, manufacturing techniques and other design variables on one particular design can be studied using this guide).

4.2 This guide is intended to be applicable to IVD prostheses that support and transmit motion by means of an articulating joint or by use of compliant materials. Ceramics, metals, or

TABLE 1 Test Profiles and Associated Parameters for Cervical IVD Prostheses

Test Profile	Axial Preload, N (3-5)	Preferred Displacement Control: Range of Motion (ROM),[A] degree (4)	Alternate Load Control: Applied Moment Ranges, Nm (4)
Flexion/extension	100	±7.5	±2.0
Lateral bend/ rotation	100	±6	±2.0
		±6	±4.0

[A] The user of the guide must determine whether the ROM will be equally divided between flexion and extension or weighted more toward one of the motion directions.

TABLE 2 Test Profiles and Associated Parameters for Lumbar IVD Prostheses

Test Profile	Axial Preload, N (6)	Preferred Displacement Control: Range of Motion (ROM), degree	Alternate Load Control: Applied Moments, Nm[A]
Flexion/extension	1200	±7.5[B]	±10
Rotation	1200	±3 (7,9)	±10
Lateral bending	1200	±6 (7,9)	±12

[A] Approximated based on a review of ROM (p. 111) and average flexibility and stiffness coefficients (p. 47) (7).
[B] Depending on the device design, the balance of ROM should be appropriate to the expected ROM in a clinical situation (8).

polymers, or combination thereof, are used in IVD prosthesis design, and it is the goal of this guide to enable a kinematic wear comparison of these devices, regardless of material and type of device.

5. Apparatus

5.1 *Total Disc Prosthesis Components*—The total disc replacement may comprise a variety of shapes and configurations. Some known forms include ball and socket articulating joints, biconcave joints having a free-floating or semi-constrained third body, metallic endplates bonded to elastomer cores, and single-axis hinge joints.

5.2 *Spinal Testing Apparatus*:

5.2.1 *Test Chambers*—In case of a multispecimen machine, each chamber shall be isolated to prevent cross-contamination of the test specimens. The chamber shall be made entirely of noncorrosive components, such as acrylic plastic or stainless steel, and shall be easily removable from the machine for thorough cleaning between tests.

5.2.2 *Component Clamping/Fixturing*—Since the purpose of the test is to characterize the wear and kinematic function of the IVD prosthesis, the method for mounting components in the test chamber shall not compromise the accuracy of assessment of the weight loss or stiffness variation during the test. For example, prostheses having complicated superior and inferior surfaces for contacting bone (for example, sintered beads, hydroxylapatite (HA) coating, plasma spray) may be specially manufactured to modify that surface in a manner that does not affect the wear simulation.

5.2.3 The device should be securely (rigidly) attached at its bone-implant interface to the mating test fixtures.

5.2.4 The motion of the superior test fixture relative to the inferior testing fixture shall be unconstrained in three-dimensional space except for the components in the direction of specified test motions/loads.

5.2.5 *Load and Motion (components in Table 1 and Table 2)*:

5.2.5.1 An axial preload is to be a compressive load applied in the direction of the negative Z-axis. Deviations from this as the IVD moves from its initial position are to be reported as shear components F_X, F_Y, and moments M_X and M_Y.

5.2.5.2 Flexion load and motion are positive moment, M_Y, and rotation about the y-axis.

5.2.5.3 Extension load and motion are negative moment, M_Y, and rotation about the y-axis.

5.2.5.4 Lateral bend load and motion are positive and negative moments, M_X, and rotations about the x-axis.

5.2.5.5 Torsional load and motion are positive and negative moments, M_Z and rotations about the z-axis.

5.2.6 *Frequency*—Test frequency is to be determined and justified by the user of this guide, and shall not exceed 2 Hz without adequate justification ensuring that the applied motion (load) profiles remain within specified tolerances and that the IVD prosthesis' wear and functional characteristics are not significantly affected. See 6.1.5.

5.2.7 *Cycle Counter*—One complete motion is the entire range from starting position through the range of motion (or load when in load control) and returning to the starting position (load). Cycles are to be counted using an automated counting device.

6. Reagents and Materials

6.1 *Testing Medium*:

6.1.1 A solution containing bovine serum diluted to a protein concentration of 20 g/L in deionized water shall be used as the testing medium.

6.1.2 To retard bacterial degradation, freeze and store the serum until needed for test. In addition, the testing medium may contain 0.2 % sodium azide (or other suitable antibiotic/antimycotic) to minimize bacterial degradation. Other lubricants should be evaluated to determine appropriate storage conditions.

6.1.3 It is recommended that ethylene-diaminetetraacetic acid (EDTA) be added to the serum at a concentration of 20m*M* to bind calcium in solution and minimize precipitation of calcium phosphate onto the bearing surfaces. The latter event has been shown to affect the friction and wear properties strongly, particularly of polyethylene/ceramic combinations. The addition of EDTA to other testing media should be evaluated.

6.1.4 The bulk temperature of the testing medium shall be maintained at 37 ± 3°C, unless otherwise specified.

6.1.5 The user is cautioned that internal heating of the prosthesis may cause localized temperatures to fall outside the 37 ± 3°C of the testing medium. Internal local temperatures may depend on a number of factors, including but not limited to joint friction, material hysteresis, conductivity of the device-fixture materials, design, and test frequency. Localized elevated temperatures may have an effect on the mechanical as well as wear properties of the prosthesis. If the device experiences localized elevated temperatures, the user must describe the effect that the selected frequency and resultant

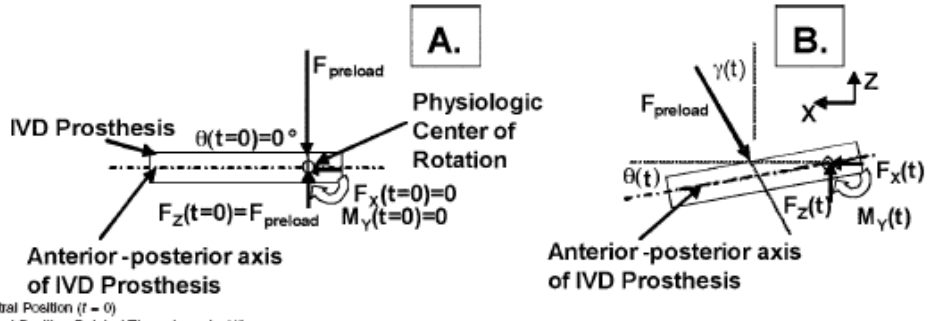

A. Neutral Position ($t = 0$)
B. Flexed Position Rotated Through Angle $\theta(t)$
γ = Angle of the Preload Relative to the Global Z-Axis

FIG. 1 2-D (*XZ* Plane Only) Loading Diagrams Showing $F_{preload}$ and its resultant Reaction Force-Moment Components Shown Acting at the Initial Physiologic Center of Rotation of the IVD Prostheses

localized temperature have on the test results, or justify that the effects are physiologically relevant. Refer to X1.6 for further information.

7. Sampling and Test Specimens

7.1 It is suggested that a minimum sample size of five be used for each kinematic/load profile. However, note that, as for any experimental comparison, the total number of needed specimens will depend on the magnitude of the difference to be established, the repeatability of the results (standard deviation), and the level of statistical significance desired.

7.2 The test assemblies (that is, IVD prosthesis components in the tested configuration) shall be labeled so they can be traced, and must be kept in a clean environment to avoid contamination. The test assembly can be disassembled to facilitate examination of surface conditions.

8. Preparation of Apparatus

8.1 The functional portion (components producing motion between vertebral bodies) of the device to be tested must be produced using equivalent manufacturing methods as the implantable form of the IVD prosthesis, including sterilization.

8.2 It is permissible to exclude nonfunctional features that may interfere with obtaining wear/functional measurements. For example, bone-implant interfaces such as HA, plasma-spray titanium, and beads may be omitted, since they may abrade the fixtures and, thereby, produce an unwanted mixture of functional and nonfunctional component wear particles (see 5.2.2).

8.3 It is permissible to fabricate entirely different bone-implant interface components (that is, superior and inferior surfaces) provided that the modification does not interfere with an accurate measurement of the wear and functional characteristics of the device. For example, a ball and socket joint prosthesis may be manufactured having the polished articulation component (that is, the functional surfaces or features of the device) and an opposite side that mounts directly to the testing apparatus, thereby simplifying the fixturing demands.

8.4 The requirements of Guide F 1714, Specimen Preparation section, shall be followed.

9. Procedure

9.1 As a weight control for the testing, a minimum of two identical loaded soak control specimens in testing medium (see 6.1) shall be used. In other words, the loaded soak control specimen must be loaded with the same preload as is applied to the wear test specimens, since it is well known that load can significantly affect fluid absorption.

NOTE 1—The user of this guide may justify not performing control tests in certain circumstances (for example, all metal components). Before, and at all specified time intervals (determined by the user) of the presoak period (defined in Guide F 1714), the wear components and soak controls should be removed from the soak bath, cleaned, dried, and weighed three times, in rotation, keeping the same specimen sequence each time. The average of the three weights may be used for the wear calculations. An analytical balance with a sensitivity of ±10 µg or less shall be used. This degree of sensitivity for weighing is necessary to detect the slight loss in weight of highly wear-resistant bearing materials (1).[3]

9.2 Always weigh specimens in the clean, dry condition (see Annex A4 of Guide F 1714). Keep the components in a dust-free container and handle with clean tools or gloves or both to prevent contamination that might affect the weight measurement. Weigh each wear and control component three times in rotation to detect random errors in the weighing process.

9.3 Record weights, W_0 and S_0, as the initial weights of the wear and soak controls, respectively. Place the loaded soak control specimens in holders in a soak chamber of the testing medium, such that the total surface area exposed to the testing medium is the same as that of the wear components when mounted in the spinal testing apparatus. Maintain the soak chamber temperature at 37 ± 3°C, or specify if different.

9.4 For all components, measure the geometry of relevant functional surfaces or features before starting the test. For example, articulating joints should have measurements of the bearing area. Prostheses having bonded polymer cores should have measurements of the external geometry such as starting

[3] The boldface numbers in parentheses refer to the list of references at the end of this standard.

circumference (to calculate changes caused by equatorial bulging) and prosthesis height.

9.5 Testing medium, temperature, and removal periods for weighing components shall be identical for all control and test specimens.

9.6 Unless otherwise justified by intended use and life expectancy of the IVD prosthesis, all tests should be conducted to a run out of 10 000 000 cycles (see Appendix X1).

9.7 The testing medium shall be collected for subsequent analysis at least once every one million cycles, and shall be replaced with fresh testing medium.

9.8 Place the prostheses in the spinal testing apparatus, add testing medium, and subject the IVD prosthesis to each of the tests as listed in 9.10. The prostheses shall be visually analyzed at a minimum once per 1 000 000 cycles, with mechanical failures noted (see Note 2). A mechanical failure (for example, considerable wear of the bearing surface) may not necessitate termination of the test since this guide attempts to characterize the time dependent wear properties of the device. The test shall be terminated if functional failure occurs (for example, gross fracture or the bearing seizes).

NOTE 2—The user may choose to analyze the specimen more frequently than recommended by the guide.

9.9 A new, unused specimen shall be used to start each test series according to 9.10.6 and 9.10.7.

9.10 *Tests*:

9.10.1 Tests should be conducted under displacement control. Load control may also be used with adequate justification.

9.10.2 The preload (initial axial load) is to be an axially applied compressive force parallel to the global Z direction through the *in vivo* physiologic instantaneous center of rotation of the IVD prosthesis (that is, the expected initial center of rotation of the IVD prosthesis when implanted *in vivo* (see X1.5). The specific methodology for fixturing and applying the preload will dictate the resultant shear load, F_X, axial load, F_Z, and bending moment, M, the device will be subject to throughout the motion profile. (F_X, F_Z, and M, are shown in Fig. 1 acting at the physiologic center of rotation of the IVD prosthesis.) θ is the rotation angle (that is, flexion/extension angle) of the prosthesis in flexion/extension motion, and γ is angle of the preload force relative to the global Z-axis. See Cripton et al (2) for a discussion of the effects of various preload fixturing configurations. (Also, see X1.7 for further comments and information about preload configurations.)

9.10.3 Loading diagrams, along with their reaction forces acting on the physiologic center of rotation of the IVD prosthesis in the neutral position ($t = 0$) and flexed position, that describe the preload configuration are given in Fig. 1.

9.10.4 An example of a specific method and fixture design for achieving the preload configuration depicted in Fig. 1 is described in Appendix X1.

9.10.5 A constant preload for all testing is to be applied with the use of a mechanism that can apply a constant magnitude force (±5 %) throughout the ranges of motion that the test rig will undergo during testing. Pneumatic or hydraulic cylinders, by virtue of their ability to apply a nearly constant force but allow movement of the actuator, are examples of devices that would be appropriate for use to apply the preload force. Note that the application of a constant preload to a spine arthroplasty during wear testing may lead to unrealistically high wear due, in part, to depletion of the lubricant between the bearing surfaces. Alternatively, the user may apply a cyclic preload, since this may drastically affect the lubrication and, thereby, the rate of wear of the prosthesis. If a cyclic axial preload is employed, minimum and maximum axial preloads shall be 50 % and 150 % respectively of the axial preloads listed in Tables 1 and 2 unless otherwise justified.

NOTE 3—If a cyclic axial preload is applied, the user must determine and justify the phase angle used between the axial preload and the other applied motions.

9.10.6 *Cervical IVD Prostheses Tests*:

9.10.6.1 Table 1 lists the test profiles and associated parameters for testing cervical spine IVD prostheses. The user shall test the same devices for each of the parameters listed. For example, after completing 10 000 000 cycles in flexion/extension, the user shall conduct lateral bend and rotational coupled motions on the same device.

9.10.6.2 An alternate method in which all of the simple motions are combined in one test may be used in lieu of testing each device sequentially under each test profile as stated in 9.10.6.1. Note that each component motion in this combined motion test must complete at least 10 000 000 cycles.

9.10.6.3 For all coupled motions, the user must report and justify the phase angle used between the motions.

9.10.6.4 The sequence of motions shall be determined and justified by the user of this guide. It should be noted, however, that the sequence of motions can affect the wear properties of the IVD prosthesis, and therefore, the user may wish to consider testing under different sequences to analyze their effect on the wear properties of the IVD prosthesis.

9.10.7 *Lumbar IVD Prostheses Tests*:

9.10.7.1 Table 2 lists the test profiles and associated parameters for testing lumbar spine IVD prostheses. There are several options open to the user for testing the prosthesis as described in this section; however, justification for the chosen methodology must be provided. As with all device testing, the user is reminded that the selected test methods should provide the most rigor and enable the most accurate characterization of the device as possible (that is, strive for identifying and then using test conditions that would produce the worst case wear that the device may experience *in vivo*). To this end, the user may wish to test according to more than one of the following options (see X1.3 for further comments):

(1) The user may test the same device under the single motion parameters defined in Table 2 (that is, the user shall test the device in flexion/extension loading for 10 000 000 cycles, followed by lateral bend testing for 10 000 000 cycles on the same device and finally rotational testing for 10 000 000 cycles on the same device).

(2) The user may wish to perform a test in which the device is tested following one of the prescribed single motions followed by a coupled test (on the same device) for the remaining two motions. As way of example, the user may wish to test the device in flexion/extension for 10 000 000 cycles and then perform a coupled test of lateral bending and rotation on the same device (10 000 000 cycles for each motion).

(3) An alternate method in which all of the component motions are combined in one test may also be employed. Note that each component motion in this combined motion test must complete at least 10 000 000 cycles.

9.10.7.2 For all coupled motions, the user must report and justify the phase angle used between the motions.

9.10.7.3 The sequence of motions shall be determined and justified by the user of this testing guide. It should be noted, however, that the sequence of motions can affect the wear properties of the IVD prosthesis, and therefore, the user may wish to consider the use of different sequences to analyze their effect on the wear properties of the IVD prosthesis.

9.10.7.4 If the device is intended for use in situations in which the facet joints are compromised, selection and justification for the amount of rotation should be provided.

9.10.8 Regardless of the selected test method, ROM data shall be recorded during the test.

9.10.9 If a device ceases to function (for example, the bearing surface has worn through, the bearing seizes, or a polymer core cracks or separates from a metal endplate), the test shall be terminated. The mechanism of failure and number of cycles at which the functional failure occurred, or was discovered, shall be noted.

9.10.10 Angular motions shall be controlled with an accuracy of ±0.5°.

9.10.11 Applied moments shall be controlled to ±5 % of the maximum moment value for the complete motion cycle when tested in load control.

9.11 At the indicated inspection interval, remove the wear and soak components, wash, rinse, and dry concurrently, in accordance with the procedure in Annex A4 of Guide F 1714. It is important that both the wear and soak components be treated identically to ensure that they have the same exposure to the wash, rinse, and drying fluids. This will provide the most accurate correction for fluid absorption by the wear specimens.

9.12 After rinsing and drying, weigh the wear components and soak controls (±10 µg).

9.13 Thoroughly rinse the wear chambers and component surfaces with distilled water.

9.14 Inspect the bearing surfaces of the components and note the characteristics of the wear process. Visual, microscopic, profilometric, replication, or other inspection techniques can be used. Geometric measurements of relevant features should also be taken. Care must be taken, however, that the surfaces do not become contaminated or damaged by any substance or technique that might affect the subsequent wear properties. If contamination occurs, thoroughly reclean the specimens before restarting the wear test.

9.15 Replace the wear components and soak controls in fresh testing medium and continue wear cycling.

9.16 *Gathering of Particulate*:

9.16.1 At appropriate intervals, representative particles should be isolated from the testing medium with appropriate digestion and filtration methods. Submicron filters (0.2 µm or below) are suggested; though, ultimately, the material type of the wear particles and their size distribution will dictate the methods used. Note that several stages of filtration may be necessary to effectively isolate the different particles of interest.

9.16.2 The particulate debris should be analyzed as appropriate. The user may wish to reference Practices F 1877 and F 561 for further information regarding particle characterization or debris isolation or both.

10. Calculation

10.1 *Correcting for Fluid Absorption*—Calculate the net wear NW_i at the end of each cycle interval i using the equation in 3.1.11 and definitions for S_i and W_i in 3.1.16 and 3.1.17, respectively. Calculate the interval net wear rate WR_i during cycle interval i using the equation in 3.1.6.

10.2 *Conversion to Volumetric Wear*—Convert net wear NW_i to volumetric wear NV_i using the equation in 3.1.5 and interval net wear rate WR_i to interval net volumetric wear rate VR_i using the equation in 3.1.5. This is recommended for comparison of wear between different materials or material grades (UHMWPE wear versus cobalt-chromium-molybdenum wear, for example). The accuracy of this calculation is dependent on the material being reasonably homogeneous, that is, having a constant density with wear depth. Report the density value used in this conversion. See Section 3 for details.

11. Report

11.1 Provide materials traceability information for all components used, such as part and lot numbers of finished parts or material grades, batch numbers, manufacturing certifications, processing variables, and any other pertinent manufacturing/material information.

11.2 All pretest bulk material properties characterizations shall be provided (for example, molecular weight average, range and distributions, percent crystallinity, density, and degree of oxidation).

11.3 The surface finish of both counterfaces shall be characterized by profilometry, photomicrography, replication, or other applicable techniques and included within the report.

11.4 All relevant geometric measurements of the IVD prosthesis throughout the duration of the test shall be reported.

11.5 Report the method of sterilization, sterilization test dates, and sterilization expiration dates. In case of sterilization using gamma radiation, report the time and storage conditions (for example, air, inert gas, vacuum, and so forth) between fabrication and irradiation, the atmosphere irradiation, the total gamma dose and dose rate, and the duration and condition of storage between sterilization and the beginning of the test, since each of these may affect the amount of oxidative degradation during or after the radiation sterilization process. If sterilization information is not available, this must be clearly stated in the report.

11.6 *Loading Conditions*:

11.6.1 Report the motion profile, load, frequency, and phase angles when using position control. When using load control, report the load profile and the associated angular motion of superior relative to inferior end plate rotations that resulted in terms of Eulerian angles. Report the maximum deviation of the

APPENDIX B

COMPARISON OF ALL PIN-ON-PLATE TESTS IN LITERATURE REVIEW

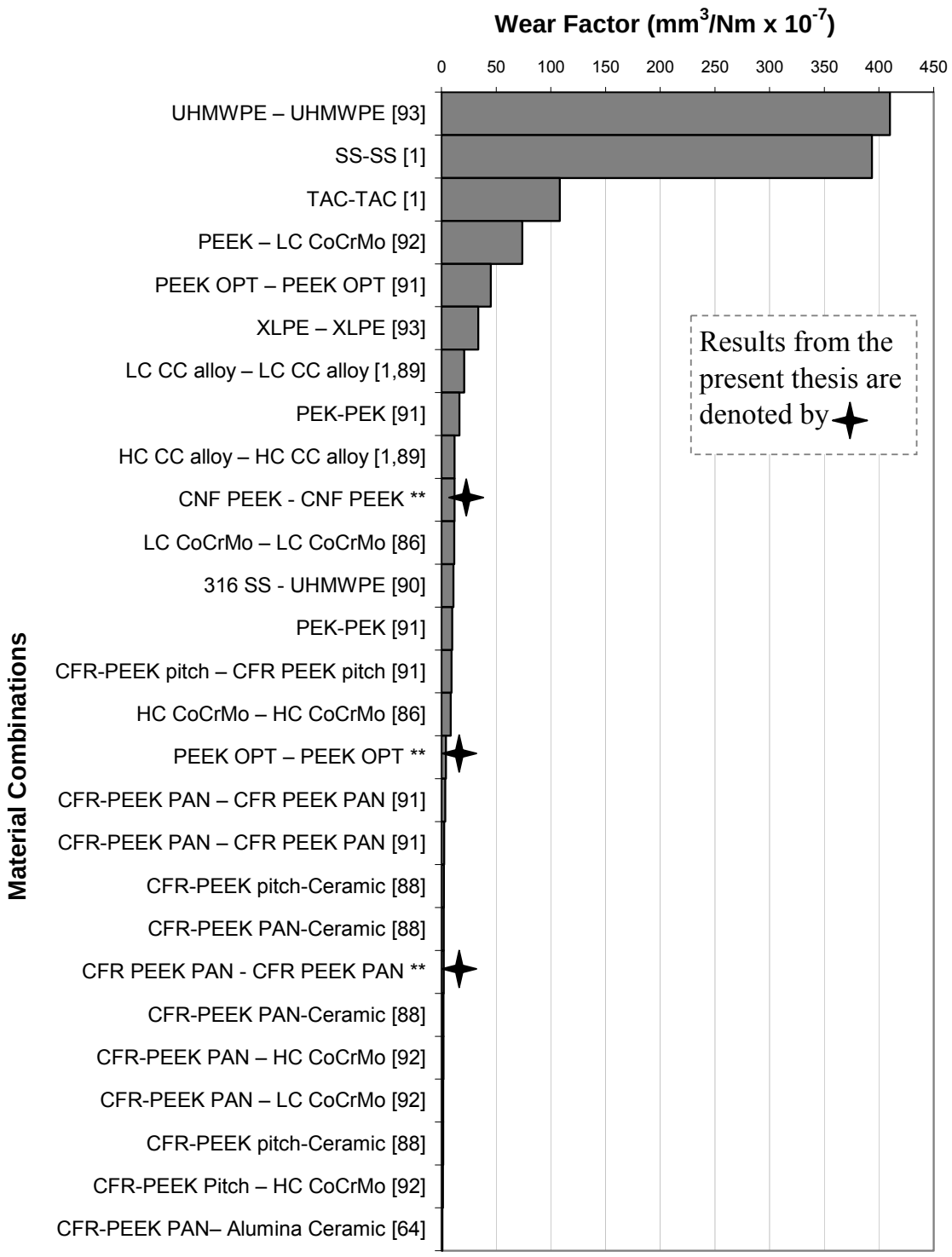
Wear Factor (mm3/Nm x 10-7)
0
50
100
150
200
250
300
350
400
450
Material Combinations
UHMWPE – UHMWPE [93]
SS-SS [1]
TAC-TAC [1]
PEEK – LC CoCrMo [92]
PEEK OPT – PEEK OPT [91]
XLPE – XLPE [93]
LC CC alloy – LC CC alloy [1,89]
PEK-PEK [91]
HC CC alloy – HC CC alloy [1,89]
CNF PEEK - CNF PEEK **
LC CoCrMo – LC CoCrMo [86]
316 SS - UHMWPE [90]
PEK-PEK [91]
CFR-PEEK pitch – CFR PEEK pitch [91]
HC CoCrMo – HC CoCrMo [86]
PEEK OPT – PEEK OPT **
CFR-PEEK PAN – CFR PEEK PAN [91]
CFR-PEEK PAN – CFR PEEK PAN [91]
CFR-PEEK pitch-Ceramic [88]
CFR-PEEK PAN-Ceramic [88]
CFR PEEK PAN - CFR PEEK PAN **
CFR-PEEK PAN-Ceramic [88]
CFR-PEEK PAN – HC CoCrMo [92]
CFR-PEEK PAN – LC CoCrMo [92]
CFR-PEEK pitch-Ceramic [88]
CFR-PEEK Pitch – HC CoCrMo [92]
CFR-PEEK PAN– Alumina Ceramic [64]
Results from the present thesis are denoted by

APPENDIX C

WEAR TEST DATA
A) PEEK OPTIMA
B) CFR PEEK
C) CNF PEEK

A) PEEK OPTIMA

PEEK OPTIMA

Weight (g)

	MC	Plate 1	Plate 2	Plate 3	Plate 4	Plate 5	Plate 6	Plate 7	Pin 1	Pin 2	Pin 3	Pin 4
Normal	0.00	6.34411	6.40487	6.38734	6.36818	6.28179	6.38958	6.36824	1.78272	1.78132	1.77762	1.77858
"	0.01	6.34410	6.40454	6.38737	6.36823	6.28217	6.38963	6.36827	1.78271	1.78059	1.77721	1.77839
"	0.05	6.34406	6.40431	6.38728	6.36810	6.28215	6.38959	6.36825	1.78258	1.78043	1.77707	1.77820
"	0.10	6.34384	6.40407	6.38709	6.36789	6.28202	6.38942	6.36807	1.78255	1.78033	1.77694	1.77818
"	0.20	6.34390	6.40399	6.38711	6.36784	6.28229	6.38952	6.36817	1.78248	1.78041	1.77712	1.77813
"	0.40	6.34384	6.40396	6.38657	6.36733	6.28231	6.38947	6.36814	1.78236	1.78027	1.77630	1.77678
"	0.60	6.34388	6.40391	6.38652	6.36727	6.28246	6.38955	6.36817	1.78233	1.78018	1.77608	1.77652
"	0.80	6.34386	6.40388	6.38638	6.36719	6.28252	6.38949	6.36813	1.78266	1.78049	1.77619	1.77658
"	1.00	6.34387	6.40399	6.38587	6.36731	6.28284	6.38965	6.36832	1.78235	1.78042	1.77599	1.77636
"	1.20	6.34372	6.40342	6.38625	6.36710	6.28294	6.38958	6.36824	1.78241	1.77964	1.77601	1.77636
"	1.40	6.34384	6.40346	6.38633	6.36717	6.28312	6.38966	6.36834	1.78229	1.77956	1.77598	1.77638
"	1.60	6.34377	6.40345	6.38623	6.36711	6.28308	6.38964	6.36830	1.78214	1.77935	1.77579	1.77612
"	1.78	6.34370	6.40340	6.38617	6.36705	6.28314	6.38963	6.36828	1.78195	1.77919	1.77558	1.77603
"	2.00	6.34352	6.40317	6.38592	6.36686	6.28303	6.38944	6.36810	1.78180	1.77901	1.77557	1.77599
Adverse	2.05	6.34352	6.40323	6.38599	6.36692	6.28304	6.38957	6.36805	1.78225	1.77941	1.77586	1.77619
"	2.10	6.34350	6.40325	6.38601	6.36694	6.28311	6.38955	6.36811	1.78193	1.77924	1.77565	1.77601
"	2.15	6.34341	6.40318	6.38594	6.36687	6.28308	6.38951	6.36809	1.78190	1.77924	1.77566	1.77598
"	2.20	6.34338	6.40321	6.38593	6.36678	6.28323	6.38961	6.36820	1.78191	1.77902	1.77536	1.77573
"	2.30	6.34283	6.40221	6.38487	6.36489	6.28312	6.38947	6.36805	1.78129	1.77874	1.77505	1.77442
"	2.45	6.34291	6.40299	6.38566	6.36628	6.28339	6.38948	6.36815	1.78159	1.77913	1.77511	1.77452
"	2.60	6.33930	6.40281	6.38538	6.36608	6.28333	6.38939	6.36807	1.77779	1.77890	1.77458	1.77409
"	2.75	6.33749	6.39888	6.38380	6.36076	6.28187	6.38800	6.36668	1.77693	1.77231	1.77403	1.76830

Weight Change for load soaks (g)

Formula = (S @ i - S @ 0)

MC	Plate 1	Plate 2	Plate 3	Plate 4	Plate 5	Plate 6	Plate 7	Average	Pin 1	Pin 2	Pin 3	Pin 4
0.00												
0.01					0.0004	0.0000	0.0000	0.0000				
0.05					0.0004	0.0000	0.0000	0.0001				
0.10					0.0002	-0.0002	-0.0002	0.0000				
0.20					0.0005	-0.0001	-0.0001	0.0001				
0.40					0.0005	-0.0001	-0.0001	0.0001				
0.60					0.0007	0.0000	-0.0001	0.0002				
0.80					0.0007	-0.0001	-0.0001	0.0002				
1.00					0.0011	0.0001	0.0001	0.0004				
1.20					0.0011	0.0000	0.0000	0.0004				
1.40					0.0013	0.0001	0.0001	0.0005				
1.60					0.0013	0.0001	0.0001	0.0005				
1.78					0.0013	0.0000	0.0000	0.0005				
2.00					0.0012	-0.0001	-0.0001	0.0003				
2.05					0.0012	0.0000	-0.0002	0.0003				
2.10					0.0013	0.0000	-0.0001	0.0004				
2.15					0.0013	-0.0001	-0.0001	0.0004				
2.20					0.0014	0.0000	0.0000	0.0005				
2.30					0.0013	-0.0001	-0.0002	0.0003				
2.45					0.0016	-0.0001	-0.0001	0.0005				
2.60					0.0015	-0.0002	-0.0002	0.0004				
2.75					0.0001	-0.0016	-0.0016	-0.0010				

Net Wear Adjusted for fluid absorbtion (mg)

Formula = (W @ 0 - W @ i) + Avg Soak Adj

MC	Plate 1	Plate 2	Plate 3	Plate 4	Plate 5	Plate 6	Plate 7	Pin 1	Pin 2	Pin 3	Pin 4
0.00	0.0000	0.0000	0.0000	0.0000				0.0000	0.0000	0.0000	0.0000
0.01	0.0033	0.3333	-0.0233	-0.0433				-0.3389	0.3778	0.0511	-0.1589
0.05	0.1800	0.6900	0.1933	0.2167				-0.1856	0.5611	0.2144	0.0511
0.10	0.2367	0.7667	0.2200	0.2667				-0.1589	0.6478	0.3444	0.0644
0.20	0.3278	1.0044	0.3544	0.4678				0.0467	0.7100	0.3000	0.2600
0.40	0.3756	1.0156	0.8756	0.9556				0.2056	0.8889	1.1589	1.6489
0.60	0.4156	1.1489	1.0189	1.1022				0.2600	1.0000	1.4033	1.9233
0.80	0.4244	1.1711	1.1378	1.1711				-0.1278	0.6322	1.2356	1.8122
1.00	0.6389	1.2822	1.8789	1.2722				0.1911	0.7178	1.4444	2.0411
1.20	0.7722	1.8289	1.4789	1.4689				0.3622	1.7256	1.6556	2.2789
1.40	0.7689	1.9122	1.5189	1.5156				0.5511	1.8678	1.7478	2.3211
1.60	0.8044	1.8944	1.5811	1.5444				0.6333	2.0133	1.8700	2.5100
1.78	0.8833	1.9533	1.6533	1.6133				0.7367	2.0933	2.0000	2.5133
2.00	0.9044	2.0211	1.7411	1.6444				0.8156	2.2022	1.9422	2.4922
2.05	0.9389	1.9922	1.7056	1.6156				0.5522	1.9789	1.8322	2.4656
2.10	0.9900	2.0100	1.7200	1.6267				0.8122	2.0922	1.9856	2.5889
2.15	1.0533	2.0467	1.7600	1.6733				0.8556	2.1089	1.9856	2.6322
2.20	1.2000	2.1400	1.8867	1.8767				0.7156	2.2022	2.1656	2.7589
2.30	1.6144	2.9978	2.8144	3.6378				1.3511	2.4978	2.4844	4.0844
2.45	1.6667	2.3500	2.1533	2.3700				1.1767	2.2333	2.5533	4.1100
2.60	5.2033	2.4500	2.3567	2.5000				4.8556	2.3389	2.9522	4.4122
2.75	5.5933	4.9733	2.5233	6.4067				5.5944	8.8044	3.3811	10.0778

Total Wear (mg)

Formula = Wear of Plate + Wear of Pin

							volumetric wear, Wear / density				PEEK OPT	
MC	1	2	3	4	MC	1	2	3	4	AVG	SD
0.00	0.0000	0.0000	0.0000	0.0000	0.00	0.0000	0.0000	0.0000	0.0000	0.0000	0.0000
0.01	-0.3356	0.7111	0.0278	-0.2022	0.01	-0.2653	0.5621	0.0220	-0.1599	0.0397	0.3679
0.05	-0.0056	1.2511	0.4078	0.2678	0.05	-0.0044	0.9890	0.3224	0.2117	0.3797	0.4283
0.10	0.0778	1.4144	0.5644	0.3311	0.10	0.0615	1.1181	0.4462	0.2617	0.4719	0.4586
0.20	0.3744	1.7144	0.6544	0.7278	0.20	0.2960	1.3553	0.5173	0.5753	0.6860	0.4621
0.40	0.5811	1.9044	2.0344	2.6044	0.40	0.4594	1.5055	1.6083	2.0588	1.4080	0.6765
0.60	0.6756	2.1489	2.4222	3.0256	0.60	0.5340	1.6987	1.9148	2.3917	1.6348	0.7889
0.80	0.2967	1.8033	2.3733	2.9833	0.80	0.2345	1.4256	1.8762	2.3584	1.4736	0.9097
1.00	0.8300	2.0000	3.3233	3.3133	1.00	0.6561	1.5810	2.6271	2.6192	1.8709	0.9472
1.20	1.1344	3.5544	3.1344	3.7478	1.20	0.8968	2.8098	2.4778	2.9627	2.2868	0.9485
1.40	1.3200	3.7800	3.2667	3.8367	1.40	1.0435	2.9881	2.5823	3.0329	2.4117	0.9344
1.60	1.4378	3.9078	3.4511	4.0544	1.60	1.1366	3.0892	2.7282	3.2051	2.5397	0.9572
1.78	1.6200	4.0467	3.6533	4.1267	1.78	1.2806	3.1989	2.8880	3.2622	2.6574	0.9323
2.00	1.7200	4.2233	3.6833	4.1367	2.00	1.3597	3.3386	2.9117	3.2701	2.7200	0.9260
2.05	1.4911	3.9711	3.5378	4.0811	2.05	1.1787	3.1392	2.7967	3.2262	2.5852	0.9558
2.10	1.8022	4.1022	3.7056	4.2156	2.10	1.4247	3.2429	2.9293	3.3325	2.7323	0.8887
2.15	1.9089	4.1556	3.7456	4.3056	2.15	1.5090	3.2850	2.9609	3.4036	2.7896	0.8740
2.20	1.9156	4.3422	4.0522	4.6356	2.20	1.5143	3.4326	3.2033	3.6645	2.9537	0.9779
2.30	2.9656	5.4956	5.2989	7.7222	2.30	2.3443	4.3443	4.1888	6.1045	4.2455	1.5366
2.45	2.8433	4.5833	4.7067	6.4800	2.45	2.2477	3.6232	3.7207	5.1225	3.6785	1.1743
2.60	10.0589	4.7889	5.3089	6.9122	2.60	7.9517	3.7857	4.1968	5.4642	5.3496	1.8761
2.75	11.1878	13.7778	5.9044	16.4844	2.75	8.8441	10.8915	4.6675	13.0312	9.3586	3.5641
					AVG	SD					
% of Wear	Plate	49.9950	36.0968	42.7362	38.8649	41.92	6.0309				
	Pin	50.0050	63.9032	57.2638	61.1351	58.08	6.0309				

CFR PEEK

Weight (g)

MC	Plate 1	Plate 2	Plate 3	Plate 5	Plate 6	Plate 7	Pin 10	Pin 2	Pin 8	Pin 4
0.00	7.1264	7.0797	7.0729	7.0506	6.9777	7.1735	1.9337	1.9524	1.9242	1.9481
0.25	7.1263	7.0795	7.0728	7.0508	6.9777	7.1735	1.9335	1.9523	1.9243	1.9481
0.59	7.1263	7.0794	7.0727	7.0506	6.9777	7.1734	1.9334	1.9523	1.9238	1.9480
0.84	7.1262	7.0794	7.0727	7.0506	6.9776	7.1734	1.9335	1.9522	1.9239	1.9480
1.09	7.1262	7.0793	7.0727	7.0506	6.9776	7.1733	1.9335	1.9521	1.9237	1.9479
1.34	7.1262	7.0793	7.0727	7.0505	6.9775	7.1733	1.9335	1.9521	1.9236	1.9480
1.59	7.1262	7.0793	7.0727	7.0506	6.9775	7.1733	1.9336	1.9521	1.9237	1.9479
2.00	7.1261	7.0792	7.0726	7.0506	6.9775	7.1732	1.9333	1.9520	1.9237	1.9478
2.15	7.1258	7.0789	7.0722	7.0501	6.9771	7.1729	1.9335	1.9518	1.9239	1.9477
2.30	7.1262	7.0793	7.0726	7.0508	6.9775	7.1732	1.9333	1.9521	1.9241	1.9478
2.45	7.1258	7.0787	7.0722	7.0497	6.9772	7.1729	1.9331	1.9518	1.9238	1.9475
2.60	7.1260	7.0789	7.0717	7.0498	6.9774	7.1731	1.9331	1.9518	1.9232	1.9474
2.75	7.1259	7.0788	7.0715	7.0500	6.9774	7.1731	1.9332	1.9518	1.9232	1.9475
2.90	7.1256	7.0775	7.0712	7.0501	6.9772	7.1728	1.9333	1.9508	1.9234	1.9474
3.05	7.1245	7.0766	7.0703	7.0491	6.9759	7.1720	1.9325	1.9502	1.9223	1.9468

Weight Change for load soaks (g)

Formula = (S @ i - S @ 0)

MC	Plate 1	Plate 2	Plate 3	Plate 4	Plate 5	Plate 6	Average	Pin 1	Pin 2	Pin 3	Pin 4
0.00											
0.25					0.0000	0.0000	0.0000				
0.59					0.0000	-0.0001	0.0000				
0.84					-0.0001	-0.0001	-0.0001				
1.09					-0.0001	-0.0001	-0.0001				
1.34					-0.0002	-0.0002	-0.0002				
1.59					-0.0002	-0.0002	-0.0002				
2.00					-0.0002	-0.0003	-0.0003				
2.15					-0.0006	-0.0006	-0.0006				
2.30					-0.0002	-0.0003	-0.0002				
2.45					-0.0005	-0.0006	-0.0005				
2.60					-0.0003	-0.0003	-0.0003				
2.75					-0.0003	-0.0004	-0.0003				
2.90					-0.0005	-0.0006	-0.0006				
3.05					-0.0018	-0.0015	-0.0017				

Net Wear Adjusted for fluid absorbtion (mg)

Formula = (W @ 0 - W @ i) + Avg Soak Adj

MC	Plate 1	Plate 2	Plate 3	Plate 5	Plate 6	Plate 7	Pin 10	Pin 2	Pin 8	Pin 4
0.00	0.0000	0.0000	0.0000	0.0000			0.0000	0.0000	0.0000	0.0000
0.25	0.1200	0.2067	0.0933	-0.2033			0.1500	0.0700	-0.1633	-0.0567
0.59	0.0367	0.2233	0.0967	-0.0600			-0.3017	-0.4983	-0.2350	-0.4683
0.84	0.0500	0.2000	0.0700	-0.1100			-0.1617	-0.1117	-0.0417	-0.2583
1.09	0.0200	0.1933	0.0767	-0.1700			-0.6617	-0.5783	-0.3850	-0.7617
1.34	0.0133	0.1600	0.0167	-0.0933			-0.5917	-0.4683	-0.2517	-0.7183
1.59	-0.0050	0.2050	0.0217	-0.1817			-0.3783	-0.1650	-0.0617	-0.3617
2.00	-0.0133	0.1567	-0.0033	-0.3233			-0.1867	-0.1267	-0.0967	-0.3100
2.15	-0.0400	0.1567	0.0700	-0.1000			-0.2333	0.1200	-0.1900	-0.1233
2.30	-0.0200	0.1933	0.0767	-0.4433			0.0900	-0.0200	-0.2767	-0.0900
2.45	0.0083	0.4717	0.1917	0.3450			0.1950	0.2383	-0.0083	0.2317
2.60	0.0233	0.5000	0.8733	0.5400			0.1567	0.1767	0.5867	0.2400
2.75	0.1367	0.5833	1.0000	0.2500			0.2067	0.2667	0.6033	0.2333
2.90	0.2133	1.6500	1.0867	-0.0433			0.0650	1.2283	0.4150	0.2850
3.05	0.2650	1.3950	0.9217	-0.1817			0.0117	1.0350	0.7083	0.0417

						AVG	SD
%Wear	Plate	95.7831	57.4074	56.5440	129.7619	84.8741	35.0758114
	Pin	4.2169	42.5926	43.4560	-29.7619	15.1259	35.0758114

Total Wear (mg)

Volumetric Wear

density 1.4

Formula = Wear of Plate + Wear of Pin

MC	1	2	3	4	MC	1	2	3	4	AVG		
0.00	0.0000	0.0000	0.0000	0.0000	0.00	0.0000	0.0000	0.0000	0.0000	0.0000	0	
0.25	0.2700	0.2767	-0.0700	-0.2600	0.25	0.1929	0.1976	-0.0500	-0.1857	0.0387	0.18907595	
0.59	-0.2650	-0.2750	-0.1383	-0.5283	0.59	-0.1893	-0.1964	-0.0988	-0.3774	-0.2155	0.11672334	
0.84	-0.1117	0.0883	0.0283	-0.3683	0.84	-0.0798	0.0631	0.0202	-0.2631	-0.0649	0.14506723	
1.09	-0.6417	-0.3850	-0.3083	-0.9317	1.09	-0.4583	-0.2750	-0.2202	-0.6655	-0.4048	0.2014357	
1.34	-0.5783	-0.3083	-0.2350	-0.8117	1.34	-0.4131	-0.2202	-0.1679	-0.5798	-0.3452	0.18858686	0.42
1.59	-0.3833	0.0400	-0.0400	-0.5433	1.59	-0.2738	0.0286	-0.0286	-0.3881	-0.1655	0.19806795	
2.00	-0.2000	0.0300	-0.1000	-0.6333	2.00	-0.1429	0.0214	-0.0714	-0.4524	-0.1613	0.20537353	
2.15	-0.2733	0.2767	-0.1200	-0.2233	2.15	-0.1952	0.1976	-0.0857	-0.1595	-0.0607	0.17815825	
2.30	0.0700	0.1733	-0.2000	-0.5333	2.30	0.0500	0.1238	-0.1429	-0.3810	-0.0875	0.22563738	
2.45	0.2033	0.7100	0.1833	0.5767	2.45	0.1452	0.5071	0.1310	0.4119	0.2988	0.18969582	
2.60	0.1800	0.6767	1.4600	0.7800	2.60	0.1286	0.4833	1.0429	0.5571	0.5530	0.37637315	
2.75	0.3433	0.8500	1.6033	0.4833	2.75	0.2452	0.6071	1.1452	0.3452	0.5857	0.40302147	
2.90	0.2783	2.8783	1.5017	0.2417	2.90	0.1988	2.0560	1.0726	0.1726	0.8750	0.89149208	
3.05	0.2767	2.4300	1.6300	-0.1400	3.05	0.1976	1.7357	1.1643	-0.1000	0.7494	0.85066417	

CNF PEEK

Weight (g)

MC	Plate 1	Plate 2	Plate 4	Plate 5	Plate 6	Plate 7	Plate 8	Pin 1	Pin 2	Pin 3	Pin 4
0.00	6.60295	6.57945	6.58752	6.57437	6.55785	6.40400	6.59510	1.85577	1.85739	1.85446	1.86450
0.25	6.60195	6.57874	6.58708	6.57381	6.55787	6.40437	6.59525	1.85460	1.85623	1.85352	1.86361
0.50	6.60154	6.57740	6.58672	6.57342	6.55765	6.40449	6.59526	1.85453	1.85469	1.85320	1.86331
0.75	6.60047	6.57687	6.58639	6.57313	6.55725	6.40462	6.59527	1.85359	1.85462	1.85307	1.86306
1.00	6.60027	6.57648	6.58458	6.57296	6.55684	6.40488	6.59547	1.85321	1.85413	1.85115	1.86271
1.25	6.59994	6.57599	6.58421	6.57260	6.55635	6.40480	6.59535	1.85288	1.85370	1.85078	1.86236
1.50	6.59977	6.57556	6.58383	6.57213	6.55615	6.40493	6.59541	1.85285	1.85341	1.85056	1.86198
1.75	6.59963	6.57512	6.58352	6.57193	6.55579	6.40507	6.59548	1.85263	1.85293	1.85029	1.86176
2.00	6.59933	6.57470	6.58327	6.57173	6.55541	6.40518	6.59558	1.85245	1.85255	1.85005	1.86162
2.15	6.59922	6.57422	6.58297	6.57147	6.55510	6.40526	6.59560	1.85215	1.85208	1.84981	1.86129
2.30	6.5970	6.5729	6.5826	6.5700	6.5554	6.4053	6.5956	1.85010	1.85100	1.84948	1.86029
2.45	6.5959	6.5710	6.5814	6.5686	6.5539	6.4054	6.5955	1.84927	1.84967	1.84860	1.85927
2.60	6.5945	6.5695	6.5800	6.5665	6.5520	6.4053	6.5956	1.8480	1.8485	1.8476	1.8579
2.75	6.5933	6.5672	6.5770	6.5643	6.5504	6.4054	6.5955	1.8473	1.8464	1.8447	1.8552
2.90	6.5912	6.5654	6.5755	6.5630	6.5495	6.4056	6.5956	1.8444	1.8446	1.8430	1.8548
3.05	6.5900	6.5630	6.5726	6.5600	6.5479	6.4055	6.5957	1.8433	1.8414	1.8384	1.8500

Weight Change for load soaks (g)

Formula = (S @ i - S @ 0)

MC	Plate 1	Plate 2	Plate 4	Plate 5	Plate 6	Plate 7	Plate 8	Average	Pin 1	Pin 2	Pin 3	Pin 4
0.00												
0.25						0.0004	0.0002	0.0003				
0.50						0.0005	0.0002	0.0003				
0.75						0.0006	0.0002	0.0004				
1.00						0.0009	0.0004	0.0006				
1.25						0.0008	0.0003	0.0005				
1.50						0.0009	0.0003	0.0006				
1.75						0.0011	0.0004	0.0007				
2.00						0.0012	0.0005	0.0008				
2.15						0.0013	0.0005	0.0009				
2.30						0.0013	0.0005	0.0009				
2.45						0.0014	0.0004	0.0009				
2.60						0.0013	0.0005	0.0009				
2.75						0.0014	0.0004	0.0009				
2.90						0.0016	0.0005	0.0010				
3.05						0.0015	0.0006	0.0011				

Net Wear Adjusted for fluid absorbtion (mg)

Formula = (W @ 0 - W @ i) + Avg Soak Adj

MC	Plate 1	Plate 2	Plate 4	Plate 5	Plate 6	Plate 7	Plate 8	Pin 1	Pin 2	Pin 3	Pin 4
0.00	0.0000	0.0000	0.0000	0.0000	0.0000			0.0000	0.0000	0.0000	0.0000
0.25	1.2633	0.9733	0.7000	0.8200	0.2433			0.9917	0.9950	0.7750	0.7150
0.50	1.7417	2.3750	1.1250	1.2750	0.5250			1.1900	2.6500	1.2133	1.1400
0.75	2.8783	2.9817	1.5283	1.6317	0.9950			2.2133	2.8167	1.4333	1.4767
1.00	3.3050	3.5950	3.5683	2.0317	1.6383			2.6750	3.3850	3.4383	1.9117
1.25	3.5383	3.9850	3.8383	2.2950	2.0250			2.9433	3.7533	3.7467	2.2033
1.50	3.8033	4.5133	4.3100	2.8567	2.3200			2.9433	4.0133	3.9300	2.5467
1.75	4.0467	5.0567	4.7333	3.1700	2.7900			3.2333	4.5633	4.2733	2.8367
2.00	4.4483	5.5783	5.0817	3.4683	3.2717			3.4600	4.9900	4.5600	3.0267
2.15	4.6150	6.1150	5.4283	3.7783	3.6283			3.7450	5.4417	4.7883	3.3450
2.30	6.8833	7.4800	5.7833	5.2333	3.3100			5.8483	6.5683	5.1617	4.3863
2.45	7.9033	9.3700	7.0400	6.6200	4.8033			6.4917	7.7183	5.8550	5.2250
2.60	9.3367	10.8700	8.4067	8.7533	6.7700			7.7750	8.9350	6.8717	6.6750
2.75	10.5367	13.1033	11.4400	10.9100	8.3367			8.3750	10.9350	9.7383	9.2417
2.90	12.8200	15.1200	13.0567	12.4367	9.3867			11.3583	12.8183	11.4217	9.7250
3.05	14.0200	17.4867	16.0233	15.4367	11.0533			12.4750	16.0017	16.0383	14.4750
						AVG	SD				
%Wear	Plate	52.9156	52.2172	49.9766	51.6075	55.2252	52.3884	1.922338089			
P	Pin	47.0844	47.7828	50.0234	48.3925	44.7748	47.6116	1.922338089			

Total Wear (mg)

Volumetric Wear density 2.0

Formula = Wear of Plate + Wear of Pin

MC	1	2	3	4	5
0.00	0.0000	0.0000	0.0000	0.0000	0.0000
0.25	2.2550	1.9683	1.4750	1.5350	0.9217
0.50	2.9317	5.0250	2.3383	2.4150	1.6650
0.75	5.0917	5.7983	2.9617	3.1083	2.2950
1.00	5.9800	6.9800	7.0067	3.9433	3.4133
1.25	6.4817	7.7383	7.5850	4.4983	4.1150
1.50	6.7467	8.5267	8.2400	5.4033	4.6933
1.75	7.2800	9.6200	9.0067	6.0067	5.4133
2.00	7.9083	10.5683	9.6417	6.4950	6.2417
2.15	8.3600	11.5567	10.2167	7.1233	6.8400
2.30	12.7317	14.0483	10.9450	9.6197	7.3550
2.45	14.3950	17.0883	12.8950	11.8450	9.4483
2.60	17.1117	19.8050	15.2783	15.4283	12.4983
2.75	18.9117	24.0383	21.1783	20.1517	14.9983
2.90	24.1783	27.9383	24.4783	22.1617	17.1317
3.05	26.4950	33.4883	32.0617	29.9117	20.0150

MC	1	2	3	4	5	AVG
0.00	0.0000	0.0000	0.0000	0.0000	0.0000	0.0000
0.25	1.1275	0.9842	0.7375	0.7675	0.4608	0.8155
0.50	1.4658	2.5125	1.1692	1.2075	0.8325	1.4375
0.75	2.5458	2.8992	1.4808	1.5542	1.1475	1.9255
1.00	2.9900	3.4900	3.5033	1.9717	1.7067	2.7323
1.25	3.2408	3.8692	3.7925	2.2492	2.0575	3.0418
1.50	3.3733	4.2633	4.1200	2.7017	2.3467	3.3610
1.75	3.6400	4.8100	4.5033	3.0033	2.7067	3.7327
2.00	3.9542	5.2842	4.8208	3.2475	3.1208	4.0855
2.15	4.1800	5.7783	5.1083	3.5617	3.4200	4.4097
2.30	6.3658	7.0242	5.4725	4.8098	3.6775	5.4700
2.45	7.1975	8.5442	6.4475	5.9225	4.7242	6.5672
2.60	8.5558	9.9025	7.6392	7.7142	6.2492	8.0122
2.75	9.4558	12.0192	10.5892	10.0758	7.4992	9.9278
2.90	12.0892	13.9692	12.2392	11.0808	8.5658	11.5888
3.0500	13.2475	16.7442	16.0308	14.9558	10.0075	14.1972

APPENDIX D

VOLUME OF SPHERICAL TIP OF PIN CALCULATIONS

Volume of a sphere

$r := 100 \qquad y := \frac{4}{3}\cdot\pi\cdot r^2 \qquad y = 4.189\times 10^4 \ mm^3$

Circumference of the pin

$d := 9.5$

$c := \pi\cdot d$

$c = 29.845 \ mm$

Area of face of flat end of pin

$y := \pi\cdot 4.75^2$

$y = 70.882$

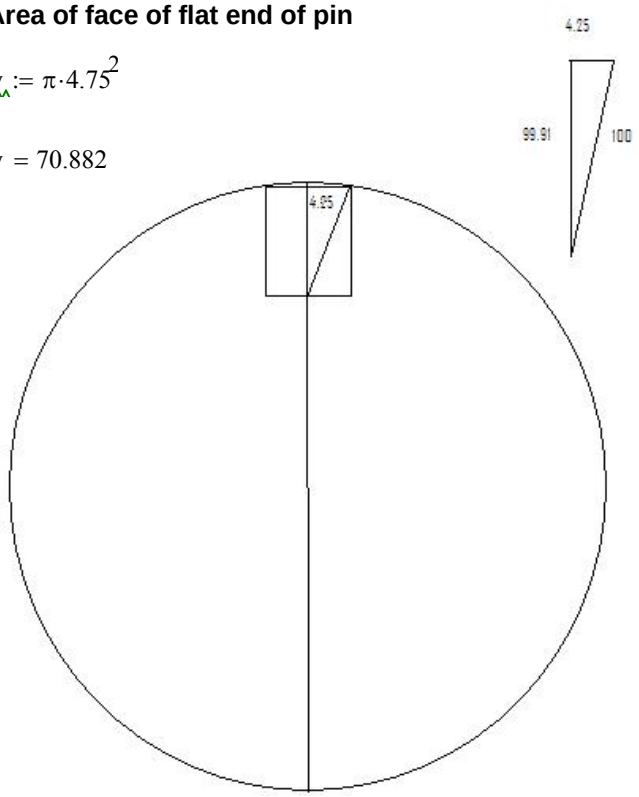

Height of a dome

$a := \sqrt{100^2 - 4.75^2}$

$a = 99.887$

Radius of curvature minus a = height of the dome

$h := 100 - a$

$h = 0.113 \ mm$

Volume of a Dome:

$V := \left(\pi\cdot r\cdot h^2\right) - \left(\frac{1}{3}\cdot\pi\cdot h^3\right)$

$V = 4.001 \ mm^3$

The above value compares to the average fluid adjusted **pin** volumetric wear values attained for the three different versions of PEEK after 2.0 Mc.

5.051 mm^3 for PEEK OPTIMA
3.599 mm^3 for CNF PEEK
0.321 mm^3 for CFR PEEK

This would imply the PEEK OPTIMA radius is totally worn down by the end of the test. The volume of the dome is removed as well as additional material. The diameter of the contact area should be the same as the pin. The PEEK OPTIMA pins reflect these findings. The load soak pins, that have not been tested, appear to have a radius in comparison to the wear test samples that appear to be flat ended.

The CNF PEEK radius is worn down; however the diameter of the contact area should be slightly smaller than the diameter of the pin.

The CFR PEEK tip maintains the radius throughout the test and has a different contact stress than PEEK OPTIMA. The pins samples reflect these finding by indicating a clear ring of unworn surface at the out edge of the pin.

APPENDIX E

LOAD SOAK INVESTIGATION

LOAD SOAK INVESTIGATION

PEEK OPTIMA – (BASELINE AND ADVERSE) PLATES

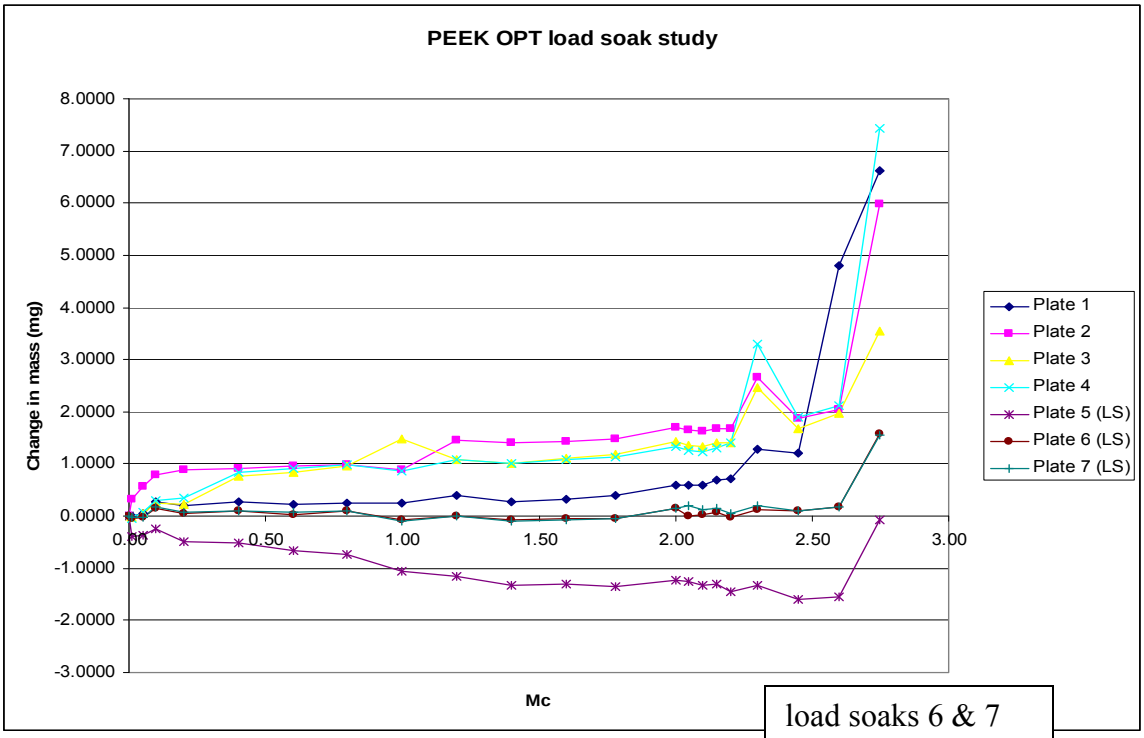

load soaks 6 & 7 are similar, not sure why 5 is so different.

PEEK OPTIMA – (BASELINE + ADVERSE) PINS

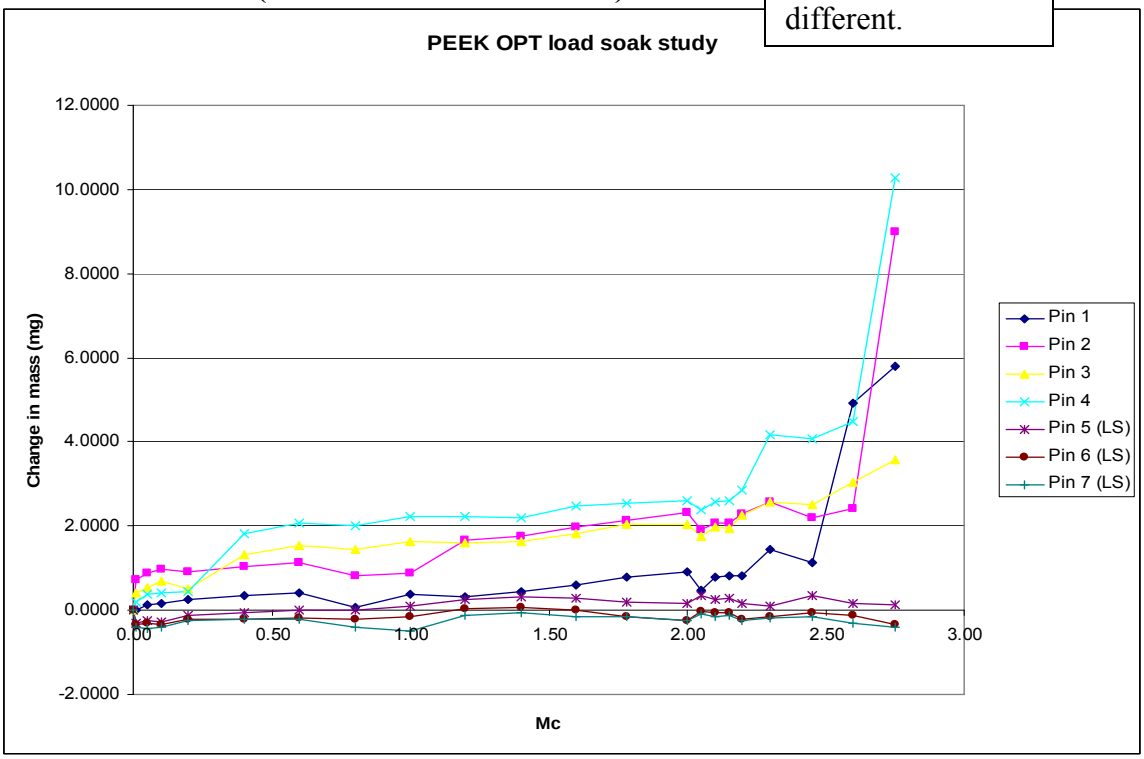

PEEK OPTIMA – ONLY BASELINE – PLATES

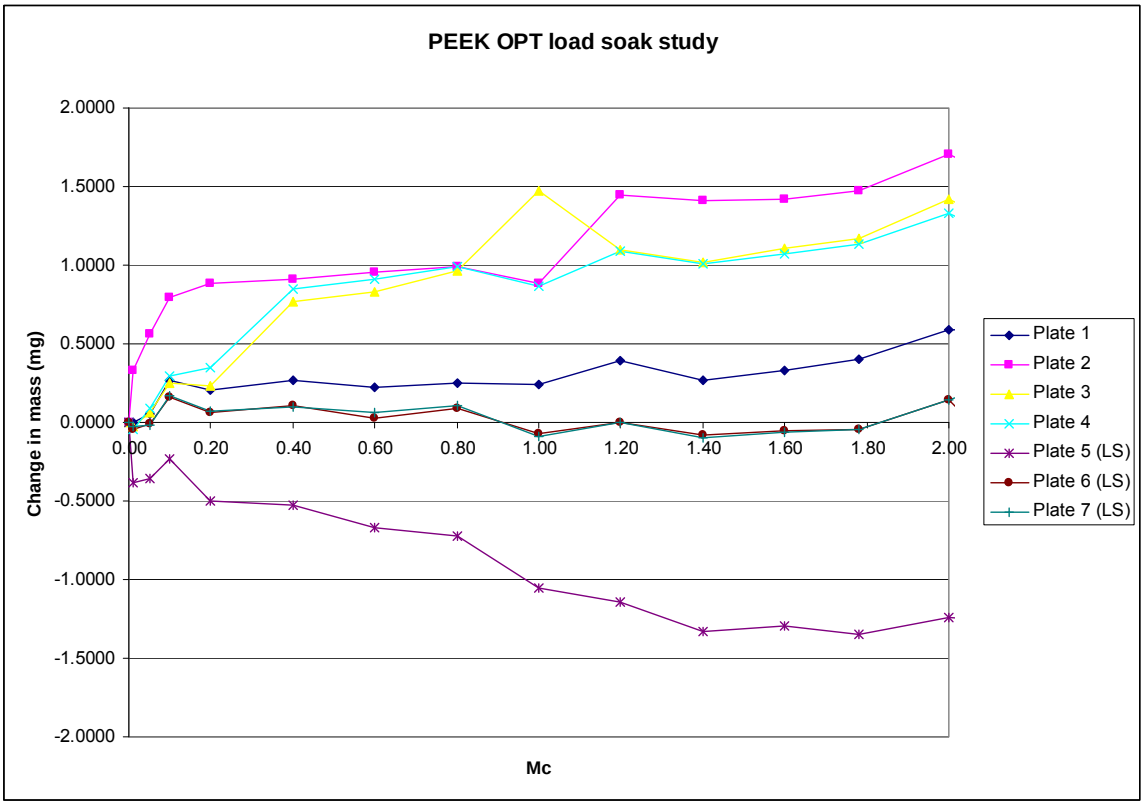

PEEK OPTIMA – ONLY BASELINE – PINS

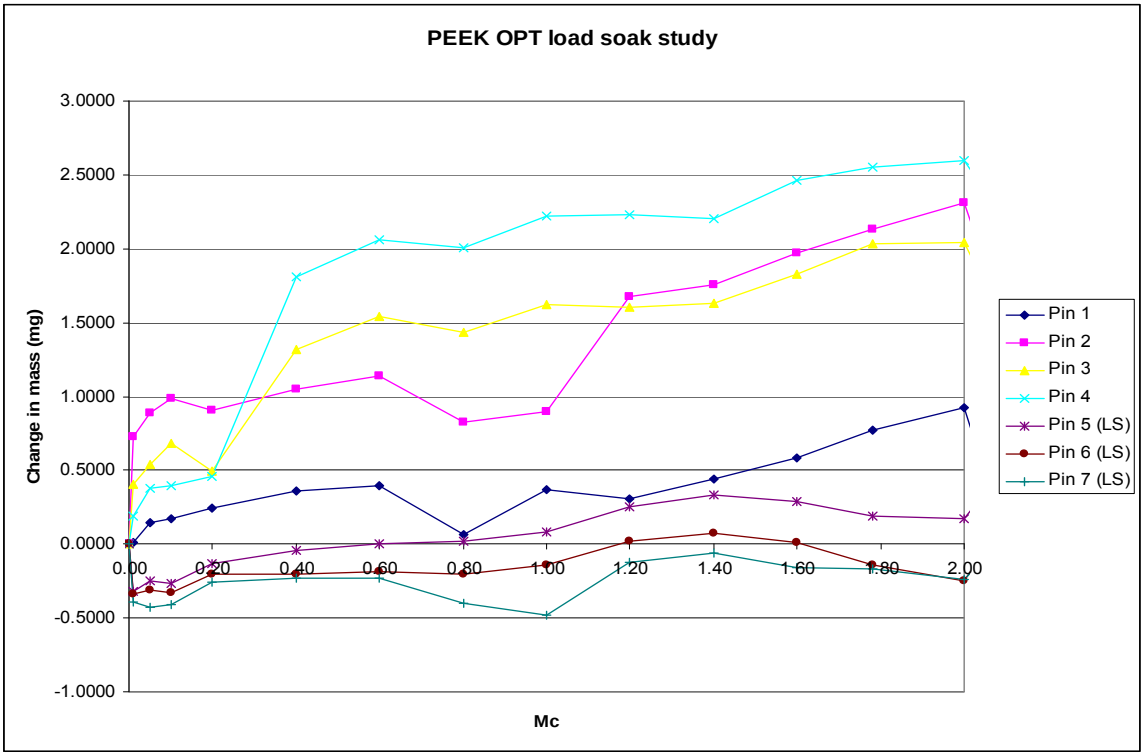

CFR PEEK – BASELINE + ADVERSE – PLATES

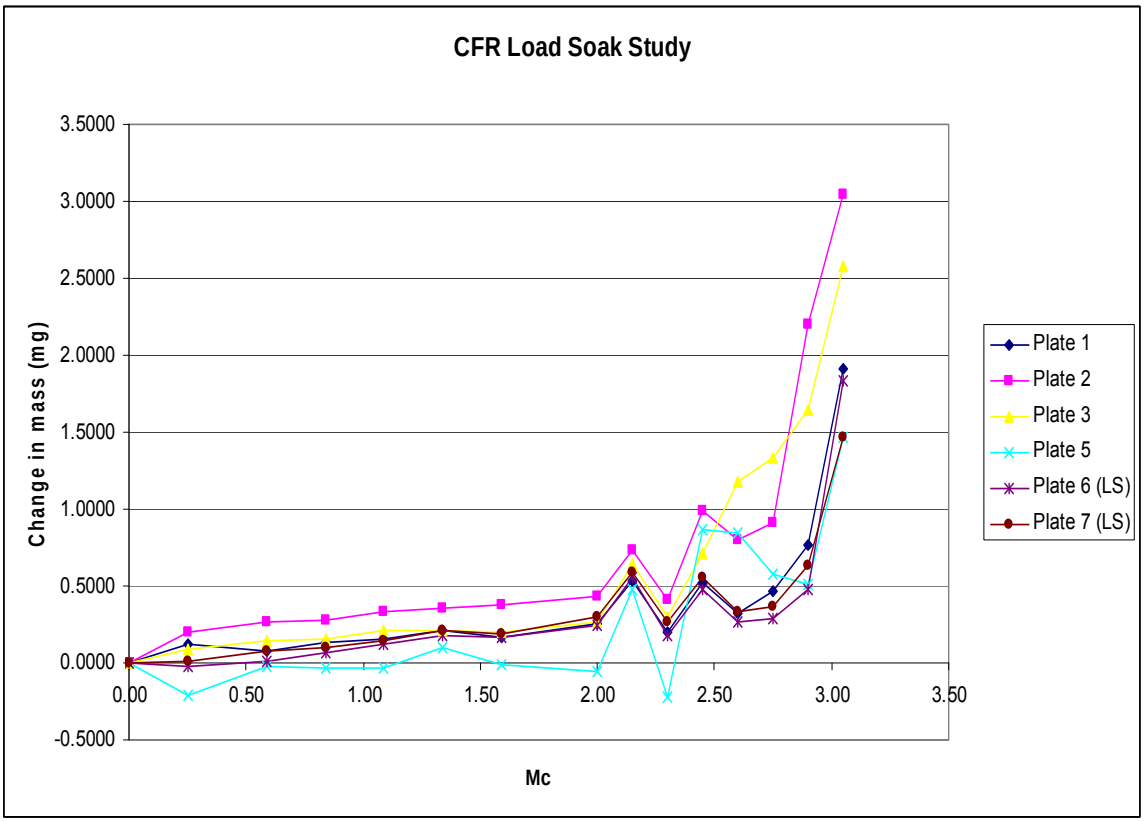

CFR PEEK – BASELINE + ADVERSE – PINS

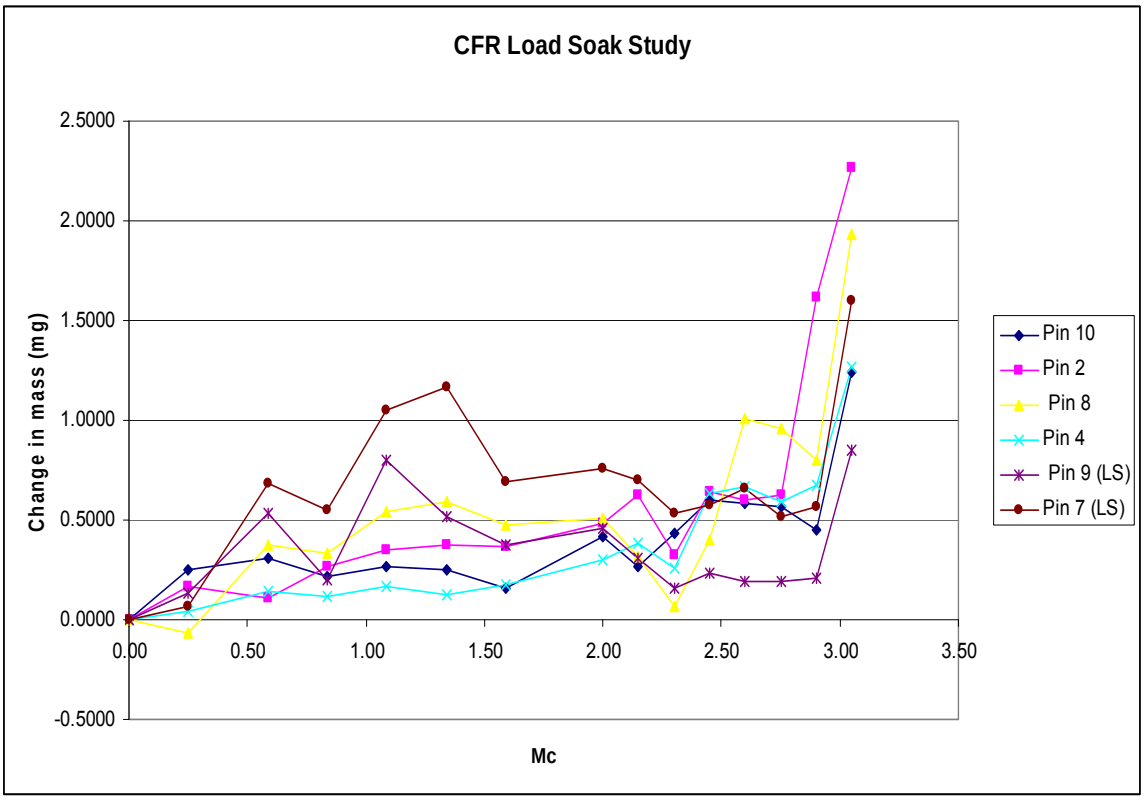

CFR PEEK – ONLY BASELINE – PLATES

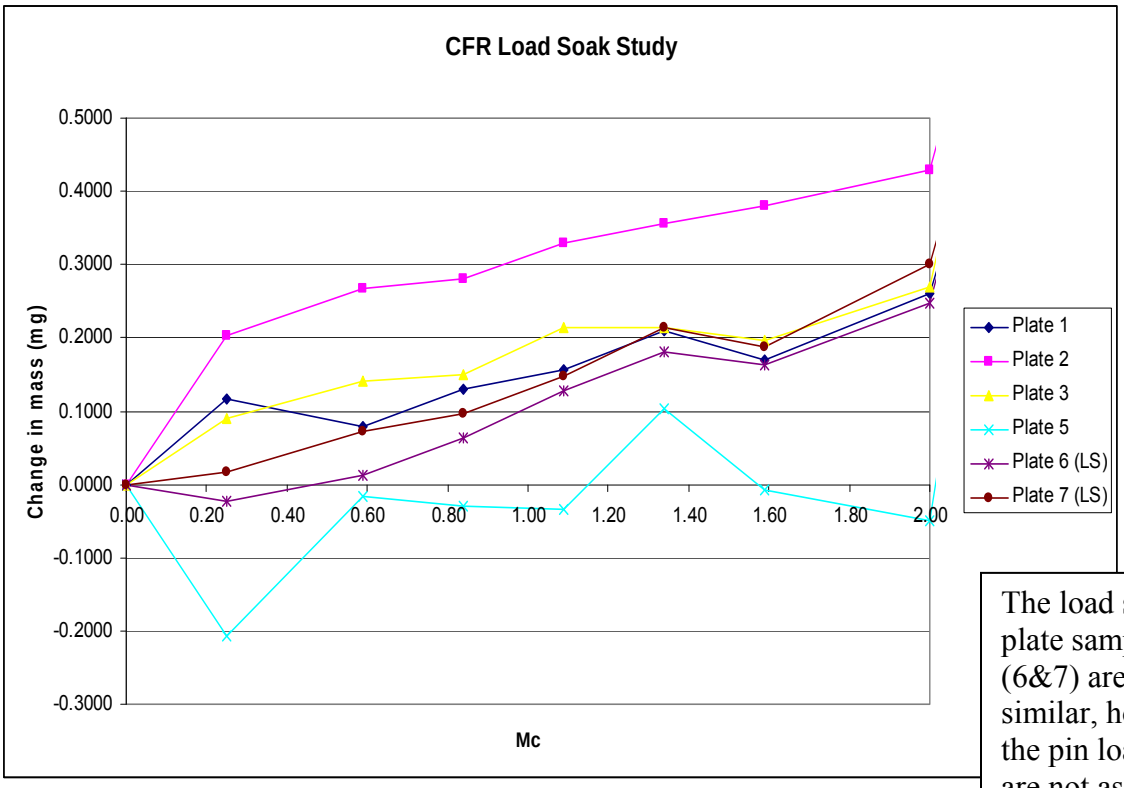

The load soak plate samples (6&7) are very similar, however the pin load soaks are not as congruent

CFR PEEK – ONLY BASELINE – PINS

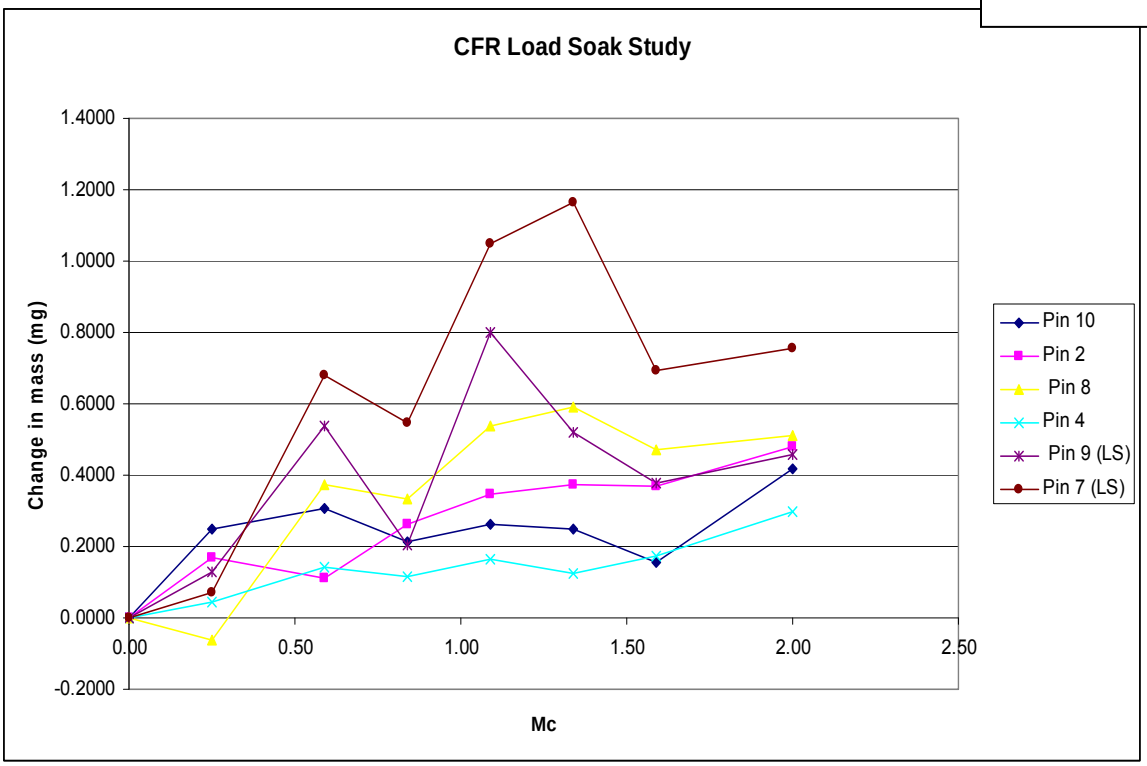

CNF PEEK – BASELINE + ADVERSE – PLATES

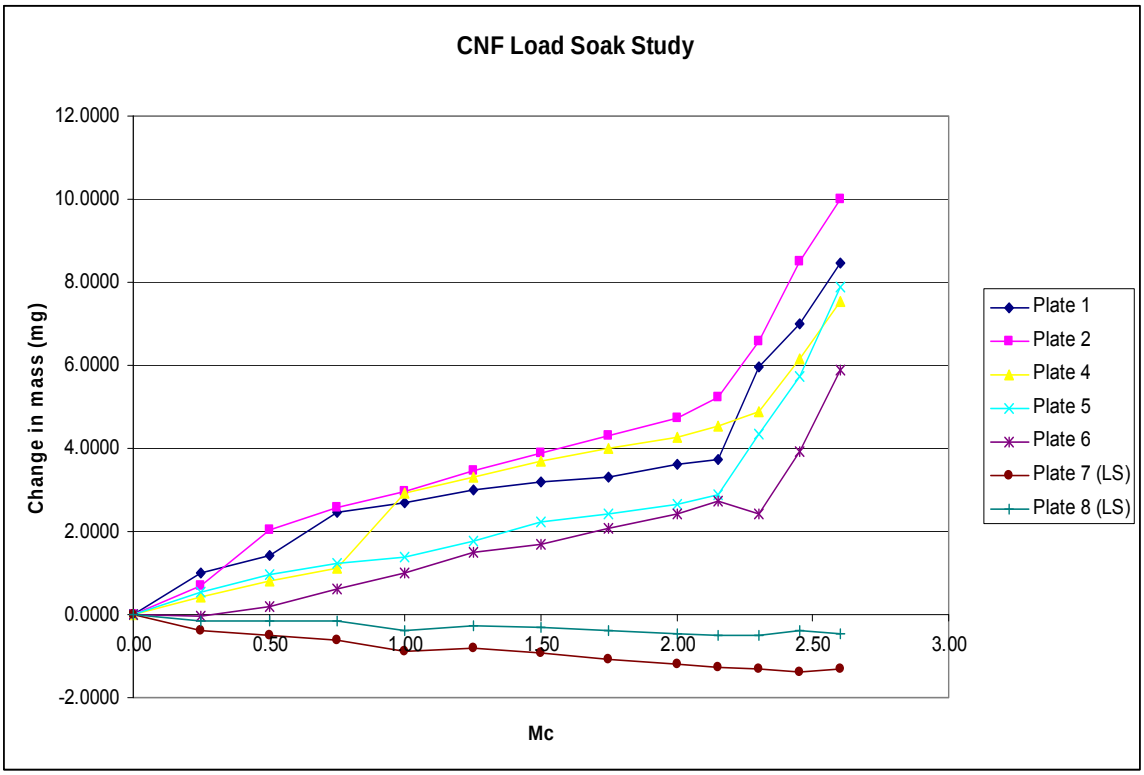

CNF PEEK – BASELINE + ADVERSE – PINS

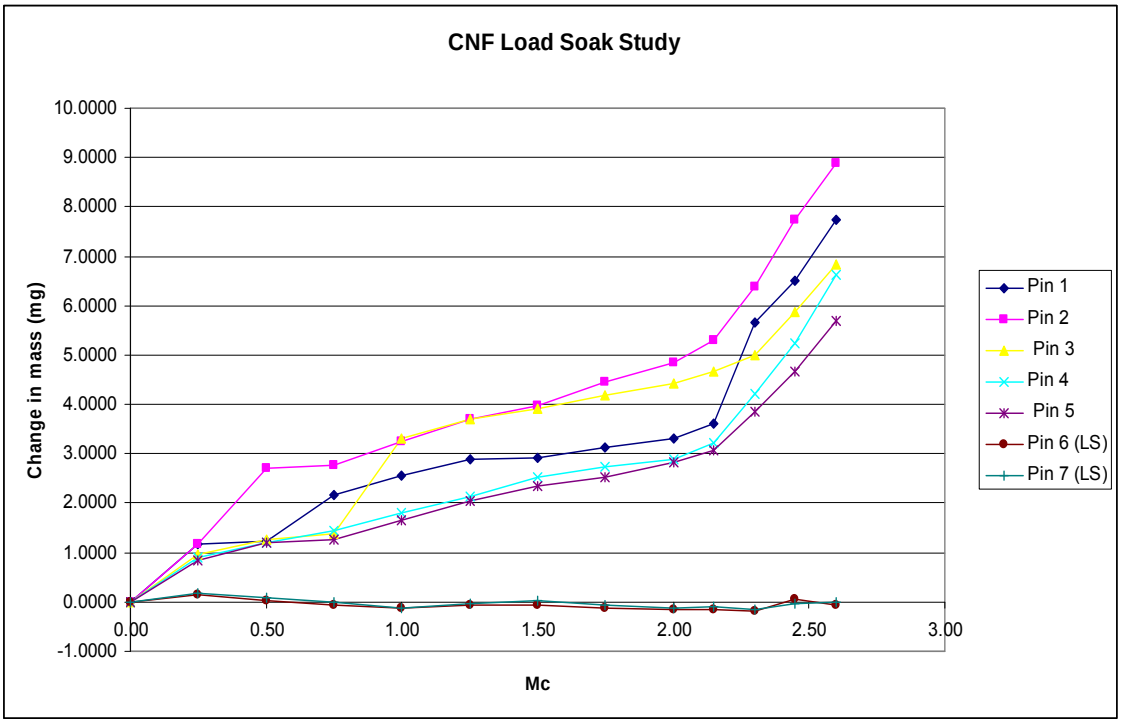

CNF PEEK – ONLY BASELINE – PLATES

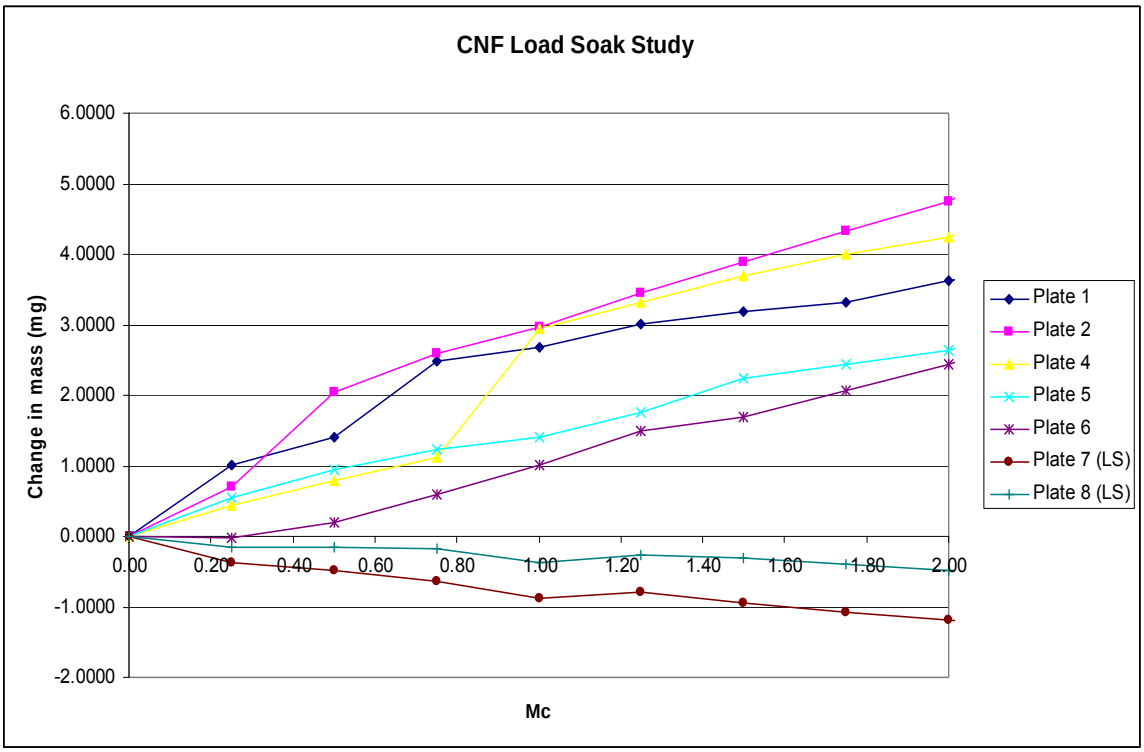
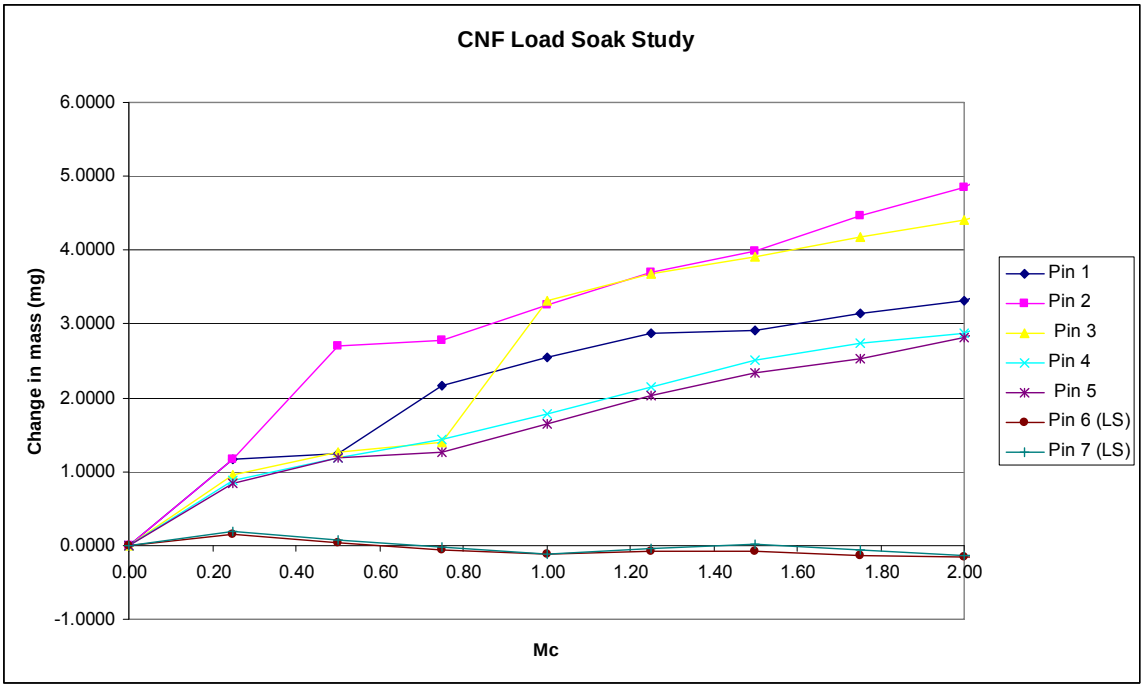
CNF PEEK – ONLY BASELINE – PINS